


Summer 8-21-2015

Detection of Iron (III) Using Magnetic Nanoparticles

Kaiya Hansen

University of Maine - Main, kaiya.hansen@umit.maine.edu

Follow this and additional works at: <http://digitalcommons.library.umaine.edu/etd>

 Part of the [Analytical Chemistry Commons](#), [Environmental Chemistry Commons](#), and the [Materials Chemistry Commons](#)

Recommended Citation

Hansen, Kaiya, "Detection of Iron (III) Using Magnetic Nanoparticles" (2015). *Electronic Theses and Dissertations*. 2334.
<http://digitalcommons.library.umaine.edu/etd/2334>

This Open-Access Thesis is brought to you for free and open access by DigitalCommons@UMaine. It has been accepted for inclusion in Electronic Theses and Dissertations by an authorized administrator of DigitalCommons@UMaine.

**DETECTION OF IRON (III) USING
MAGNETIC NANOPARTICLES**

By

Kaiya Hansen

B.S. University of Maine, 2014

A THESIS

Submitted in Partial Fulfillment of the

Requirements for the Degree of

Master of Science

(in Chemistry)

The Graduate School

University of Maine

August 2015

Advisory Committee:

Carl P. Tripp, Professor of Chemistry, Advisor

Alice E. Bruce, Associate Professor of Chemistry

Mark Wells, Professor of Marine Science

DETECTION OF IRON (III) USING

MAGNETIC NANOPARTICLES

By Kaiya Hansen

Thesis Advisor: Dr. Carl Tripp

An Abstract of the Thesis Presented
in Partial Fulfillment of the Requirements for the
Degree of Master of Science
(in Chemistry)
August 2015

The goal of this work was to develop an iron (III) sensor which can be mounted on buoys and gliders and automatically measure iron (III) in the ocean. The method investigated in this thesis was based on anchoring the iron (III) chelator desferrioxamine B (DFB) to magnetic particles. DFB selectively binds iron (III), resulting in a complex which produces a broad absorbance band at 430 nm. This band can be measured via UV-Vis spectroscopy (UV-Vis). However, measuring oceanic iron (III) directly in solution is difficult because the concentrations can be very low, sometimes less than 1 nM. This problem could be solved if one were able to concentrate the iron (III) from a sample and magnetic particles (which can be removed from a solution by introducing a magnet to the side of the container) were used to accomplish this task.

In Chapter 2, it was found that the untreated carbon-coated cobalt magnetic (Co-C) particles were able to capture iron (III) from a solution. This offered the opportunity to use untreated Co-C particles to capture iron (III) and then in a second

step, remove the iron (III) from the particles for analysis in solution. Most of the studies in Chapter 3 were directed at developing a protocol for extracting iron (III) from the untreated Co-C particles. In one case, 100% of the iron (III) was removed from the particles with DFB. However, this result was not repeatable – in all other cases, 72% or less of the iron (III) captured from solution was recovered by the DFB. It was determined that this was because the Co-C particles were exposed to the air between removing the remaining iron solution and adding the DFB. This allowed the iron (III) on the surface to react and form iron oxyhydroxides, meaning that the DFB was not able to capture it all.

In Chapter 4, a variety of magnetic nanoparticles were derivatized with DFB on the surface: Co-C particles, TurboBeads Silica™ (Co-C particles purchased with a silica coating), and silica-coated nickel nanoparticles (Ni-SiO₂). It was found that TurboBeads Silica™ treated with DFB or DFB-Fe (DFB already bound to iron), as well as Ni-SiO₂ treated with DFB-Fe could capture iron (III) from solution. Some of the iron (III) could be removed from the particles by adding oxalate adjusted to a pH of 1.5. However, no more than 70% (usually less) of the iron (III) captured by these particles was ultimately recovered by the oxalate. The DFB on the particles' surface should have captured the iron (III), preventing it from forming oxyhydroxides. However, to measure iron (III) in the oxalate required adding DFB and adjusting the pH to form the DFB-Fe complex in solution. It was discovered that in a solution of oxalate, DFB-Fe can be reduced to iron (II) when exposed to light. Because measurements were not performed in a dark room, some of the iron (III) was rendered undetectable.

ACKNOWLEDGEMENTS

First and foremost, I would like to thank my advisor, Dr. Carl Tripp. He has now guided me through not one but two research projects. As an undergraduate student, I became a part of his research group, and it was probably one of the best decisions I have made as a student at the University of Maine. Throughout the past four years, he has really helped shape my skills as a scientist. That training has culminated in this thesis, so I have him to thank for that as well as the skills I have acquired while working in his lab. Finally, I must thank him for the tremendous editing help he gave me for this thesis.

I would also like to thank Dr. Alice Bruce and Dr. Wells. They graciously agreed to be a part of my committee, which I am thankful for. They also gave me a few odd supplies here and there to help with this project. Additionally, Dr. Wells gave me a crash course in avoiding iron (III) contamination in the laboratory, which was very important for this research.

Outside of my committee, I would like to thank Dr. George Bernhardt for his help with the SEM, EDX, and XPS measurements made for this thesis in LASST. I could not have done those without him. I would also like to thank Dr. Kelly Edwards, for showing me how to use the TEM instrument in the School of Biology and Ecology's Electron Microscope Lab. The TEM images taken in that lab added to this thesis. Additionally, I thank Michael Handley of the University of Maine's Climate Change Institute for lending me a 5 cm cuvette, which was important to the work done in Chapter 4. Another person

whom I would like to thank is Dr. Whitney King of Colby College. He provided the Toyoparl® column used to remove iron (III) contaminants from oxalate solutions.

There are two fellow students I would like to thank: Silas Owusu-Nkwantabisah and Roghi Kalan. Silas was a great help at the start of this experiment before he graduated, showing me how to do certain procedures (such as using the TGA instrument) and giving advice about how to design particular procedures. He helped me start to become an independent researcher. Roghi has always been willing to lend a hand, teach me something I didn't know, or help me with predicaments in the lab. I am very glad she has been around throughout my time in Dr. Tripp's research group.

I would also like to thank Carol Tripp for reading over this thesis and assisting with the editing process, as well as the rest of the Tripp research group for being supportive of my work throughout my time here.

The work done in this thesis was partially supported by the National Science Foundation under Grant No. OCE-0826098, and I am very thankful for their contribution.

Last but not least, I would like to thank my family for their general support throughout my time as a student at the University of Maine. In addition to the kind assistance from everyone mentioned above, my family's support has been invaluable to me.

TABLE OF CONTENTS

ACKNOWLEDGEMENTS.....	iii
LIST OF TABLES.....	xii
LIST OF FIGURES.....	xvi
LIST OF EQUATIONS.....	xxi
LIST OF ABBREVIATIONS.....	xxii
Chapter	
1. INTRODUCTION.....	1
1.1. Motivation for Automated Iron Detection.....	1
1.2. A Potential Basis for Automated Iron (III) Detection – Desferrioxamine B.....	3
1.3. Detection of Iron (III) Using Infrared Spectroscopy.....	5
1.4. Capture of Iron (III) on Transparent Membrane and Detection with UV-Vis Spectroscopy.....	10
1.5. Capture of Iron (III) on Transparent Column and Detection with UV-Vis Spectroscopy.....	17
1.6. Capture of Iron (III) with Magnetic Particles and Subsequent Concentration for In-Solution Detection.....	19
1.7. References.....	24

2. INITIAL WORK.....	29
2.1. Introduction.....	29
2.2. Experimental	31
2.2.1. Materials.....	31
2.2.2. Washing Particles	32
2.2.3. Treatment of Co-C with Sodium Polyacrylate (NaPA).....	33
2.2.4. Treatment of Co-C with 3-(triethoxysilyl)propylsuccinic Anhydride (Silane)	33
2.2.5. Derivatization of Carboxylic Acid-Treated Co-C with DFB.....	33
2.2.6. Characterization with Thermogravimetric Analysis	35
2.2.7. Characterization of DFB-Derivatized Co-C Particles with SEM and EDX	35
2.2.8. Characterization of DFB-Derivatized Co-C Particles with ATR-IR Spectroscopy.....	36
2.2.9. Iron (III) Removal with Oxalate from DFB-Derivatized Co-C Particles.....	36
2.2.10. Iron (III) Uptake of DFB-Derivatized Co-C Particles	37
2.2.11. Calculations.....	38
2.3. Results and Discussion	39
2.3.1. Characterization with Thermogravimetric Analysis	39
2.3.2. Characterization of DFB-Treated Co Nanoparticles – SEM and EDX.....	46

2.3.3. Characterization of DFB-Derivatized Co-C Particles with ATR-IR Spectroscopy.....	50
2.3.4. Iron (III) Uptake & Removal with Oxalate from DFB-Derivatized Co-C	56
2.4. Conclusions.....	58
2.5. References.....	59
3. IRON UPTAKE WITH UNMODIFIED, CARBON-COATED COBALT NANOPARTICLES	62
3.1. Introduction.....	62
3.2. Experimental	63
3.2.1. Materials.....	63
3.2.2. Washing the Particles	65
3.2.3. The Effect of NaCl on Bare Co-C Particles' Uptake of Iron (III) from Solution.....	65
3.2.4. Removing Iron (III) from Bare Co-C Nanoparticles with DFB – Initial Attempt.....	66
3.2.5. Removing Iron (III) from Bare Co-C Nanoparticles with DFB: Varying DFB pH	67
3.2.6. Removing Iron (III) from Bare Co-C Nanoparticles with DFB – Adding NaCl.....	68

3.2.7. Investigation of Particles' Interference in UV-Vis Spectra	69
3.2.8. Removing Iron (III) from Bare Co-C Nanoparticles with DFB – Substituting DI Water with pH 2 HCl	70
3.2.9. Removing Iron (III) from Bare Co-C Particles – Concentrating Iron (III) from <10 μM FeCl_3	71
3.2.10. Calculation of Amount of Iron (III).....	73
3.2.11. Detection Limits and Error Bars.....	73
3.3. Results and Discussion	73
3.3.1. The Effect of NaCl on Bare Co-C Particles' Uptake of Iron (III) from Solution.....	73
3.3.2. Removing Iron (III) from Bare Co-C Nanoparticles with DFB – Initial Attempt.....	78
3.3.3. Removing Iron (III) from Bare Co-C Nanoparticles with DFB: Varying DFB pH	80
3.3.4. Removing Iron (III) from Bare Co-C Nanoparticles with DFB – Adding NaCl.....	83
3.3.5. Removing Iron (III) from Bare Co-C Nanoparticles with DFB – Interference of Particles.....	86
3.3.6. Investigation of Particles' Interference in UV-Vis Spectra	87

3.3.7. Removing Iron (III) from Bare Co-C Nanoparticles with DFB – Using pH 2 HCl for Washes	91
3.3.8. Removing Iron (III) from Bare Co-C Particles – Concentrating Iron (III) from <10 μM FeCl_3	93
3.4. Conclusion	97
3.5. References.....	99
4. IRON UPTAKE WITH SILICA-COATED, DESFERRIOXAMINE B-TREATED MAGNETIC NANOPARTICLES	100
4.1. Introduction.....	100
4.2. Experimental	101
4.2.1. Materials.....	101
4.2.2. Washing the Particles	103
4.2.3. Treatment of Co-C Particles with Silica, Anhydride Silane, and DFB.....	103
4.2.4. Iron Uptake of Silica- and DFB-Treated Co-C Particles.....	105
4.2.5. Treatment of Fe_3O_4 , Ni Nanoparticles with Silica.....	107
4.2.6. Transmission Electron Microscopy (TEM) Of Silica-Treated Nanoparticles.....	107
4.2.7. Derivatizing TurboBeads Silica™ and Ni-SiO ₂ with DFB.....	108

4.2.8. Characterization of Silica- and DFB-Treated Magnetic Nanoparticles	108
4.2.9. Iron (III) Uptake of Ni-SiO ₂	109
4.2.10. Iron (III) Uptake of Ni-SiO ₂ -DFB	110
4.2.11. Iron (III) Uptake of Ni-SiO ₂ -FB; Removal of Iron (III) from Particles	110
4.2.12. UV-Vis Spectra of 0.1 M NiCl ₂ , Product of Oxalic Acid and Ni Nanoparticles	112
4.2.13. Iron (III) Uptake of TurboBeads Silica™	112
4.2.14. Iron (III) Uptake of Co-SiO ₂ -DFB	112
4.2.15. Iron (III) Uptake of Co-SiO ₂ -FB.....	114
4.2.16. Calculations.....	114
4.3. Results and Discussion	115
4.3.1. Characterization of Co-C Particles Treated with Silica and DFB.....	115
4.3.2. Iron Uptake of Silica- and DFB-Treated Co-C Particles.....	117
4.3.3. TEM Images of Silica-Coated Nanoparticles.....	122
4.3.4. Characterization of Silica-Treated, DFB-Treated Nanoparticles: IR Spectroscopy.....	127
4.3.5. Characterization of Silica-Treated, DFB-Treated Nanoparticles: XPS	131
4.3.6. Iron (III) Uptake of Ni-SiO ₂ (Prior to DFB Exposure)	141
4.3.7. Iron (III) Uptake of Ni-SiO ₂ -DFB	143

4.3.8. Iron (III) Uptake and Removal with Oxalate of Ni-SiO ₂ -FB Particles	144
4.3.9. UV-Vis Spectra of 0.1 M NiCl ₂ , Product of Oxalic Acid and Ni Nanoparticles.....	149
4.3.10. Iron (III) Uptake of TurboBeads Silica™	150
4.3.11. Iron (III) Uptake of Co-SiO ₂ -DFB	152
4.3.12. Iron (III) Uptake of Co-SiO ₂ -FB.....	153
4.4. Conclusions.....	155
4.5. References.....	158
5. FUTURE WORK	160
BIBLIOGRAPHY	162
BIOGRAPHY OF THE AUTHOR	166

LIST OF TABLES

Table 2.1.	Final Volume of Oxalate/DFB Mixture After pH Adjustment and Necessary Dilutions	37
Table 2.2.	Amounts of NaOH Added for pH Adjustments – Measuring Iron (III) in Oxalate Supernatants	38
Table 2.3.	Elemental Analysis of Untreated, NaPA-Treated, and Silane-Treated Cobalt Nanoparticles by Atom.....	49
Table 2.4.	DFB-Fe Absorbance Measurements in Oxalate Washes	56
Table 2.5.	DFB-Fe Absorbance Measurements in Iron (III) Supernatants.....	57
Table 3.1.	Amounts of NaOH Added for pH Adjustments – Measuring Iron (III) in FeCl ₃ Solutions.....	66
Table 3.2.	pH of DFB Used with Each Sample; Mass of Each Sample	68
Table 3.3.	Amount of Iron (III) in the FeCl ₃ Solution, FeCl ₃ Supernatant, and DFB Supernatants (pH 1.88) as a Function of Time Stirred	78
Table 3.4.	Amounts of Iron (III) in FeCl ₃ Solution, FeCl ₃ Supernatant, and DFB Supernatants.....	81
Table 3.5.	Amounts of Iron (III) in FeCl ₃ Solution, FeCl ₃ Supernatant, and DFB Supernatants.....	84

Table 3.6.	Observations and Spectral Features of Supernatants Sonicated/Shaken with Co-C Nanoparticles.....	88
Table 3.7.	Iron (III) in FeCl ₃ Solution, Supernatant, and DFB after Shaking with Co-C.....	92
Table 3.8.	Amounts of Iron (III) in FeCl ₃ Solution, FeCl ₃ Supernatant, and DFB Supernatants.....	94
Table 3.9.	Amounts of Iron (III) in FeCl ₃ Solution, FeCl ₃ Supernatant.....	96
Table 4.1.	Amounts of NaOH Added for pH Adjustments – Measuring Iron (III) in Oxalate Supernatants	106
Table 4.2.	Amounts of NaOH Added for pH Adjustments – Measuring Iron (III) in Oxalate Supernatants from Ni-SiO ₂ -FB.....	111
Table 4.3.	Amounts of NaOH Added for pH Adjustments – Measuring Iron (III) in Oxalate Supernatants from Co-SiO ₂ -DFB.....	113
Table 4.4.	Amounts of NaOH Added for pH Adjustments – Measuring Iron (III) in Oxalate Supernatants from Co-SiO ₂ -FB	114
Table 4.5.	Amount of Iron (III) in FeCl ₃ Solution Before and After Stirring with Co-C/Silica/DFB Particles	119
Table 4.6.	Atom Percent of Elements in Ni-SiO ₂ Sample.....	132
Table 4.7.	Atom Percent of Elements in TurboBeads Silica™ Sample.....	134

Table 4.8.	Atom Percent of Elements in Ni-SiO ₂ -DFB Sample.....	136
Table 4.9.	Atom Percent of Elements in Ni-SiO ₂ -FB Sample, Excluding Fe	137
Table 4.10.	Atom Percent of Elements in Co-SiO ₂ -DFB.....	139
Table 4.11.	Atom Percent of Elements in Co-SiO ₂ -FB	140
Table 4.12.	Amount of Iron (III) in FeCl ₃ Solution Before and After Stirring with Ni-SiO ₂	142
Table 4.13.	Amount of Iron (III) Adsorbed by Ni-SiO ₂ Samples.....	142
Table 4.14.	Amount of Iron (III) in FeCl ₃ Solution Before and After Stirring with Ni-SiO ₂ -DFB	143
Table 4.15.	Amount of Iron (III) Measured in FeCl ₃ , Oxalate Samples from Ni-SiO ₂ -FB Particles.....	147
Table 4.16.	Amount of Iron (III) Measured for Each Step (Removed from Particles with Oxalate or Added to Ni-SiO ₂ -FB from FeCl ₃ Solution).....	148
Table 4.17.	Amount of Iron (III) in FeCl ₃ Solution Before and After Stirring with TurboBeads Silica™	151
Table 4.18.	Amount of Iron (III) Adsorbed by TurboBeads Silica™ Samples.....	152
Table 4.19.	Amount of Iron (III) in FeCl ₃ Solution Before and After Stirring with Co-SiO ₂ -DFB, in Oxalate Washes	153

Table 4.20. Amount of Iron (III) in FeCl_3 Solution Before and After Stirring with
Co-SiO₂-FB, in Oxalate Washes..... 154

LIST OF FIGURES

Figure 1.1.	The structure of desferrioxamine B.	4
Figure 1.2.	The structure of desferrioxamine B complexed with iron (III)	5
Figure 1.3.	Summary of process to attach DFB to silica-coated silicon wafer	6
Figure 1.4.	Reaction between DFB and carboxylic acid with EDC and mechanism	7
Figure 1.5.	Infrared spectra of DFB-treated silicon wafer surface before and after reaction with iron (III)	8
Figure 1.6.	Iron (III) concentrations measured off the coast of Alaska at various depths with chemiluminescence and IR spectroscopy.....	10
Figure 1.7.	The process by which a Teflon® membrane is derivatized with PS-b-PAA	12
Figure 1.8.	A Teflon® membrane before and after exposure to water.....	13
Figure 1.9.	Process for detecting iron (III) on a DFB-treated Teflon® membrane	14
Figure 1.10.	Flow rate dependence of iron (III) captured on Teflon® membranes	15
Figure 1.11.	Thickness of membrane compared to thickness of column	18
Figure 1.12.	Process proposed to detect iron (III) using a transparent column treated with DFB.....	18
Figure 1.13.	Structure of agarose and picture of agarose beads suspended in water	18

Figure 1.14.	Steps to remove and concentrate iron (III) using magnetic particles.....	21
Figure 1.15.	Controlling the chelation of iron (III) by DFB and oxalate.....	22
Figure 1.16.	Images of TurboBeads™	23
Figure 2.1.	Scheme depicting the initial goals for the beginning of this project	29
Figure 2.2.	Structures of chemicals used for carboxylic acid derivatization	31
Figure 2.3.	Thermogravimetric plot of unmodified Co-C nanoparticles	40
Figure 2.4.	Derivative of weight with respect to temperature (weight%/°C) for the graph shown in Figure 2.3	41
Figure 2.5.	Thermogravimetric plot of NaPA-treated Co-C nanoparticles.....	42
Figure 2.6.	Derivative of weight with respect to temperature (weight%/°C) for the graph shown in Figure 2.5	43
Figure 2.7.	Thermogravimetric plot of silane-treated Co-C nanoparticles	44
Figure 2.8.	Derivative of weight with respect to temperature (weight%/°C) for the graph shown in Figure 2.7	45
Figure 2.9.	SEM image of unmodified Co-C nanoparticles.....	46
Figure 2.10.	SEM images of NaPA-treated Co-C nanoparticles	47
Figure 2.11.	SEM image of silane-treated Co-C nanoparticles.....	47
Figure 2.12.	EDX spectrum of unmodified Co-C nanoparticles.....	48
Figure 2.13.	EDX spectrum of NaPA-treated Co-C nanoparticles	48

Figure 2.14.	EDX spectrum of silane-treated Co-C nanoparticles.....	49
Figure 2.15.	ATR-IR spectra of a NaPA-treated Co-C nanoparticle sample after DFB derivatization.....	51
Figure 2.16.	ATR-IR spectra of a silane-treated Co-C nanoparticle samples after DFB derivatization.....	52
Figure 2.17.	ATR-IR spectra before and after using Method #3 for DFB derivatization on NaPA-treated Co-C nanoparticles	54
Figure 2.18.	ATR-IR spectra before and after using Method #3 for DFB derivatization on silane-treated Co-C nanoparticles.....	55
Figure 3.1.	Steps to remove and concentrate iron (III) using unmodified Co-C nanoparticles	63
Figure 3.2.	UV-Vis absorbance spectra of FeCl ₃ -containing supernatants after being stirred with Co-C nanoparticles for 3 hours	75
Figure 3.3.	UV-Vis spectra of FeCl ₃ supernatants prior to stirring with particles	77
Figure 3.4.	Sample structures of graphite and graphite oxide.....	77
Figure 3.5.	The amount of iron (III) measured in the DFB supernatant as a function of the amount of time spent stirring with the particles	79
Figure 3.6.	The amount of iron (III) measured in the DFB/NaCl supernatant as a function of the amount of time spent stirring with the particles	84

Figure 3.7.	Absorbance UV-Vis spectra of a FeCl ₃ solution with DFB added and a DFB solution used to remove iron (III) from Co-C nanoparticles.....	87
Figure 3.8.	Amount of iron (III) in DFB as a function of time shaken	93
Figure 3.9.	The amount of iron (III) measured in the DFB supernatant from Co-C nanoparticles as a function of the amount of time spent stirring with the particles.....	95
Figure 4.1.	DRIFT spectra of Co-C particles	116
Figure 4.2.	UV-Vis spectrum of the second oxalate wash of silica/DFB-treated Co-C nanoparticles.....	118
Figure 4.3.	UV-Vis spectrum of the seventh oxalate wash of silica/DFB-treated Co-C nanoparticles.....	119
Figure 4.4.	DRIFT spectra of silica- and DFB-treated Co-C nanoparticles	121
Figure 4.5.	TEM images of nickel nanoparticles.....	123
Figure 4.6.	TEM images of silica-treated nickel nanoparticles.....	124
Figure 4.7.	TEM image of a Co-C nanoparticle	125
Figure 4.8.	TEM images of TurboBeads Silica™	126
Figure 4.9.	DRIFT spectra of TurboBeads Silica™ before and after addition of anhydride silane.....	128

Figure 4.10.	DRIFT spectra of Ni-SiO ₂ before and after addition of anhydride silane	129
Figure 4.11.	DRIFT spectra of Fe ₃ O ₄ -SiO ₂ before and after addition of anhydride silane	130
Figure 4.12.	XPS spectrum of silica-treated nickel nanoparticles.....	132
Figure 4.13.	XPS spectrum of TurboBeads Silica™	134
Figure 4.14.	XPS spectrum of Ni-SiO ₂ -DFB	135
Figure 4.15.	XPS spectrum of Ni-SiO ₂ -FB.....	137
Figure 4.16.	XPS spectrum of Ni-SiO ₂ -FB, showing the small nitrogen peak at 398 eV	138
Figure 4.17.	XPS spectrum of Co-SiO ₂ -DFB.....	139
Figure 4.18.	XPS spectrum of Co-SiO ₂ -FB	140
Figure 4.19.	UV-Vis spectra of the final oxalate washes of DFB-Fe-treated Ni-SiO ₂	146
Figure 4.20.	UV-Vis spectra for Section 4.3.9.....	150
Figure 5.1.	Scheme to prevent magnetic nanoparticles' exposure to air when changing solutions	161

LIST OF EQUATIONS

Equation 2.1.....	39
Equation 2.2.....	39
Equation 2.3.....	39

LIST OF ABBREVIATIONS

ATR-IR: Attenuated Total Reflectance Infrared

Co-C: Carbon-coated magnetic cobalt nanoparticles (TurboBeads™)

Co-SiO₂-DFB: TurboBeads Silica™ treated with DFB

Co-SiO₂-FB: TurboBeads Silica™ treated with DFB-Fe

DFB: Desferrioxamine B, also known as deferoxamine

DFB-Fe: Ferrioxamine B (desferrioxamine B which is binding iron (III))

DI Water: Deionized water

DRIFT: Diffuse Reflectance Infrared Fourier Transform

EDX: Energy-Dispersive X-Ray Spectroscopy

EDC: 1-ethyl-3-(3-dimethylaminopropyl)carbodiimide, also known as *N*-(3-Dimethylaminopropyl)-*N'*-ethylcarbodiimide hydrochloride

FeCl₃: Iron (III) Chloride

Fe₃O₄: Iron (II, III) Oxide

GF-AA: Graphite Furnace Atomic Absorption

HCl: Hydrochloric Acid

HNLC: High-Nitrate, Low-Chlorophyll

ICP-MS: Inductively-Coupled Plasma Mass Spectrometry

IR: Infrared (referring to infrared spectroscopy)

KBr: Potassium Bromide

MES: 2-(N-morpholino)ethanesulfonic acid

NaCl: Sodium Chloride

NaOH: Sodium Hydroxide

NaPA: Sodium Polyacrylate

NiCl₂: Nickel (II) Chloride

Ni-SiO₂: Silica-coated nickel nanoparticles

Ni-SiO₂-DFB: Ni-SiO₂ treated with DFB

Ni-SiO₂-FB: Ni-SiO₂ treated with DFB-Fe

PS-b-PAA: Polystyrene-b-Poly(acrylic acid)

SEM: Scanning Electron Microscopy

Silane or Anhydride Silane: 3-(triethoxysilyl)propylsuccinic anhydride

TEA: Triethylamine

TEOS: Tetraethyl Orthosilicate

TGA: Thermogravimetric Analysis

TEM: Transmission Electron Microscopy

UV-Vis: Ultra-Violet-Visible spectroscopy

XPS: X-ray Photoelectron Spectroscopy

CHAPTER 1: INTRODUCTION

1.1. Motivation for Automated Iron Detection

The increase in atmospheric carbon dioxide levels has been affecting the world's climate. A major source of carbon dioxide sequestering occurs through phytoplankton growth in the world's oceans. However, in as much as 40% of the world's oceans, it has been found that the amount of phytoplankton and hence, carbon dioxide uptake is limited by the amount of dissolved iron. Some areas of the ocean, known as "high-nitrate, low-chlorophyll" (HNLC) areas, have an excess amount of the macronutrients (phosphates, nitrates, and silicates) needed for phytoplankton growth. Seeding these areas with iron has been shown to increase the amount of phytoplankton which grow there, indicating that a lack of iron is what is preventing more phytoplankton from growing.^{1,2,3}

Adding iron to HNLC areas allows more phytoplankton to grow, and in turn, to consume carbon dioxide. Thus, the amount of iron in the ocean plays a role in determining how much carbon dioxide can be taken out of the atmosphere. For this reason, it is very important to understand the distribution and role of iron in oceanic waters as well as to understand the mechanisms by which organisms extract iron from the ocean. This information would also aid in developing a better understanding of oceanic ecosystems because phytoplankton are at the base of the food chain in the ocean.

The development of models and an understanding of the role of iron in oceanic ecosystems will require a database of the spatial concentration of iron in the oceans. Currently, there is insufficient data on iron levels in the oceans because measuring iron at trace levels can be quite difficult. Concentrations can be very low – less than 1 nM – because iron is not very soluble and is constantly being consumed by phytoplankton. Additionally, some of the iron present is complexed to organic molecules rather than free in solution.¹

Contemporary methods for measuring iron at sub-nanomolar levels are primarily lab-based, though a few ship-based methods have also been developed. Common lab-based methods for measuring low concentrations of iron (III) include inductively-coupled plasma mass spectrometry (ICP-MS) and graphite furnace atomic adsorption (GF-AA). When using either of these methods for seawater analysis, the analyte must first be removed from the sample. This is because the sensitivity can be reduced by the presence of other ions in solution. This is particularly problematic when measuring iron in seawater, because other ions are present in much higher concentrations. Additionally, because these are lab-based methods, samples must be collected from the ocean and brought to a laboratory. Therefore, collection and transportation of samples is time-consuming and tedious. It is also possible to perform analysis from aboard a ship rather than in a lab.^{4,5} These methods still require user involvement, so someone must be present on a ship to analyze the samples. Ship time is expensive, and the sampling can still be tedious. Therefore, to increase the volume of data collected on iron levels throughout the world's oceans, a fully automated detection system is needed.

Furthermore, this automated system needs to be one which can be deployed on buoys and gliders in the ocean.

There have been some methods developed which can be deployed on a buoy and provide continuous iron measurements automatically. These methods use a variety of detection techniques, such as fluorescence^{6,7}, colorimetry⁸, and flow-injection analysis/spectrophotometric detection⁹. However, only one of these methods has a detection limit below 1 nM, and it cannot be used with acidified samples.⁶ Acidification is necessary for comparison with historical data. Therefore, there is still a need to develop new sensor platforms which are not only automatized but have detection limits below 1 nM and can be performed on acidified samples.

The work in this thesis was ultimately motivated by the need to develop such a sensor. The research presented herein was done to bring us one step closer to developing sufficiently sensitive iron detectors on buoys and gliders.

1.2. A Potential Basis for Automated Iron (III) Detection – Desferrioxamine B

All the work described herein, including the previous work toward the goal of developing iron (III) sensors, is based on the chemistry of desferrioxamine B. The structure of desferrioxamine B (also called deferoxamine) is shown in Figure 1.1.

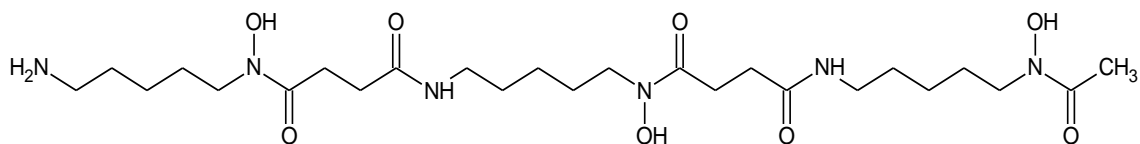


Figure 1.1. The structure of desferrioxamine B.

Desferrioxamine B (abbreviated as DFB) is known as a siderophore, meaning that it chelates iron (III). In fact, it is naturally produced by prokaryotes such as *Streptomyces pilosus* for the purpose of collecting the iron (III) needed for survival.^{10, 11} Desferoxamine chelates iron (III), forming a hexadentate structure as shown in Figure 1.2. It has a high affinity for iron (III), with a thermodynamic binding constant on the order of 10^{31} to 10^{32} . DFB does not have such high binding constants with other metals. The metal with the next-highest binding constant, copper (II), has a binding constant about 15 orders of magnitude lower than that of iron (III).^{1, 11, 12} Therefore, not only does it have a high affinity for iron (III) – it will also bind iron (III) at the exclusion of other metal ions. The high affinity is due to the fact that a hexadentate structure is formed, making a rather stable coordination complex. The selectivity is due to the fact that iron (III) is ideal for fitting into the cavity formed when DFB curls around to chelate a metal.

The fact that DFB possesses both a high affinity and selectivity for iron (III) makes it ideal for use as an iron (III) sensor. The high binding constant with iron (III) enables DFB to chelate it even at very low concentrations. Its high selectivity means that interference from other metal ions in the sample (which will always occur with sea water samples) is unlikely. Finally, DFB is commercially available and therefore easy to obtain.

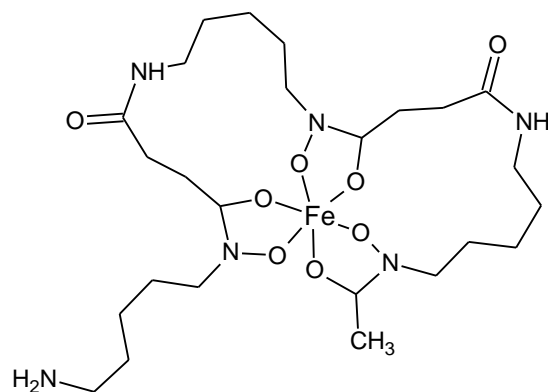


Figure 1.2. The structure of desferrioxamine B complexed with iron (III) (also known as ferrioxamine B).

1.3. Detection of Iron (III) Using Infrared Spectroscopy

One method of DFB-based iron (III) detection which has been explored was the use of infrared spectroscopy to detect DFB-Fe on a silicon wafer.¹ A silicon wafer was first treated with mesoporous silica. The silica layer was then functionalized using 3-(triethoxysilyl)propylsuccinic anhydride. Upon exposure to water, the anhydride became a dicarboxylic acid. Carboxylic acids can undergo reactions with amines in the presence of a carbodiimide to form an amide linkage. Note in Figures 1.1 and 1.2 that DFB contains an amine group which is not utilized in the chelation of iron (III). Therefore, by adding *N*-(3-Dimethylaminopropyl)-*N'*-ethylcarbodiimide hydrochloride (EDC) and DFB, DFB could be covalently linked to the wafer. More specifically, it is covalently linked via formation of an amide linkage through a reaction between the amine group in DFB with the carboxylic acid groups on the surface of the wafer. This process is summarized in Figure 1.3.

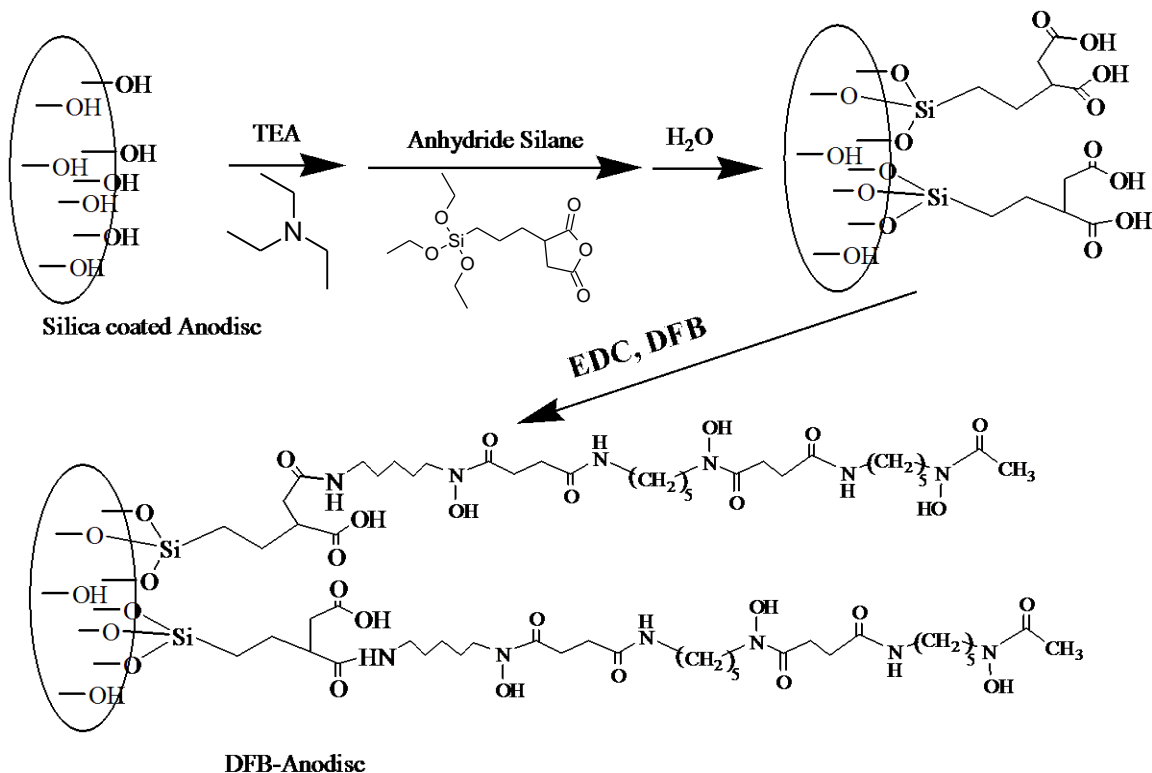
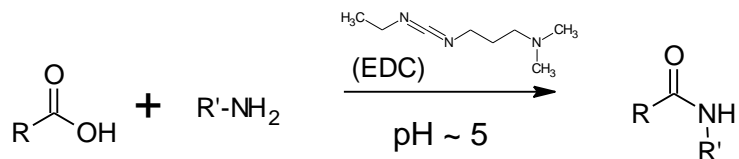


Figure 1.3. Summary of process to attach DFB to silica-coated silicon wafer. TEA stands for triethylamine, and “anhydride silane” refers to 3-(triethoxysilyl)propylsuccinic anhydride. Figure from Cuihong Jiang’s Ph.D thesis (University of Maine). Structures for TEA and anhydride silane added for clarity.

The mechanism for the general reaction between a carboxylic acid and amine with carbodiimide present is shown in Figure 1.4. The addition of EDC is necessary to ensure that the amide linkage is formed. This is because when only carboxylic acid and DFB are present, they will undergo an acid-base reaction (with the amine group on the DFB acting as a base), forming a salt.

Overall Reaction



General Mechanism

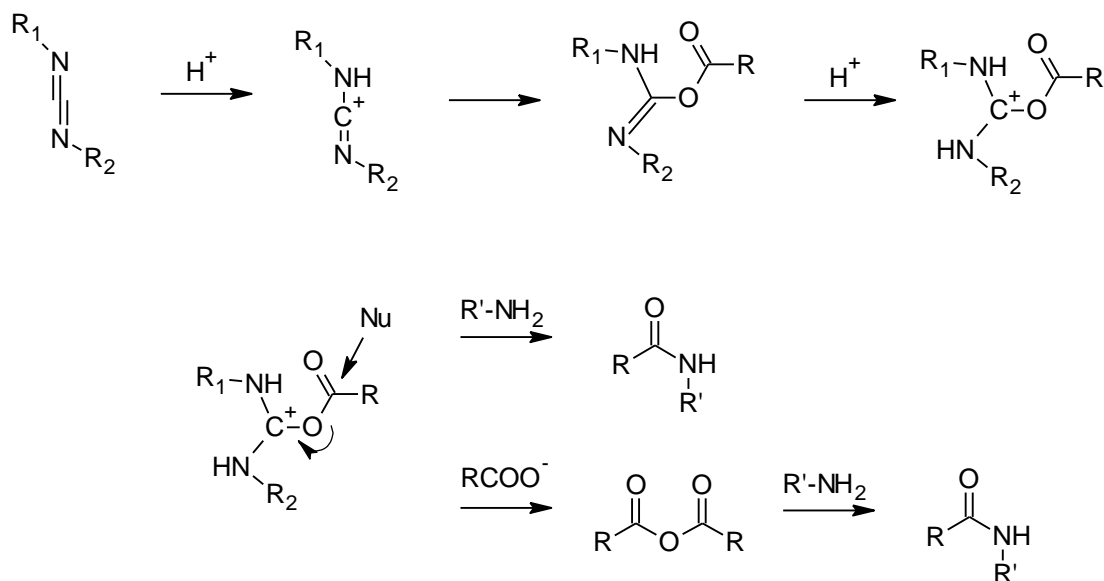


Figure 1.4. Reaction between DFB and carboxylic acid with EDC and mechanism. Adapted from mechanism stated by Nakajima and Ikada, 1995.¹³ Side reactions have been left out for simplicity.

Once the DFB was successfully attached to the surface of a silica-coated silicon wafer, it was exposed to a 1 L sample, and the DFB extracted any iron (III) in the sample. The silicon wafer was analyzed using infrared spectroscopy, using a wafer not treated with DFB as the background. Figure 1.5 shows two difference spectra – one spectrum recorded before DFB has chelated iron (III) and the second one recorded after it has done so. When DFB has chelated iron (III), a band appears at 560 cm^{-1} , which is due to a Fe-O stretching mode. This band is not present in the spectrum of DFB without iron (III).

The intensity of the band was proportional to the amount of iron (III) present, so it was used to quantify iron (III).¹

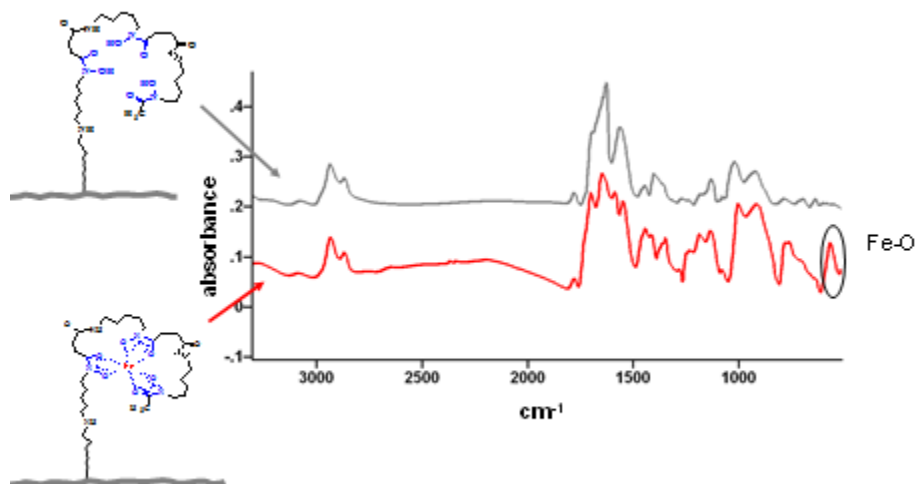


Figure 1.5. Infrared spectra of DFB-treated silicon wafer surface before and after reaction with iron (III). The top spectrum is of the wafer before the reaction while the bottom spectrum is of the wafer after the reaction. A reference spectrum was recorded through an unmodified silica-coated wafer.¹

It was found that the presence of other metal cations in a sample did not interfere with the ability of this method to measure iron (III). Iron-containing colloids and organic compounds did not interfere with the Fe-O peak either. It was also determined that this method can be used with samples which have been acidified to pH 1.8. This is necessary for comparison to historical measurements. Ocean samples have, in the past, been acidified to free any iron complexed to organic ligands in the ocean. Acidification also prevents the formation of iron hydroxides, which occurs naturally in iron solutions of higher pH.

Additionally, the infrared-based detection method was field-tested off the coast of Alaska. The concentrations of iron (III) were measured at various depths in the ocean with the infrared detection method and by flow-injection analysis with chemiluminescence. As shown in Figure 1.6, the error bars for the values obtained in each method overlap, meaning that the two measurements are not significantly different. In other words, the infrared detection method was in agreement with a more well-established chemiluminescence method.¹

Despite the advantages of the infrared detection method, it is still restricted to use on a ship. This is primarily due to the fact that water absorbs very strongly in the infrared region. This means that wafers must be dried before measurements can be taken, to avoid the interference of water with the detection of other bands. Another disadvantage is that the wafer was stirred in the sample for 24 hours to ensure complete mass transport of iron (III). Neither drying nor long stirring times are practical for deployment on buoys and gliders.

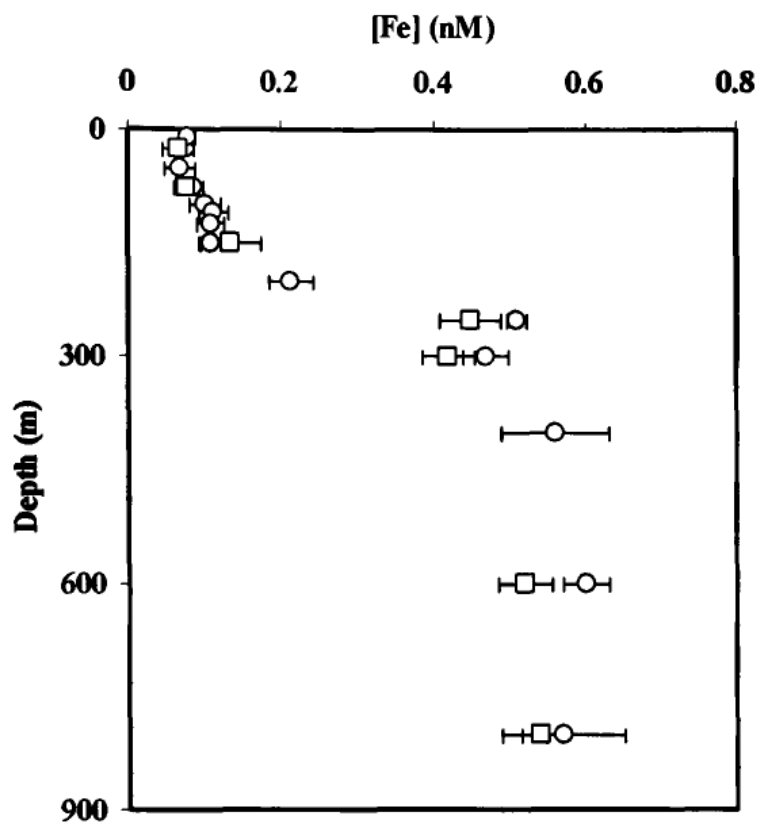


Figure 1.6. Iron (III) concentrations measured off the coast of Alaska at various depths with chemiluminescence and IR spectroscopy. The circles represent chemiluminescence measurements while the squares represent measurements with the newly-developed infrared detection method. Data points represent mean measurements with three replicates; the error bars represent ± 1 standard deviation.¹

1.4. Capture of Iron (III) on Transparent Membrane and Detection with UV-Vis Spectroscopy

Subsequent work in iron (III) detection systems using DFB focused on a different method which would not require drying nor become limited by mass transport. This work was begun by Zachary Helm for his M.S. thesis. Instead of attaching DFB to a silicon wafer, a Teflon[®] membrane was used. The membrane is capable of withstanding flow rates of up to 10 mL/min, allowing a water sample to be flowed through it. But to

accommodate these flow rates, the pores have to be large, meaning that the membranes have a low surface area.¹⁴

To compensate for the low surface area, the membranes were treated with a block copolymer of polystyrene-b-poly(acrylic acid) (PS-b-PAA). Treatment simply involved exposing the membranes to a solution of PS-b-PAA in water. Because the PS block is hydrophobic, it is not particularly soluble in water. The PAA block is hydrophilic and therefore this block extends out from the surface into the water. Initially, the polymers lie flat on the surface, but as the surface becomes more crowded, they will arrange to accommodate additional polymers which adsorb from the solution phase. Eventually, the polymers adopt a “brush-like” configuration, where the PAA extends from the surface into solution.^{14, 15} This process is illustrated in Figure 1.7.

Once the surface of the membrane has been treated with PS-b-PAA, one can use the reaction between DFB/EDC and a carboxylic acid (see Figure 1.4)¹³ to covalently attach DFB to the acrylic acid units of the PAA. The PAA units are long chains extending from the surface, which increases the number of binding sites for DFB. This is known as vertical amplification, and it helps account for the low surface area of the original membranes.¹⁴

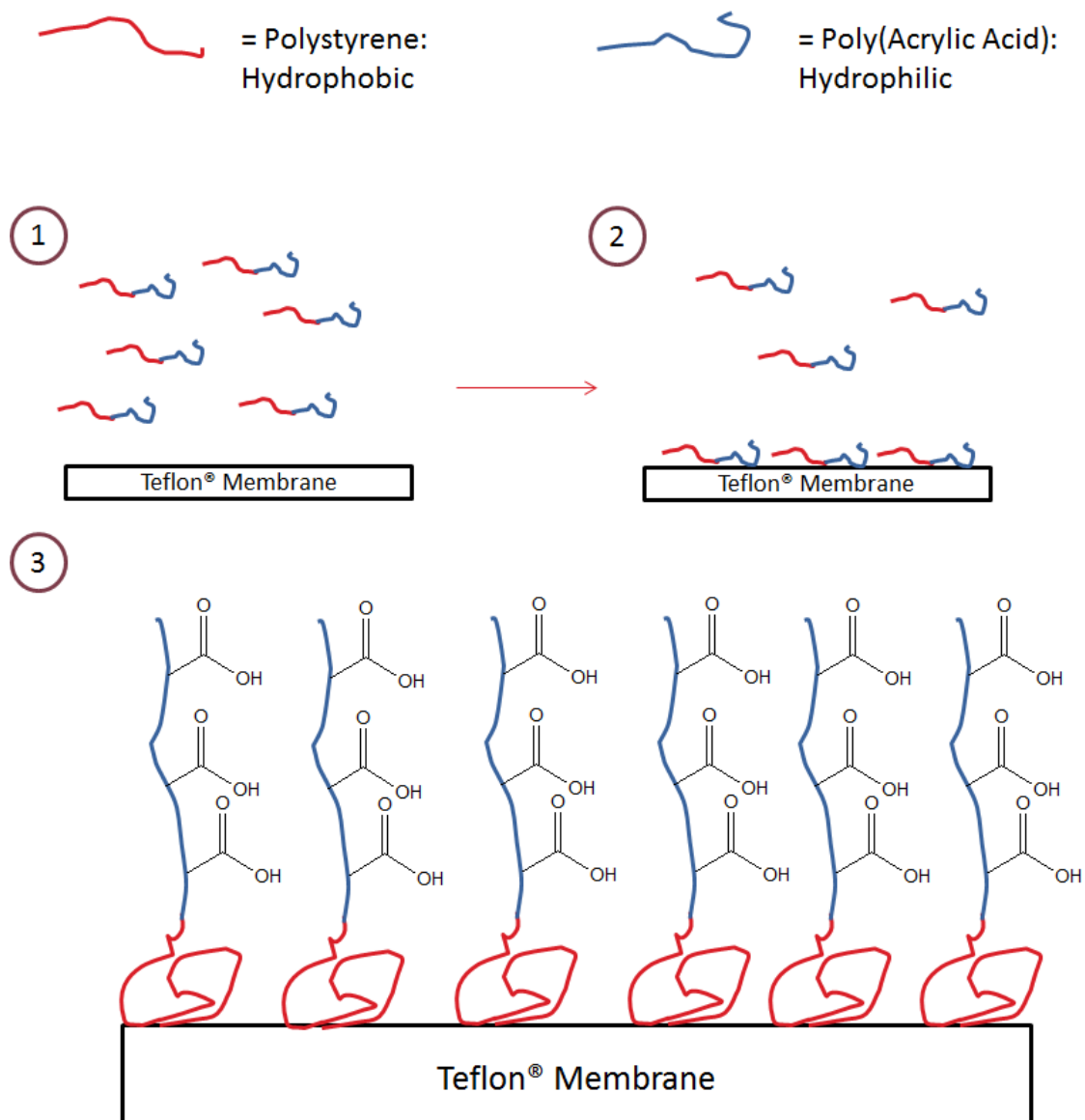


Figure 1.7. The process by which a Teflon® membrane is derivatized with PS-b-PAA. The red lines are PS blocks and the blue lines are PAA blocks. 1) PS-b-PAA in solution near a Teflon® membrane. 2) Some PS-b-PAA adsorbed, flat, onto the membrane surface. 3) The block copolymers have adsorbed, with the PS blocks attached to the surface and PAA blocks extending out into solution. The carboxylic acid functional groups of the PAA are shown.

Thus, one can mitigate the problem of mass transport by flowing sample through a membrane. However, infrared spectroscopy is still sensitive to the presence of water.

Therefore, another detection technique is needed which is not sensitive to the presence

of water. Ultra-Violet-Visible spectroscopy (UV-Vis) is an attractive option, as it is often used for aqueous samples. The membranes are opaque when dry, which may at first appear to be problematic for using UV-Vis to measure the surface. However, the membranes become transparent when wetted by water (see Figure 1.8). This is due to the fact that the membranes have a refractive index similar to that of water and that the surface is hydrophilic, meaning it can be completely wetted by water. This means that when water fills the porous network of the membrane, there is one continuous phase of similar refractive index. Therefore, as long as the membranes are wet, they are amenable to analysis by transmission UV-Vis. The detection process is illustrated in Figure 1.9.

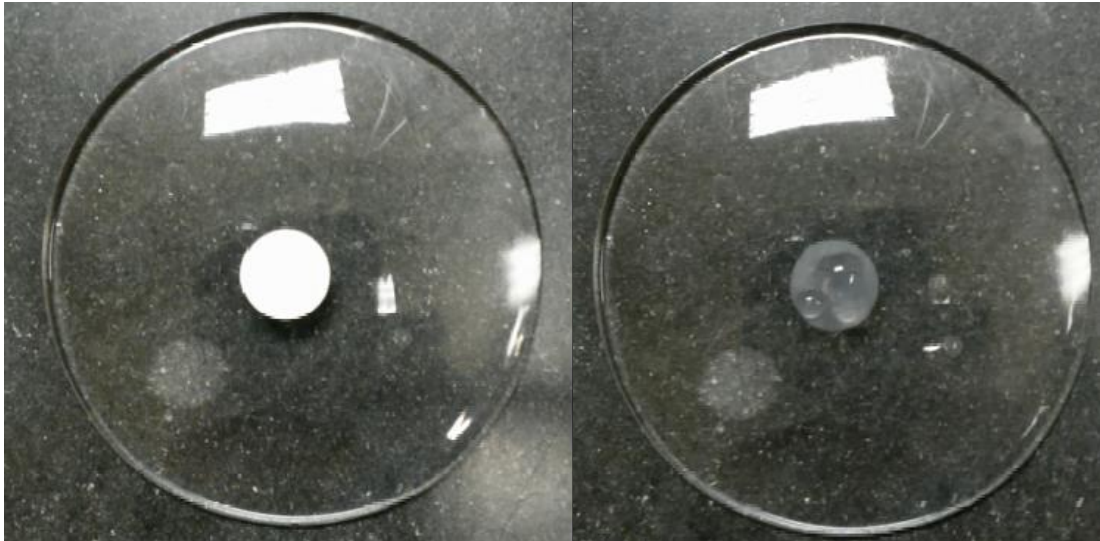


Figure 1.8. A Teflon® membrane before and after exposure to water. The left image shows a membrane before its exposure to water while the right image shows the same membrane after exposure to water. Some water droplets can be seen on the membrane exposed to water.

The DFB-Fe complex is a deep red color with a broad absorbance band between 430 and 470 nm. No such band is observed when a solution containing iron (III) is passed through a membrane which has not been derivatized with DFB. Since the intensity of this peak is proportional to the amount of iron (III) present on the membrane, the absorbance at 470 nm provides a measure of the amount of iron (III) present.¹⁴

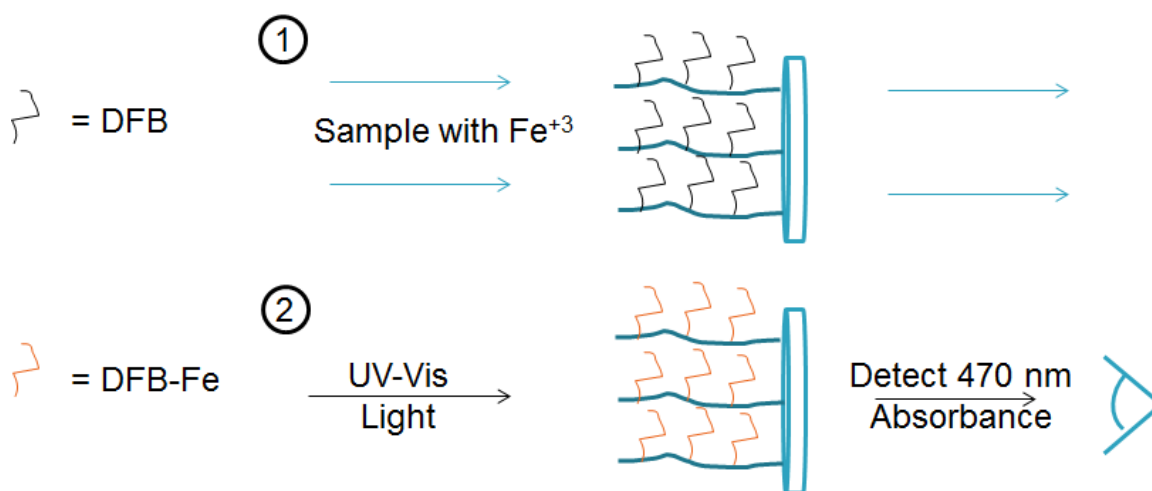


Figure 1.9. Process for detecting iron (III) on a DFB-treated Teflon[®] membrane. 1) A sample which contains iron (III) is flowed through a Teflon[®] membrane which has been treated with DFB. The DFB captures the iron (III). 2) The Teflon[®] membrane now has DFB-Fe on the surface. DFB-Fe absorbs light at 470 nm, which can be detected with UV-Vis spectroscopy.

Helm found that the membranes were able to extract iron (III) from both fresh water and sea water samples. The iron (III) uptake was more efficient at higher pH – for instance, when increasing the pH from 9 to 9.3, the rate constant for DFB-Fe complexation increased from 1.65 to 6.87 M⁻¹s⁻¹. The amount of iron (III) which could be captured also increased as the flow rate was decreased, as shown in Figure 1.10. It was suspected that this was due to increased contact time, which allowed more time for DFB to capture the iron (III). The detection limit for a 5 mL sample was found to be 0.24 nM

at a pH of 2 and a flow rate of 0.1 mL/min. However, this is not sufficiently low to measure iron (III) in all parts of the ocean, because the iron (III) concentrations can be as low as 30 pM.¹⁴ This means that in order to use this system to measure oceanic iron (III), the detection limit would first have to be improved.

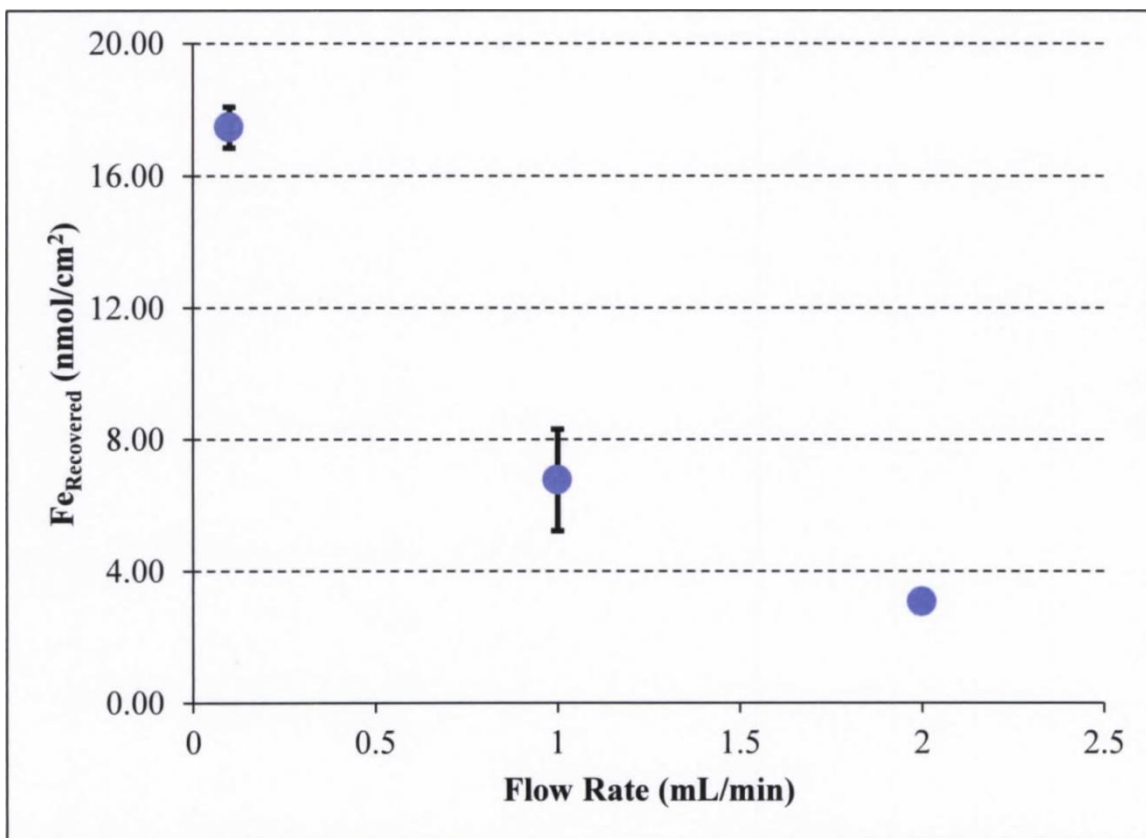


Figure 1.10. Flow rate dependence of iron (III) captured on Teflon[®] membranes. This shows the amount of iron (III) captured by a DFB-treated Teflon[®] membrane at varying flow rates.¹⁴

Madhira Gammana followed up Helm's work as part of her Ph.D thesis.¹⁶ In this work, membranes treated with PS-b-PAA were reacted with varying amounts of DFB. More specifically, she compared membranes fully reacted with DFB and membranes where only 50% of the reactive sites were bound with DFB. She found that membranes

with half the amount of DFB on the surface were able to capture more iron (III) and at a faster rate than their fully-bound counterparts. In other words, the membranes less densely-packed with DFB were better able to take up iron (III). It was suspected that this was because although more DFB was present on the fully-bound membranes, the denser packing interfered with some of the DFB molecules' ability to bind iron (III). As shown in Figure 1.2, the DFB must wrap around the iron (III) in order to capture it. If the DFB is densely-packed enough, there may be steric hindrance preventing DFB from forming that curled structure.

Further follow-up work was done by Silas Owusu-Nkwantabisah in his Ph.D thesis.¹⁷ When reacting DFB with a PS-b-PAA-treated membrane, he used DFB bound to iron (III), an approach called molecular imprinting. The iron (III) was then removed from the DFB by washing the membrane with 0.1 M oxalate at pH 1.5. It was found that when using DFB-Fe, the carboxylic acid on the surface only partially reacted with the DFB. What percentage of the carboxylic acid groups reacted depended on the length of the PAA block used, but in all cases, less than half of the acrylic acid groups on the surface actually reacted with the DFB. Additionally, it was found that for DFB-derivatized membranes prepared in this manner, the amount of iron (III) which could be recovered from solution was not flow-rate dependent. Nonetheless, not all of the iron (III) could be captured from solution, possibly due to a limitation from contact time.

Thus, two problems still remained: an insufficiently low detection limit and flow rate dependence in the uptake of iron (III) by the membrane. In order to improve the

detection limit, one needs to concentrate as much iron (III) into the path of the detection beam as possible. In this author's B.S. thesis work, the amount of iron (III) needed in the beam to produce a DFB-Fe absorbance of 0.02 was calculated. The result was that to produce an absorbance of 0.02 in a 1 cm cuvette with a 3 mm UV-Vis beam, there needed to be 36 ng of iron (III). This translates to $4.5 \times 10^{-7} \text{ g/cm}^3$ in general.¹⁸

1.5. Capture of Iron (III) on Transparent Column and Detection with UV-Vis Spectroscopy

Based on the work done by Helm, it seemed to be necessary to use very slow flow rates – around 0.1 mL/min – to get iron (III) capture greater than 90% out of a sample.¹⁴ Passing 1 L of sample at such a slow flow rate would be impractical. It was thought that increasing the contact time with a DFB-treated surface would allow for greater capture rates. Rather than decreasing the flow rate, it was thought that a column could be used in place of a membrane, as illustrated in Figures 1.11 and 1.12. This membrane would have to be made of a transparent material so that measurements could be taken directly on the column, as with the work done with the membranes. Still, a sample flowed through a column would have a longer contact time with the column surface than with a membrane experiencing an equivalent flow rate. It was thought that this would allow for higher iron (III) capture rates without the need to decrease the flow rate.^{16, 18}

This author's B.S. work strove to develop a transparent, DFB-treated column which could be used to capture iron (III) from a sample. Agarose beads were selected as

the column material. Because they have a refractive index close to that of water (1.333 to 1.337)¹⁹, they are somewhat transparent in water. The structure of agarose and a suspension of agarose beads in water are shown in Figure 1.13.

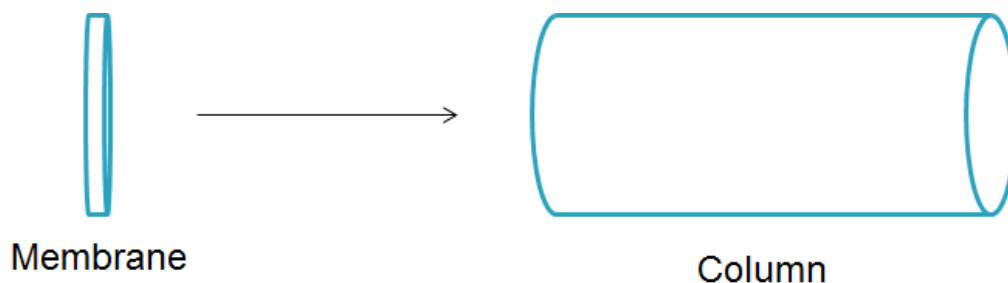


Figure 1.11. Thickness of membrane compared to thickness of column. A sample will take longer to flow through a column than it would through a membrane, increasing contact time with the surface.

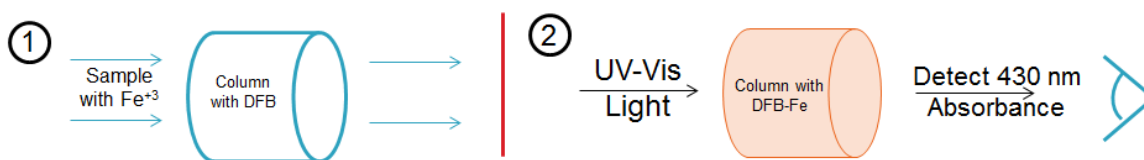


Figure 1.12. Process proposed to detect iron (III) using a transparent column treated with DFB. 1) A sample which contains iron (III) is flowed through a transparent column which has been treated with DFB. The DFB captures the iron (III). 2) The transparent column now has DFB-Fe on the surface. DFB-Fe absorbs light at 430 nm, which can be detected with UV-Vis spectroscopy.

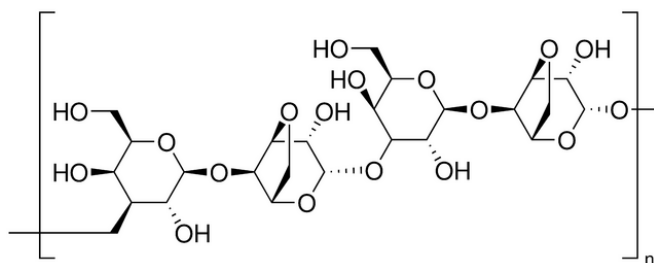


Figure 1.13. Structure of agarose and picture of agarose beads suspended in water. The former is on the left while the latter is on the right.

As was done to the membranes, the agarose beads were first treated with PS-b-PAA. The acrylic acid groups of the PAA were then reacted with DFB to produce an amide linkage. Derivatization with DFB was successful, and these derivatized beads were able to capture iron (III), which could then be measured on a suspension of the particles. However, even at the maximum amount of iron (III) which could be captured by the beads, the DFB-Fe absorbance was only 0.016. Furthermore, due to the beads' movement in the water, there were many fluctuations in the baseline. For this reason, it was determined that this system would be difficult to automate.¹⁸

1.6. Capture of Iron (III) with Magnetic Particles and Subsequent Concentration for In-Solution Detection

The simplest way to measure iron (III) is to add DFB to a solution containing iron (III) and then take a UV-Vis spectrum to determine the concentration of DFB-Fe. The reason this method cannot directly be used to measure iron (III) in the ocean is due to the low concentration – even though DFB would capture the iron (III), the concentration of the resulting complex would be too small to measure effectively with UV-Vis. However, if one were able to concentrate the iron (III) from a sample, and then add DFB to the concentrated solution, it may in fact be possible to detect the resulting DFB-Fe complex.

In this author's B.S. work, iron (III) was captured on agarose beads derivatized with DFB by stirring the beads in an iron (III) solution in a beaker. The beads were somewhat difficult to capture from solution afterward.¹⁸ However, this problem could

be circumvented by using magnetic beads. Adapting the iron (III) capture onto magnetic particles is the focus of the work presented in this thesis. First, magnetic particles would be treated with DFB. Then, the beads could be stirred in a water sample, the DFB on the surface capturing any iron (III) present. Once all the iron (III) is captured, the particles can be drawn to a magnet, allowing for the remaining water in the sample to be removed. The complete process is outlined step-by-step in Figure 1.14.

To remove iron from the DFB on the particles, one can stir them in a solution of oxalate at pH 1.5. As determined in Helm's M.S. work, oxalate has a higher affinity for iron (III) than DFB at this pH.¹⁴ Therefore, using a smaller volume of pH 1.5 oxalate than the original sample volume, the iron (III) can be removed from the beads. Because a smaller volume was used, the iron (III) will now be concentrated. By adding DFB to the concentrated iron (III)/oxalate solution and raising the pH to around 8 (where DFB has the higher affinity for iron¹⁴), one will concentrate the iron (III) and form a detectable DFB-Fe complex. The chemistry upon which this process is based is illustrated in Figure 1.15.

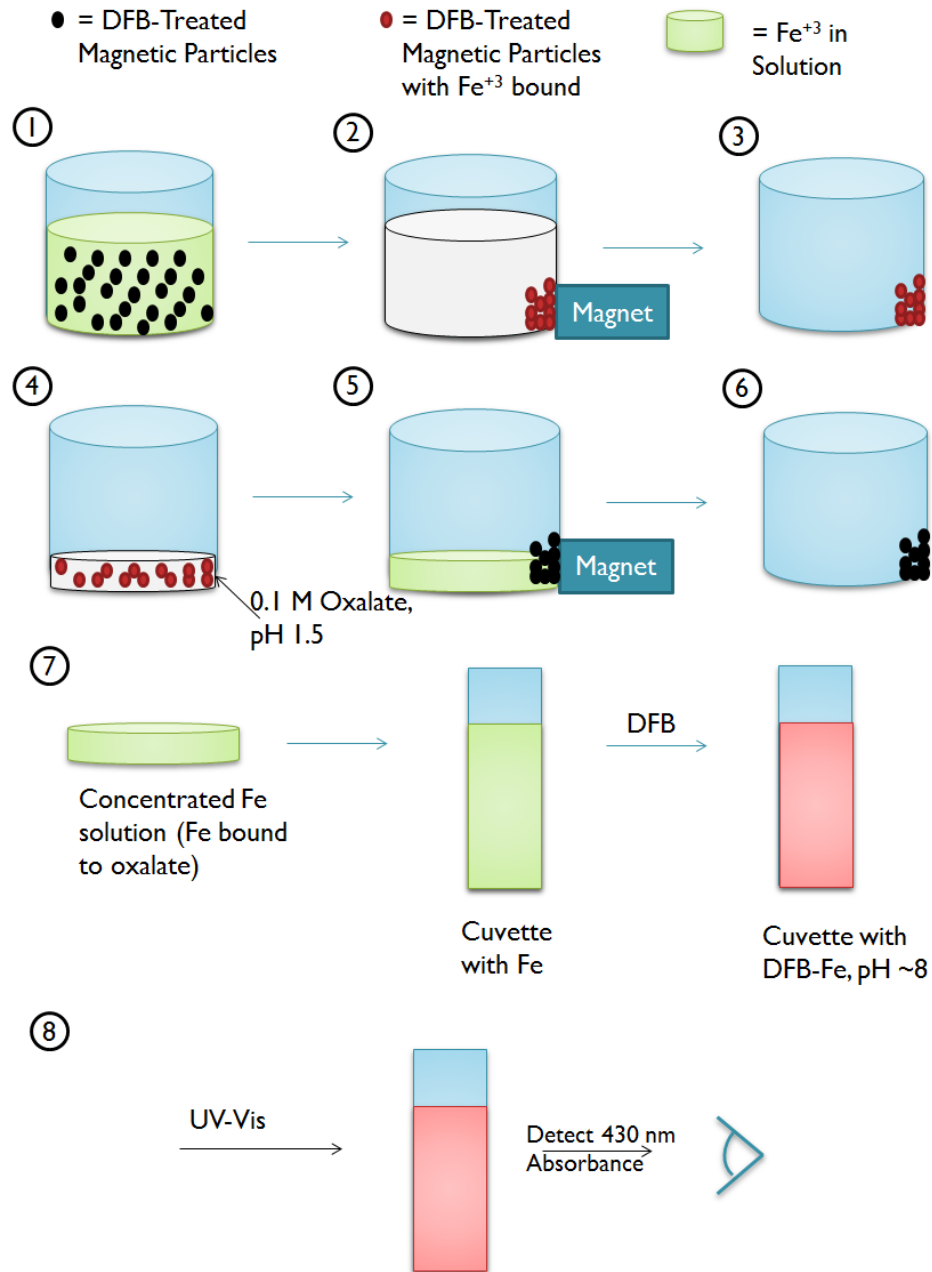


Figure 1.14. Steps to remove and concentrate iron (III) using magnetic particles. 1) DFB-treated magnetic particles are dispersed in solution. 2) DFB on particles takes iron out of solution and particles are drawn to a magnet. 3) Supernatant is removed. 4) Smaller volume of 0.1 M oxalate (pH 1.5) than that of the original solution is added. 5) Oxalate removes iron from DFB on particles. 6) Supernatant, now containing oxalate chelating iron, is removed. 7) Supernatant from step 6 is added to a cuvette; DFB is added and the pH is adjusted to around 8, causing the DFB to chelate the iron. 8) UV-Vis spectrum is taken to measure DFB-Fe absorbance of solution from step 7.

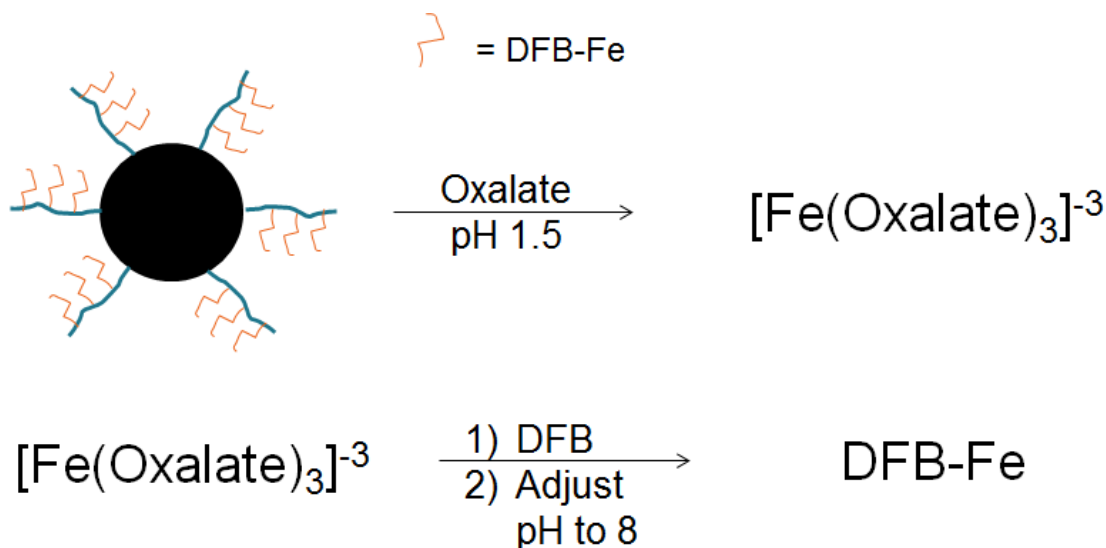


Figure 1.15. Controlling the chelation of iron (III) by DFB and oxalate. a) A particle derivatized with DFB has captured iron (III). A solution of oxalate at pH 1.5 is added, removing the iron (III) from the DFB on the particles. b) The oxalate solution, now containing iron (III), is mixed with DFB solution. The pH of the oxalate/DFB solution is raised to 8, causing DFB to chelate the iron (III).

Many magnetic particles are made of iron or iron oxides. However, due to concerns that some of the iron could leak out into solution, thereby providing false readings of iron (III), it was necessary to avoid using those for this work. Therefore, this work primarily focuses on the use of carbon-coated magnetic cobalt particles known as TurboBeads™ (Co-C), pictured in Figure 1.16. TurboBeads™ are about 50 nm in diameter, and the carbon coating prevents oxidation of the cobalt. They were developed for the purpose of derivatization for the use of capturing particular elements and molecules from solution.²⁰ For this reason, they appeared to be an ideal choice for this project. They can also be purchased with a variety of functional groups already on the surface.

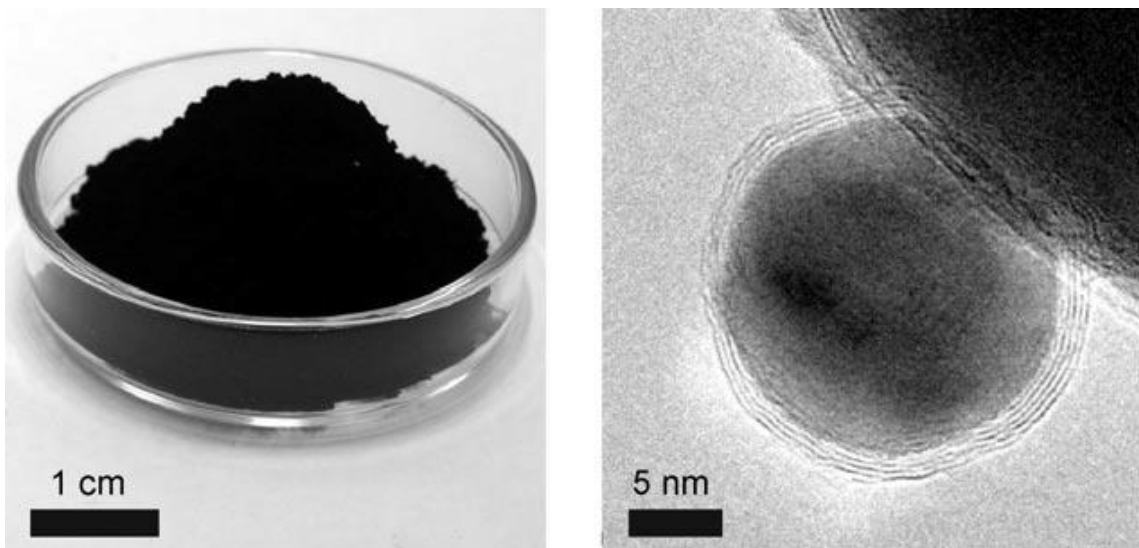


Figure 1.16. Images of TurboBeads™. Left: Macroscopic photograph of TurboBeads™. Right: TEM image of TurboBeads™ showing the graphene layers on the surface.

The research described herein was done in an attempt to develop a method of concentrating iron (III) from a sample using functionalized magnetic particles. The bulk of this work was performed on carbon-coated cobalt (TurboBeads™, Co-C). The first goal was to treat the surface of these particles with DFB. The next goal was to use the derivatized particles to take iron (III) out of a sample solution. The final goal was to remove the iron (III) from the particles into another solution with a smaller volume than the original sample. By decreasing the volume in which the iron (III) is dissolved, a more concentrated iron (III) solution would be obtained.

In the process of performing this research, it was discovered that untreated TurboBeads™ will take iron (III) from solution; therefore, some work was done to explore the possibility of taking advantage of this characteristic. Finally, due to the limited success of concentrating and measuring iron (III) using TurboBeads™, the

possibility of using other magnetic nanoparticles for this concept was also explored. More specifically, this concept was applied to nickel nanoparticles and TurboBeads Silica™ (TurboBeads™ which have been coated in silica).

1.7. References

1. Roy, E. G.; Jiang, C. H.; Wells, M. L.; Tripp, C., Determining Subnanomolar Iron Concentrations in Oceanic Seawater Using a Siderophore-Modified Film Analyzed by Infrared Spectroscopy. *Analytical Chemistry* **2008**, *80* (12), 4689-4695.
2. Martin, J. H.; Fitzwater, S. E., Iron-Deficiency Limits Phytoplankton Growth in the Northeast Pacific Subarctic. *Nature* **1988**, *331* (6154), 341-343.
3. Martin, J. H.; Coale, K. H.; Johnson, K. S.; Fitzwater, S. E.; Gordon, R. M.; Tanner, S. J.; Hunter, C. N.; Elrod, V. A.; Nowicki, J. L.; Coley, T. L.; Barber, R. T.; Lindley, S.; Watson, A. J.; Vanscoy, K.; Law, C. S.; Liddicoat, M. I.; Ling, R.; Stanton, T.; Stockel, J.; Collins, C.; Anderson, A.; Bidigare, R.; Ondrusek, M.; Latasa, M.; Millero, F. J.; Lee, K.; Yao, W.; Zhang, J. Z.; Friederich, G.; Sakamoto, C.; Chavez, F.; Buck, K.; Kolber, Z.; Greene, R.; Falkowski, P.; Chisholm, S. W.; Hoge, F.; Swift, R.; Yungel, J.; Turner, S.; Nightingale, P.; Hatton, A.; Liss, P.; Tindale, N. W., Testing the Iron Hypothesis in Ecosystems of the Equatorial Pacific-Ocean. *Nature* **1994**, *371* (6493), 123-129.

4. Lohan, M. C.; Aguilar-Islas, A. M.; Bruland, K. W., Direct Determination of Iron in Acidified (pH 1.7) Seawater Samples by Flow Injection Analysis with Catalytic Spectrophotometric Detection: Application and Intercomparison. *Limnology and Oceanography-Methods* **2006**, *4*, 164-171.
5. King, D. W.; Lounsbury, H. A.; Millero, F. J., Rates and Mechanism of Fe(II) Oxidation at Nanomolar Total Iron Concentrations. *Environmental Science & Technology* **1995**, *29* (3), 818-824.
6. Lam, C.; Jickells, T. D.; Richardson, D. J.; Russell, D. A., Fluorescence-Based Siderophore Biosensor for the Determination of Bioavailable Iron in Oceanic Waters. *Analytical Chemistry* **2006**, *78* (14), 5040-5045.
7. Barrero, J. M.; Camara, C.; Perezconde, M. C.; Sanjose, C.; Fernandez, L., Pyoverdine-Doped Sol-Gel Glass for the Spectrofluorometric Determination of Iron(III). *Analyst* **1995**, *120* (2), 431-435.
8. Chapin, T. P.; Jannasch, H. W.; Johnson, K. S., In Situ Osmotic Analyzer for the Year-Long Continuous Determination Of Fe in Hydrothermal Systems. *Analytica Chimica Acta* **2002**, *463* (2), 265-274.

9. Laes, A.; Vuillemin, R.; Leilde, B.; Sarthou, G.; Bournot-Marec, C.; Blain, S., Impact of Environmental Factors on In Situ Determination of Iron in Seawater by Flow Injection Analysis. *Marine Chemistry* **2005**, *97* (3-4), 347-356.
10. Keberle, H., The Biochemistry of Desferrioxamine and its Relation to Iron Metabolism. *Annals of the New York Academy of Sciences* **1964**, *119*, 758 - 768.
11. Hernlem, B. J.; Vane, L. M.; Sayles, G. D., Stability Constants for Complexes of the Siderophore Desferrioxamine B with Selected Heavy Metal Cations. *Inorganica Chimica Acta* **1996**, *244* (2), 179-184.
12. Martel, A. E.; Smith, R. M., *Critical Stability Constants*. Plenum Press: New York 1982; Witter, A. E.; Hutchins, D. A.; Butler, A.; Luther, G. W., Determination of Conditional Stability Constants and Kinetic Constants for Strong Model Fe-Binding Ligands in Seawater. *Marine Chemistry* **2000**, *69* (1-2), 1-17.
13. Nakajima, N.; Ikada, Y., Mechanism of Amide Formation by Carbodiimide for Bioconjugation in Aqueous-Media. *Bioconjugate Chemistry* **1995**, *6* (1), 123-130.
14. Helm, Z. Determining Oceanic Iron Concentrations Using a Siderophore Based Sensor. University of Maine, 2013, M.S. Thesis.

15. Tripp, C. P.; Hair, M. L., Kinetics of the Adsorption of a Polystyrene-Poly(Ethylene Oxide) Block Copolymer on Silica: A Study of the Time Dependence in Surface/Segment Interactions. *Langmuir* **1996**, *12* (16), 3952-3956.
16. Gammana, M. A UV-Vis. Spectroscopic Based Method for Iron Detection in Aqueous Solutions by Using DFB Tethered to Membranes. University of Maine, 2014, Ph.D Thesis.
17. Owusu-Nkwantabisah, S. Polymer Adsorption on Solid Surfaces: Layer-by-Layer Studies and Development of an Iron (III) Sensor. University of Maine, 2014, Ph.D Thesis.
18. Hansen, K. Detection of Iron (III) Using Agarose Beads Derivatized with Desferrioxamine B. University of Maine, 2014, B.S. Thesis.
19. Byron, M. L.; Variano, E. A., Refractive-Index-Matched Hydrogel Materials for Measuring Flow-Structure Interactions. *Experiments in Fluids* **2013**, *54* (2), 6;
Gupta, R.; Bastani, B.; Goddard, N. J.; Grieve, B., Absorption Spectroscopy in Microfluidic Flow Cells Using a Metal Clad Leaky Waveguide Device With a Porous Gel Waveguide Layer. *Analyst* **2013**, *138* (1), 307-314.

20. Grass, R. N.; Athanassiou, E. K.; Stark, W. J., Covalently Functionalized Cobalt Nanoparticles as a Platform for Magnetic Separations in Organic Synthesis. *Angewandte Chemie-International Edition* **2007**, *46* (26), 4909-4912.

CHAPTER 2: INITIAL WORK

2.1. Introduction

As outlined in Chapter 1, DFB can be attached by reaction of its amine group to a surface containing carboxylic acid groups through the formation of an amide linkage. This section details the initial work done toward the derivatization of carbon-coated cobalt nanoparticles (Co-C) with carboxylic acids and the subsequent derivatization with DFB. The original goal was to be able to perform the procedures outlined in Figure 2.1.

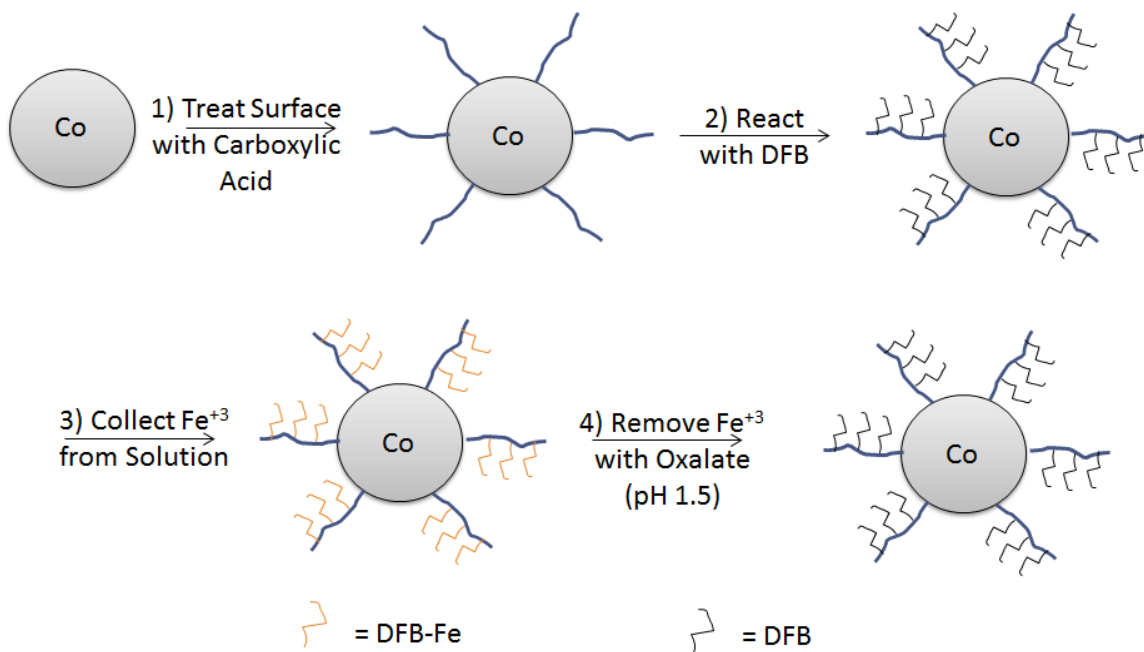


Figure 2.1. Scheme depicting the initial goals for the beginning of this project. 1) Treat the surface of Co-C particles with a carboxylic acid. 2) React the carboxylic acid groups on the surface of the particles with DFB. 3) Use the DFB-treated particles to collect iron (III) from a solution. 4) Use oxalate at a pH of 1.5 to remove the iron (III) from the particles.

Two methods of derivatizing the surface with carboxylic acid groups were attempted. The first was the adsorption of sodium polyacrylate (NaPA) onto the surface. The structure of NaPA is shown in Figure 2.2. As with block copolymers¹, NaPA adsorbs on a nanoparticle surface from a solution due to its relatively low solubility in water. NaPA was used in place of the block copolymers in this work for a couple reasons. First, it is easier and cheaper to obtain than PS-b-PAA. Second, the NaPA is available as a 60,000 molecular weight polymer, so it has an average of 833 acrylic acid units per polymer chain. This is far more carboxylic acid units per polymer chain than the PS-b-PAA, which has an average of 180 units per polymer chain. The adsorbed amount of a homopolymer such as NaPA on surfaces (approximately 5 mg/m²) is about the same as, if not more than, that of a block copolymer.² Therefore, it was thought that with the higher molecular weight NaPA, there would be more carboxylic acid groups on the surface and therefore, more DFB could be added to the surface.

The second method involved the polymerization of 3-(triethoxysilyl)propylsuccinic anhydride (“silane”) around the particles. The structure of this molecule is shown in Figure 2.2. Trialkoxysilanes are known to polymerize with water³, and though water was not explicitly added to the reaction vessel, the silane reacts with the surface water to form a coating on the particle.

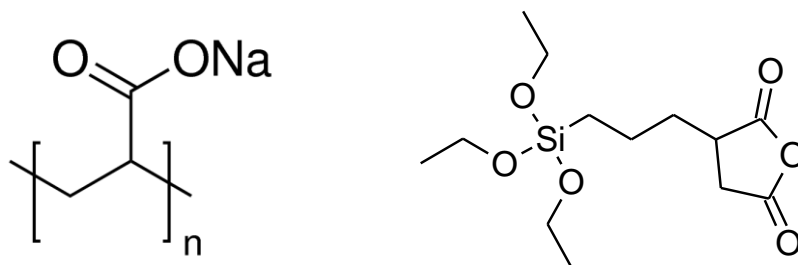


Figure 2.2. Structures of chemicals used for carboxylic acid derivatization. Left: sodium polyacrylate (image from Sigma Aldrich). Right: 3-(triethoxysilyl)propylsuccinic anhydride.

2.2. Experimental

2.2.1. Materials

The following materials were obtained from Sigma-Aldrich: <50 nm carbon-coated magnetic cobalt nanopowder (Co-C), deferoxamine mesylate salt (DFB), iron (III) chloride (FeCl_3), and 1-ethyl-3-(3-dimethylaminopropyl)carbodiimide (EDC). Sodium hydroxide and hydrochloric acid were purchased from Fisher. The sodium polyacrylate with MW 60,000 (NaPA) was purchased from Polysciences as a 35% solution, while the 3-(triethoxysilyl)propylsuccinic anhydride (“silane”) was from Gelest, Inc.

An iron-free 0.1 M oxalate solution was provided by Dr. Mark Wells. The iron-free 0.1 M oxalate solution was prepared by flowing it through a Toyopearl column derivatized with DFB. The pH was adjusted as necessary using dilute sodium hydroxide and hydrochloric acid solutions.

The 35% NaPA solution was first diluted to a 3500 ppm solution by diluting 1 mL of 35% NaPA to 100 mL with DI water. The 3500 ppm solution was then further diluted

to make a 700 ppm solution using 1 part 3500 ppm NaPA to 4 parts DI water. The exact volumes prepared depended on how much 700 ppm solution was needed.

The FeCl_3 was received as a powder. To make a 1 mM solution of FeCl_3 , the solid material was dissolved in DI water (16.2 mg per 100 mL). The pH was adjusted to 2.5 – 2.8 with concentrated HCl to prevent the formation of iron hydroxides in solution. Solutions older than 1 week were discarded.

All other materials listed above were used as received. The DFB and EDC were stored at $-50\text{ }^\circ\text{C}$ when not in use.

All UV-Vis spectra were recorded on an Ocean Optics USB 2000 UV-Vis spectrometer with SpectraSuite software. Attenuated total reflectance infrared spectra (ATR-IR) were taken using an Alpha-P Bruker spectrometer at a resolution of 4 cm^{-1} . Mass was recorded on a Mettler Toledo AG245 analytical balance. Thermogravimetric analysis was performed using a TGA Q500. SEM and EDX measurements were performed using a Zeiss NVision 40 system. Mechanical shaking was performed using a Vibramax 100 from Heidolph.

2.2.2. Washing Particles

Washing was performed by adding the desired solvent (usually DI water unless otherwise noted), mixing for approximately 2 seconds, drawing the particles to the side of the container using an external magnet, and then decanting the wash liquid or extracting the liquid with a pipette.

2.2.3. Treatment of Co-C with Sodium Polyacrylate (NaPA)

A 700 ppm NaPA solution was prepared as described in Section 2.2.1. The pH of the NaPA solution was adjusted to 3. Next, 20 mL of this solution was added to 50 mg Co-C particles. This suspension was sonicated for 1 hour, then mechanically shaken at 450 rpm with a Vibramax 100 for periods ranging from 11 to 24 hours. The particles were then washed 3 times with DI water.

2.2.4. Treatment of Co-C with 3-(triethoxysilyl)propylsuccinic Anhydride (Silane)

Approximately 50 mg Co-C particles were added to 85 mL toluene in a 125-mL Erlenmeyer flask. The flask was covered with a rubber septum. Using a syringe, 2 mL of the anhydride silane were added to the flask. The syringe was washed 3 times with toluene into the reaction mixture (thereby adding an additional 15 mL toluene). The suspension was sonicated for 1 hour and then mechanically shaken at 450 to 600 rpm with a Vibramax 100 for 2 hours. The supernatant was decanted. After that, the particles were then washed once with toluene, followed by an acetone wash, further followed by 3 DI water washes.

2.2.5. Derivatization of Carboxylic Acid-Treated Co-C with DFB

The derivatization of carboxylic acid-treated Co-C with DFB was attempted in a number of different ways at the beginning of this project.

For Method #1, 20 mL of the 1.96 mM DFB was added to the NaPA- and anhydride silane-treated particles. Next, 10 mg EDC was added to each mixture and the

pH of the supernatant was adjusted to 5 (± 0.2). Then, 10 mg FeCl_3 was added to each sample to bind the DFB to iron (III). The suspension was shaken at 450 rpm with a Vibramax 100 for 4 hours, then 600 rpm for another 20 hours. Fresh EDC was added at 3 different points during this time period to make up for loss of EDC (it can hydrolyze in solution at room temperature; the exact rate depends on the pH^4). After 24 hours, the particles were sonicated for 1 hour, shaken for 1 hour, sonicated again for 1 hour, and then shaken for two additional days. After this, the supernatant was removed and the particles were washed 3 times with DI water.

For Method #2, 20 mL 2 mM DFB was added to the NaPA- and anhydride silane-treated particles. This was followed by an addition of 10 to 16 mg EDC, and then approximately 40 μmol FeCl_3 . The supernatant was adjusted to a pH between 4 and 5. The silane-treated particles were sonicated for 1 hour, and then both samples were mechanically shaken at 450 rpm for 3.5 days. Each sample was then washed 3 times with DI water. For the NaPA-treated nanoparticles, the pH of the last water supernatant was adjusted to 2 before it was removed from the particles.

For Method #3, first, two 20-mL samples of 2 mM DFB were prepared. To one sample, 20 mg EDC was added. To the other sample, 20 mg EDC and 6.6 mg FeCl_3 was added. The sample which contained FeCl_3 was added to 50 mg anhydride silane-treated Co-C, while the aliquot without FeCl_3 was added to 50 mg of NaPA-treated Co-C. The pH of each suspension was adjusted to 4.5. Each suspension was sonicated for 30 minutes and then mechanically shaken at 450 rpm with a Vibramax 100 for 5 hours. After the

sonication step and after each hour of shaking, 25 mg fresh EDC was added. After the reaction, the supernatants were removed and each sample was washed 3 times with DI water.

2.2.6. Characterization with Thermogravimetric Analysis

After treating the Co-C particles with NaPA (Section 2.2.3) or silane (Section 2.2.4), they were analyzed by thermogravimetric analysis (TGA). These measurements were performed in the following way. A small amount of the sample (5 to 8 mg) was put onto a TGA sample tray. The sample was heated to 80 °C at 10 °C/min under a N₂ atmosphere. To ensure that any remaining water in the sample evaporated, the temperature was held at 80 °C for 30 minutes. The temperature was increased to 800 °C at 10 °C/min. After this, the atmosphere was changed from N₂ to O₂ gas and the temperature was increased to 1000 °C at the same rate. This last step was done for easier cleaning of the sample trays.

As a control, TGA was also performed on a sample of untreated Co-C particles. In this case, the procedure was the same except the temperature was only held at 80 °C for 20 minutes.

2.2.7. Characterization of DFB-Derivatized Co-C Particles with SEM and EDX

After using Method #1 for derivatization of Co-C with DFB (Section 2.2.5), the particles were analyzed with SEM and EDX. Before taking these measurements, the particles were washed with water and then dried.

2.2.8. Characterization of DFB-Derivatized Co-C Particles with ATR-IR Spectroscopy

After using Methods #2 and #3 for derivatization of Co-C particles with DFB (Section 2.2.5), the particles were characterized with ATR-IR spectroscopy. A few milligrams of the sample to be analyzed were spread onto the single pass diamond crystal and pressed onto the crystal with the plunger. If the sample was wet, it was allowed a few minutes to dry before a spectrum was taken. In all cases, the background used was of the bare crystal.

2.2.9. Iron (III) Removal with Oxalate from DFB-Derivatized Co-C Particles

As discussed in Section 2.3.2, the EDX measurements performed after using Method #1 to derivatize Co-C with DFB show that there was iron on the surface of the particles. The iron (III) had to be removed prior to measuring iron (III) uptake from solution by the particles. To do this, 5 mL 0.1 M oxalate at pH 1.5 was added to each derivatized bead sample (note: these samples underwent Method #1 for DFB derivatization). The mixtures were sonicated for 30 minutes and then shaken at 450 rpm with a Vibramax 100 for 30 minutes. Then, the particles were drawn out of suspension with a magnet and the supernatant was drawn off.

After that, 1000 μ L of 1.96 mM DFB was added to the 0.1 M oxalate supernatant and the pH of this mixture was adjusted to near 8. The volume of NaOH required to make this pH adjustment was recorded. A UV-Vis spectrum was taken of this oxalate/DFB mixture. If necessary to ensure that the absorbance was not too high for proper quantification of the peak, the mixture was diluted and another spectrum was

taken. In all cases, the final volume was recorded after pH adjustments and necessary dilutions, as stated in Table 2.1.

This procedure was repeated 4 more times. After that, a similar procedure was performed wherein the oxalate was stirred with the particles for 18 hours rather than just 30 minutes.

Table 2.1. Final Volume of Oxalate/DFB Mixture After pH Adjustment and Necessary Dilutions

Sample	Wash Number	Final Volume (mL)
NaPA-Treated Co-C Nanoparticles	1	9.3
	2	9.9
	3	9.8
	4	6.1
	5	5.8
	6	5.8
Silane-Treated Co-C Nanoparticles	1	7.9
	2	8.8
	3	8.9
	4	7.7
	5	9.4
	6	9.4

2.2.10. Iron (III) Uptake of DFB-Derivatized Co-C Particles

After washing the particles with oxalate (Section 2.2.9), the ability of each particle sample to remove iron (III) from solution was tested. To do this, 20 mL 1 mM FeCl₃ was added to the NaPA- and silane-treated particles as well as to 25.5 mg untreated Co-C. Each suspension was shaken at 450 rpm with a Vibramax 100 for 3 hours. After that, the particles were drawn out of solution with a magnet and the supernatant was removed.

A 1 mL aliquot of each FeCl₃ supernatant was mixed with 1 mL 1.76 mM DFB. The pH of each mixture was adjusted to 8 using NaOH. The volume of NaOH required to make this pH adjustment was recorded, as stated in Table 2.2. A UV-Vis spectrum was taken of each of these mixtures after pH adjustment. The iron (III) content of the original solution was also measured using the same procedure.

Table 2.2. Amounts of NaOH Added for pH Adjustments – Measuring Iron (III) in Oxalate Supernatants

Oxalate Wash Sample	NaOH (+ any HCl) Added to Oxalate/DFB Mixture (mL)
Fresh FeCl ₃ Solution (not exposed to nanoparticles)	0.4
Untreated Co-C Nanoparticles	0.8
NaPA-Treated Co-C Nanoparticles	1.4
Silane-Treated Co-C Nanoparticles	0.3

Note: When the pH of the oxalate/DFB mixture went over 9, some HCl was added to bring the pH to between 8 and 9.

2.2.11. Calculations

For all DFB-Fe measurements, the concentration was calculated from the UV-Vis absorbance using Beer's Law (Equation 2.1). The molar absorptivity of the DFB-Fe complex used is $2.5 \times 10^6 \text{ cm}^2/\text{mol}$.⁵ Then, the original concentration in the oxalate or FeCl₃ sample (prior to adjusting the pH or adding DFB) had to be calculated (Equation 2.2). Finally, the amount of iron in μmol could be calculated knowing the volume of solution added (Equation 2.3).

Equation 2.1 $c = \frac{A}{\varepsilon \ell}$

Equation 2.2 $M_c = \frac{M_D V_D}{V_c}$

Equation 2.3 $Fe = M_c V_s \times \frac{10^6 \mu mol}{1 mol}$

In Equation 2.1, A represents absorbance, c represents concentration, ε represents the molar absorptivity, and ℓ represents the path length. In Equation 2.2, M represents concentration, V represents the volume of a solution, subscript C indicates the more concentrated solution (before dilution), and subscript D indicates the diluted solution. Finally, in Equation 2.3, Fe is the amount of iron (III) in a particular volume (V_s) of a sample of solution in L with a concentration M_c in mol/L.

2.3. Results and Discussion

2.3.1. Characterization with Thermogravimetric Analysis

Figures 2.3 and 2.4 show the thermogravimetric analysis data for unmodified Co-C nanoparticles. Figure 2.3 shows the weight % versus temperature, where weight % is the percent of the original weight of the sample at the start of the experiment. Though there are a few small fluctuations and perhaps a slight decrease of less than 5% weight above 700 °C, the largest change appears just before 800 °C. At that temperature, oxygen was introduced to the sample, allowing the sample to oxidize. This easily accounts for the increase in weight to 115% weight at 800 °C.

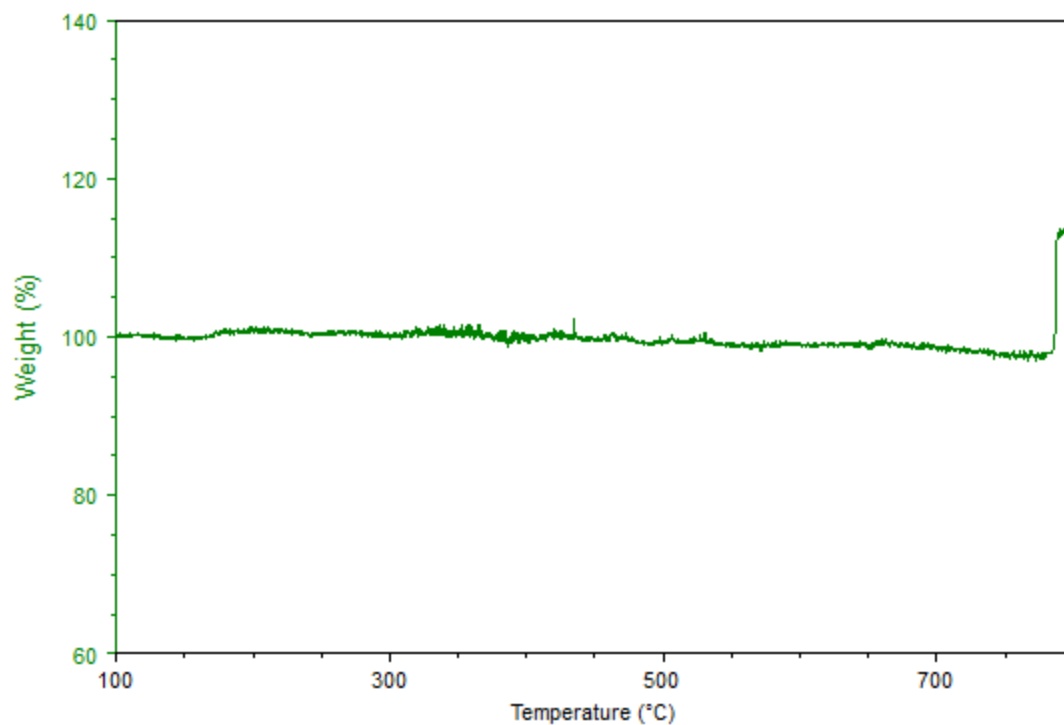


Figure 2.3. Thermogravimetric plot of unmodified Co-C nanoparticles.

Figure 2.4 shows the derivative of the weight rather than the raw weight data. There is only one notable peak in this spectrum just before 800 °C, where a dramatic increase to 115% weight can be seen in Figure 2.3. Peaks in graphs of the derivative of weight with respect to °C correspond to a change in weight. Here, the derivative indicates the rate of weight loss, showing the peak to be negative because weight was gained. Below 800 °C, this graph shows no peaks, and hence there was no significant change in the weight below 800 °C.

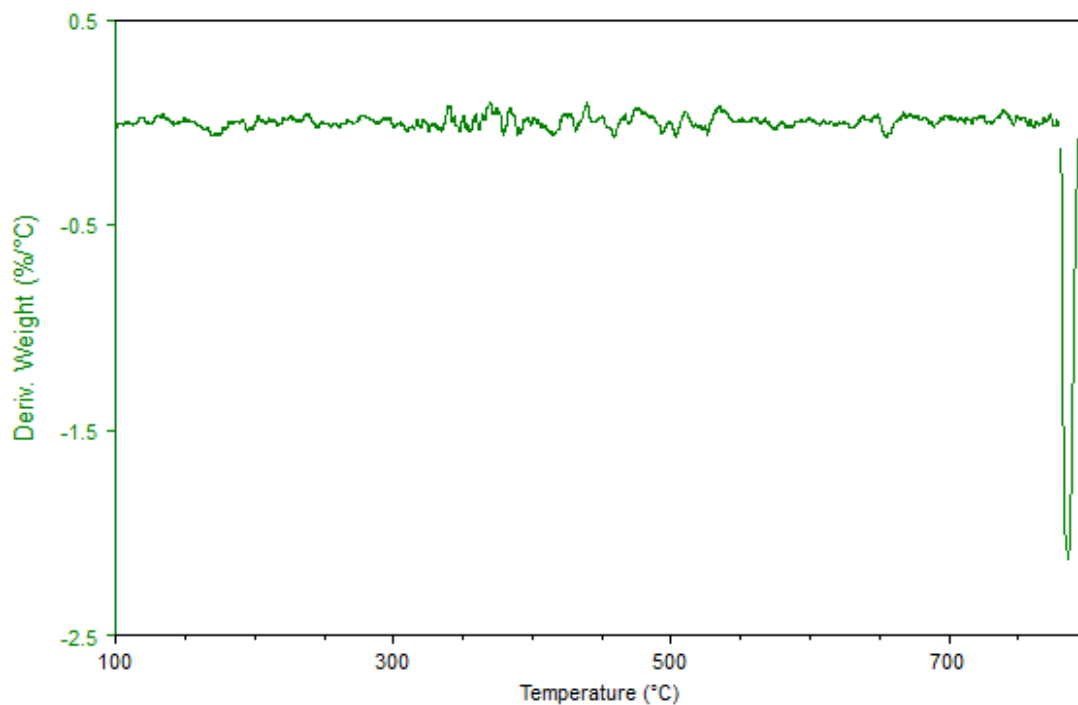


Figure 2.4. Derivative of weight with respect to temperature (weight%/°C) for the graph shown in Figure 2.3.

Figures 2.5 and 2.6 show a representative set of thermogravimetric analysis data for a NaPA-treated Co-C nanoparticle sample. Similar data was obtained for all such samples analyzed. Unlike the unmodified Co-C nanoparticles, there is a significant decrease in the weight, most prominently at 400 °C. This can be seen in Figure 2.5 as a decrease in the weight % curve. The weight percent dropped from 17.5% to 14.5% (the weight percent is not 100% at 100 °C because the sample was wet when added to the sample tray, so water weight was lost prior to that temperature). If 17.5% weight is considered to be the full weight of the dry sample, then this means almost one fifth of the weight of the sample was lost over the 100 °C – 700 °C temperature range.

Figure 2.6 confirms that there is a significant change in the weight at 400 °C, because the derivative is greater than 0 at that point. This indicates that at this temperature, there is a positive rate of weight loss. Because such a loss was not observed at this temperature for the unmodified particles, we conclude that this was due to the loss of NaPA. This provides evidence that the NaPA was adsorbed onto the surface of the particles.

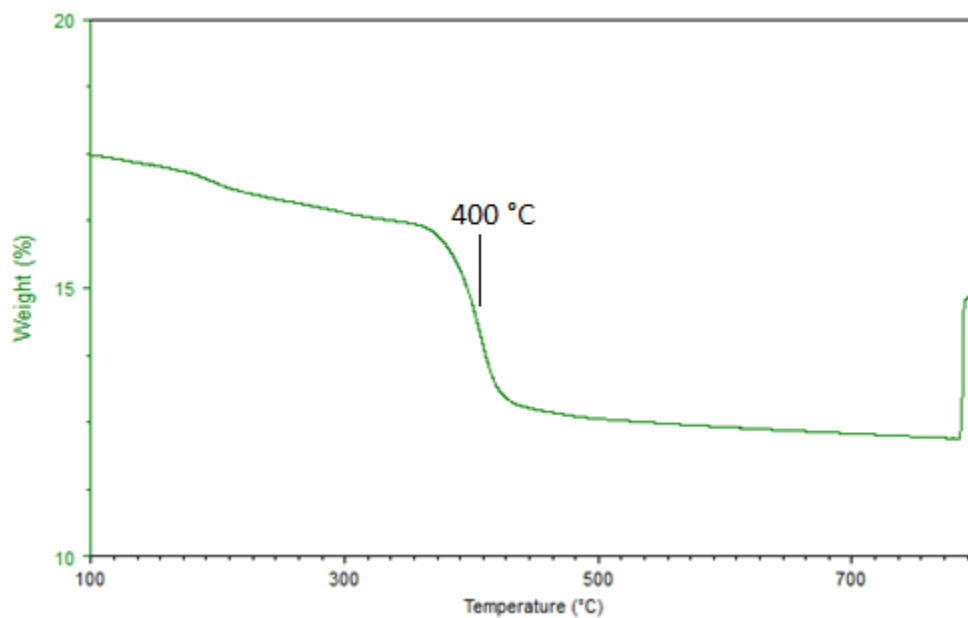


Figure 2.5. Thermogravimetric plot of NaPA-treated Co-C nanoparticles. Note: the sample was wet when the experiment began, so weight loss occurred below 100 °C due to the evaporation of water.

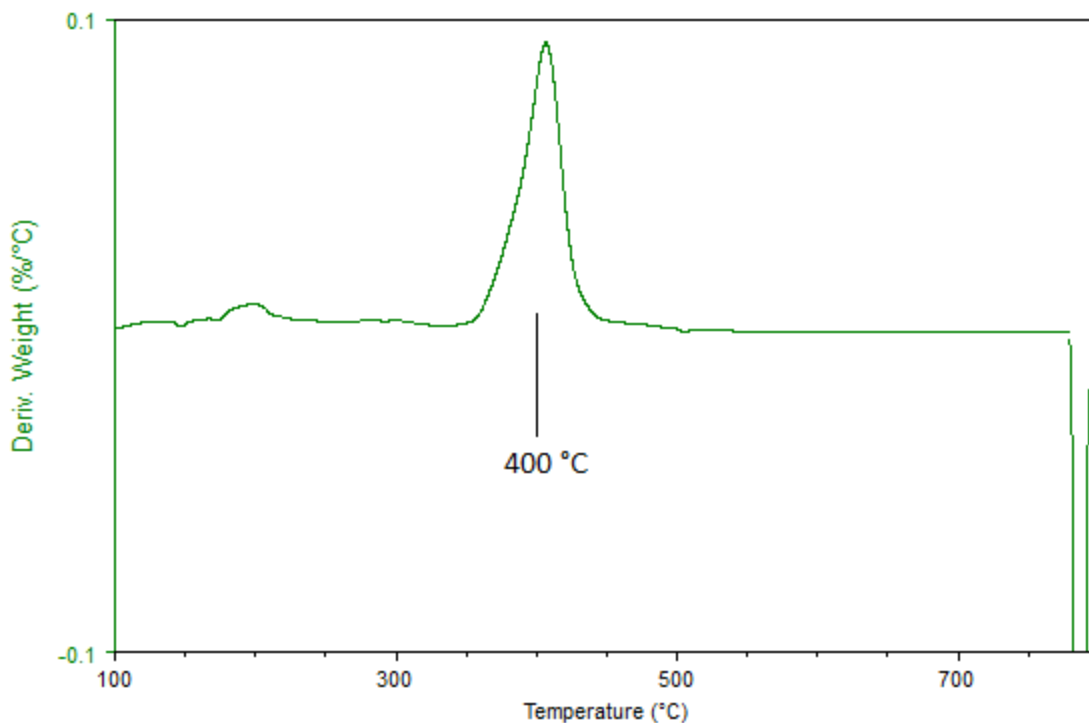


Figure 2.6. Derivative of weight with respect to temperature (weight%/°C) for the graph shown in Figure 2.5.

The next two figures, Figures 2.7 and 2.8, show a set of thermogravimetric analysis data for a sample of silane-treated Co-C nanoparticles. In this case, Figure 2.7 has two weight decreases, one centered around 250 °C and another centered around 450 °C. In total, between 100 °C and 500 °C, the weight percent decreased from 59% to 52.5%. As with the NaPA-treated sample, the weight percent is not at 100% because the initial sample weight included adsorbed water, which was lost before 100 °C. Considering 59% to be the total sample weight, this means a loss of 11% of the sample weight occurred between 100 °C and 500 °C.

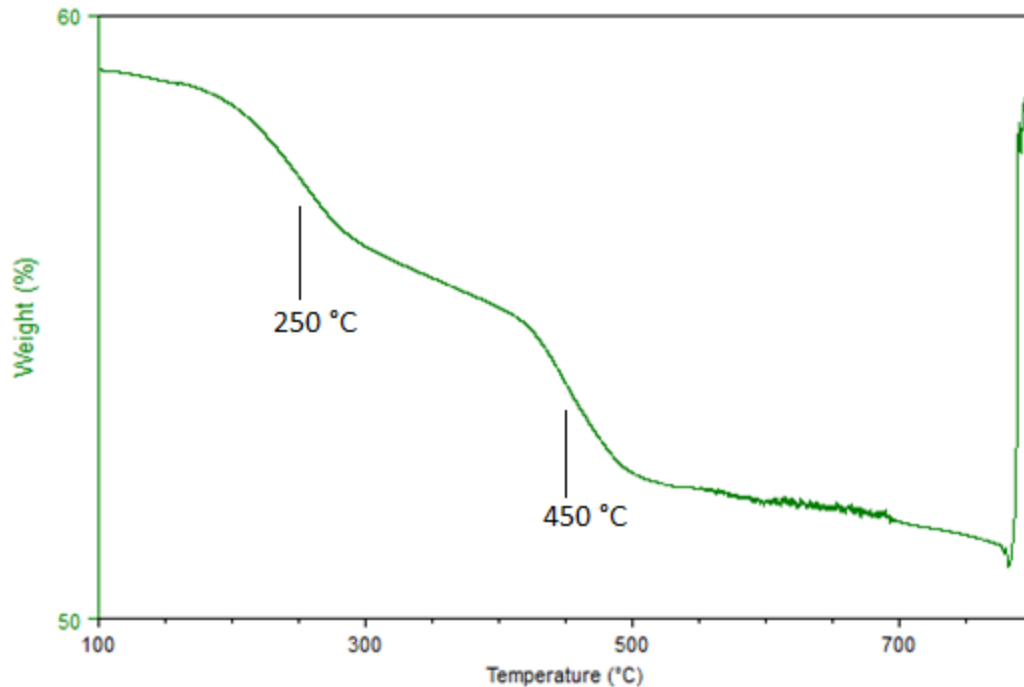


Figure 2.7. Thermogravimetric plot of silane-treated Co-C nanoparticles. Note: the sample was wet when the experiment began, so significant weight loss occurred below 100 °C due to the evaporation of water.

In Figure 2.8, which shows the derivative graph, positive peaks at 250 °C and 450 °C indicate a loss of weight at these temperatures. Similar results were seen by García-González *et. al.* when performing TGA measurements on titania particles treated with various organosilanes. They saw one peak at 525-650 K or 252 to 377 °C (depending on the exact silane used). This was attributed to a combination of factors.⁶ When silanes polymerize, they first undergo hydrolysis, producing silanol groups. These silanol groups undergo a condensation reaction, leading to polymerization of the silane through formation of Si-O-Si bonds and liberation of water.⁷ García-González *et. al.* thought that their 525-650 K peak was due in part to the loss of hydrolyzed silanes which were merely interacting with the surface via hydrogen bonding. Additionally,

some of the weight loss was thought to be the evolution of water from additional condensation reactions between adjacent silanol groups on the surface. A similar explanation can be used for the peak at 250 °C in Figure 2.8.

García-González *et. al.* also saw another peak at 650 to 850 K or 377 to 577 °C (depending on the exact silane used). They attributed this to cleavage of C-C and Si-C bonds in the coating – in other words, oxidation of the coating.⁶ This provides an explanation for the peak at 450 °C in Figure 2.8.

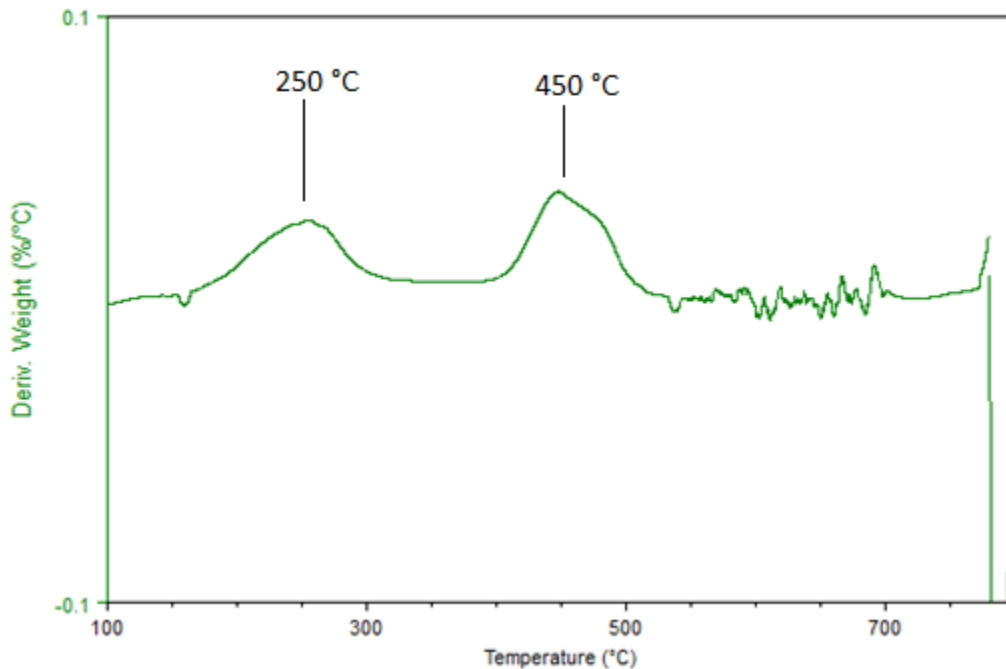


Figure 2.8. Derivative of weight with respect to temperature (weight%/°C) for the graph shown in Figure 2.7.

2.3.2. Characterization of DFB-Treated Co Nanoparticles – SEM and EDX

Figures 2.9, 2.10, and 2.11 show the SEM images taken of unmodified Co-C nanoparticles, NaPA-treated Co-C, and silane-treated Co-C, respectively. These samples were treated using Method #1 for derivatizing carboxylic acid-coated particles with DFB-Fe (see Section 2.2.5 for more details).

The SEM in Figure 2.9 shows that the starting Co-C particles are small, approximately 50 nm in size or less. In Figures 2.10 and 2.11, one can see that the NaPA- or silane-treated particles aggregated into larger chunks which are 5 to 10 μm in size. This is particularly true of the silane-treated particles (Figure 2.11). These appear to have a smooth surface, indicating that the silane polymerized around many nanoparticles at once rather than around individual particles.

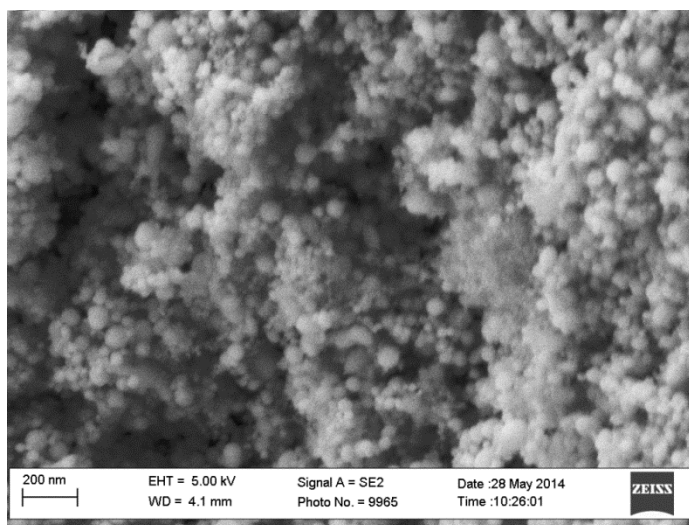


Figure 2.9. SEM image of unmodified Co-C nanoparticles. The scale bar indicates 200 nm.

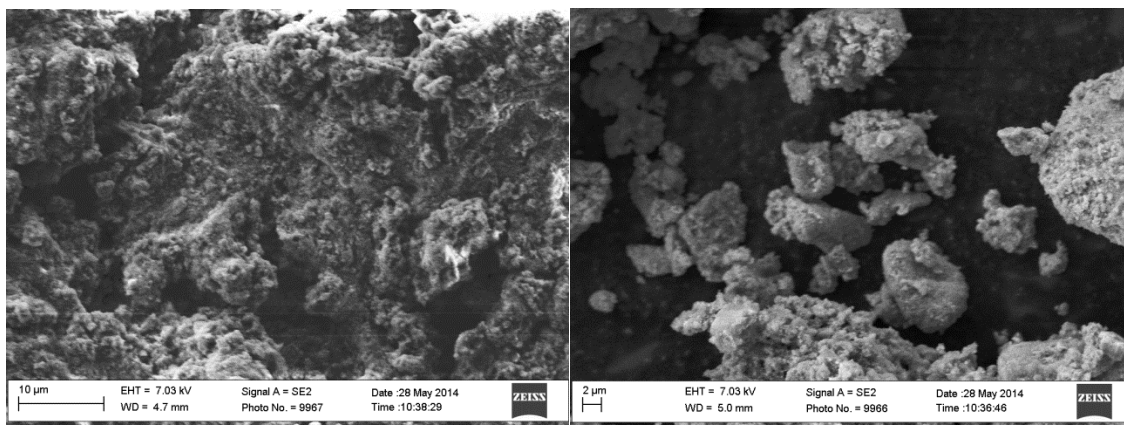


Figure 2.10. SEM images of NaPA-treated Co-C nanoparticles. The scale bars indicate 10 μm (left) and 2 μm (right).

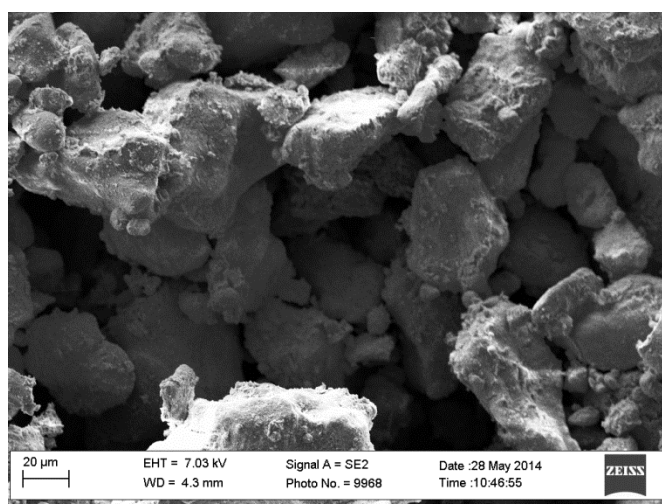


Figure 2.11. SEM image of silane-treated Co-C nanoparticles. The scale bar indicates 20 μm .

Figures 2.12, 2.13, and 2.14 show the EDX spectra taken of each of these samples. As expected, the unmodified Co-C nanoparticles only have peaks due to carbon and cobalt (see Figure 2.12). Figure 2.13 shows the spectrum of the NaPA-treated sample, and in addition to the cobalt and carbon peaks, there are peaks due to oxygen, iron, and nitrogen. Figure 2.14 shows the spectrum of the silane-treated sample, which is similar to Figure 2.13 but with the addition of a silicon peak.

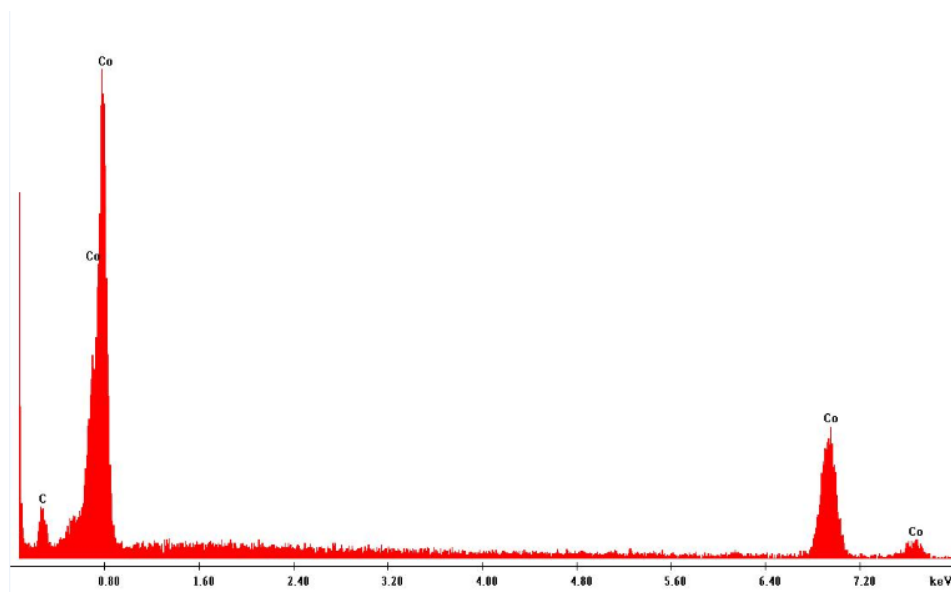


Figure 2.12. EDX spectrum of unmodified Co-C nanoparticles.

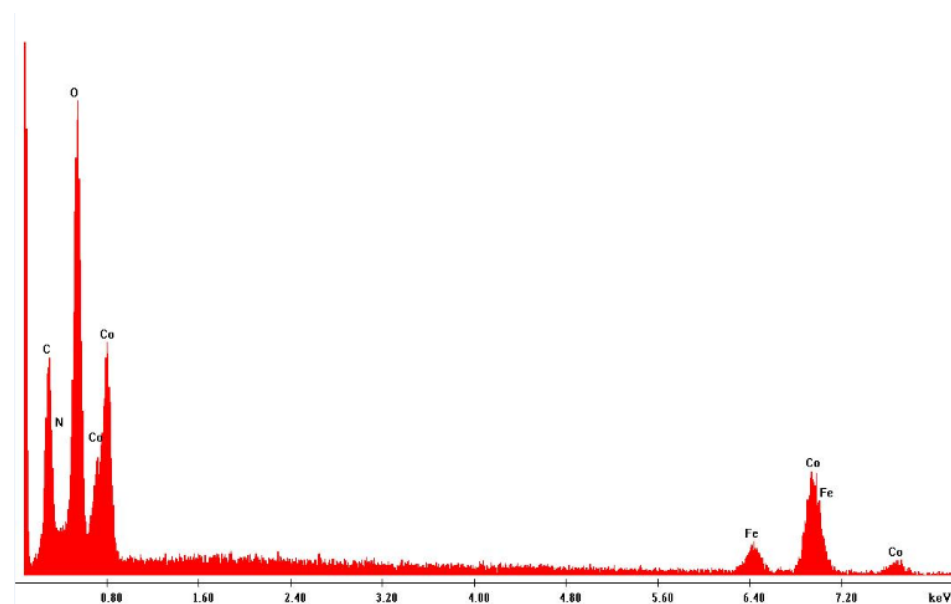


Figure 2.13. EDX spectrum of NaPA-treated Co-C nanoparticles.

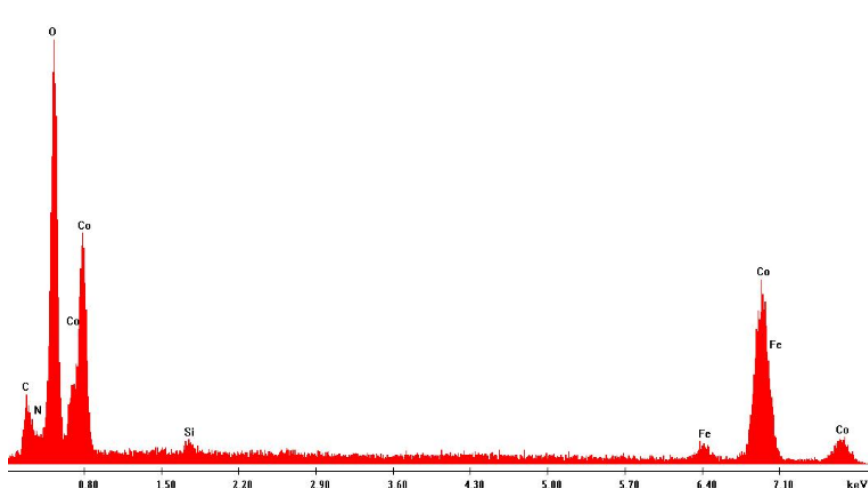


Figure 2.14. EDX spectrum of silane-treated Co-C nanoparticles.

The percent of each element was also determined by the EDX software. These calculated values are shown in Table 2.3. The presence of nitrogen indicates that there is DFB on the surface of the NaPA- and silane-treated particles. However, there is no way to be certain from this data whether the amide linkage was successfully formed, which is why IR spectroscopy was used to characterize subsequent samples.

Table 2.3. Elemental Analysis of Untreated, NaPA-Treated, and Silane-Treated Cobalt Nanoparticles by Atom

Element	Untreated Co-C (atom %)	NaPA-Treated Co-C (atom %)	Silane-Treated Co-C (atom %)
Co	90 %	45 %	34 %
C	10 %	29 %	23 %
O	-	15 %	34 %
N	-	4 %	6 %
Fe	-	7 %	2.5 %
Si	-	-	0.5 %

It is also interesting to compare the percentages of nitrogen and iron on these two samples. All of the nitrogen signal originates from the DFB. Each molecule of DFB can chelate 1 atom of iron (III). Because one DFB molecule contains 6 nitrogens, there should be 6 nitrogen molecules for every 1 iron atom, if all of the iron present is bound to DFB. However, the percentages in Table 2.3 show that the NaPA-treated particle sample is 4% nitrogen and 7% iron – in other words, there is actually 1.8 times *more* iron atoms than nitrogen atoms in this sample. Table 2.3 also shows that the silane-treated sample is 6% nitrogen and 2.5% iron. This means there is 2.4 times more nitrogen than iron in this sample, but if all the iron were bound to DFB, there would be 6 times more nitrogen.

Thus, in both cases, a portion of the iron in the sample must not be bound to DFB and therefore, there is some non-specific adsorption onto the surface. This excess iron comes from the approach used for the addition of DFB to the surface. When generating DFB-Fe, excess FeCl_3 was added so that all the DFB in the solution would be bound to iron. Thus, when the DFB-Fe was exposed to the samples, there was excess iron (III) in solution which could also adsorb on the surface of the particles.

2.3.3. Characterization of DFB-Derivatized Co-C Particles with ATR-IR Spectroscopy

Figures 2.15 and 2.16 show the ATR-IR spectra of a NaPA-treated Co-C nanoparticle sample and a silane-treated Co-C nanoparticle sample, respectively. In both cases, the samples were derivatized with DFB using Method #2 (see Section 2.2.5 for more details).

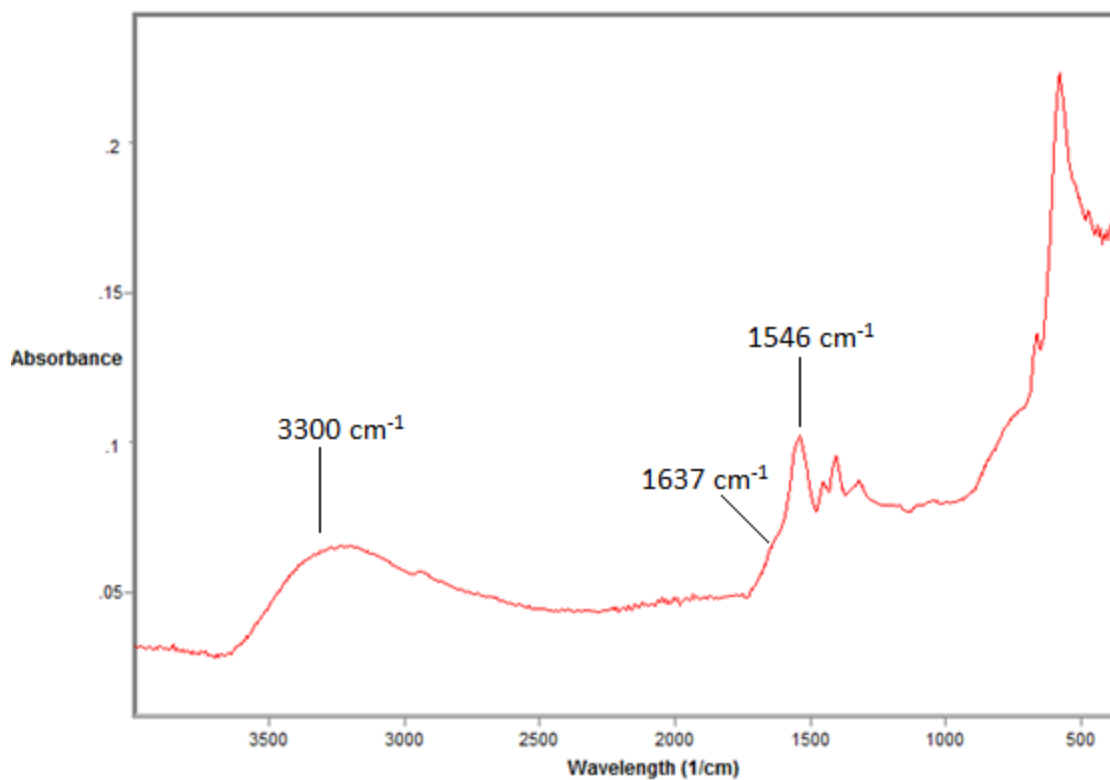


Figure 2.15. ATR-IR spectra of a NaPA-treated Co-C nanoparticle sample after DFB derivatization. The derivatization technique used was Method #2.

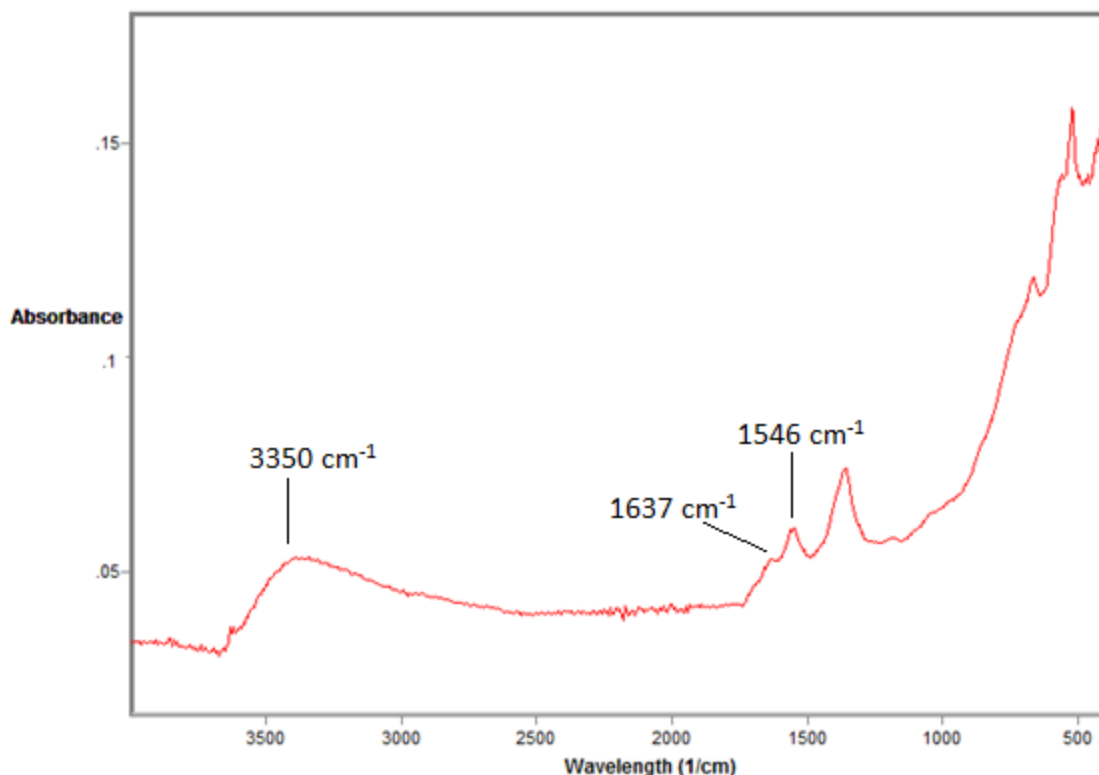


Figure 2.16. ATR-IR spectra of a silane-treated Co-C nanoparticle samples after DFB derivatization. The derivatization technique used was Method #2.

Both spectra in Figures 2.15 and 2.16 have a band at 1546 cm^{-1} . However, neither have a peak equal in intensity near 1650 cm^{-1} . Each of the two seem to have a small peak or shoulder at 1637 cm^{-1} . However, each spectrum also has a broad band centered at 3300 cm^{-1} (Figure 2.15) or 3350 cm^{-1} (Figure 2.16) which is the O-H stretching mode of a water peak. This shows that there is water on the surface. Therefore, the 1637 cm^{-1} peak is a water bending mode in both cases. The 1546 cm^{-1} peak is probably the C=O stretching mode from a deprotonated carboxylic acid (COO^-).

If the DFB derivatization reaction had occurred, then it would have produced bands due to an amide linkage in the IR spectrum. These bands (more specifically, the

C=O stretching modes for an amide) should appear around 1650 cm^{-1} and 1550 cm^{-1} and be approximately the same intensity. If anything, the former peak should be larger, as it can easily overlap with the water O-H bending mode which often appears near 1630 to 1640 cm^{-1} when water is present. However, in the case of Figures 2.15 and 2.16, the 1546 cm^{-1} peak was larger than the 1637 cm^{-1} peak, leading to the conclusion that the 1637 cm^{-1} peak was due to water and that no amide linkage formed.

One possibility for why the amide linkage did not form during this attempt at DFB derivatization is that the EDC was added to the particles *after* the DFB was added. Thus, the carboxylic acid groups on the particles were exposed to the DFB without the EDC, allowing the amine group on the DFB to undergo an acid-base reaction with the carboxylic acids. Therefore, when performing Method #3 of DFB derivatization, EDC and DFB were mixed into one solution prior their addition to the particles.

For the particles which underwent Method #3 for DFB derivatization, ATR-IR spectra were taken before and after the reaction. Figure 2.17 shows the spectra before and after using Method #3 for DFB derivatization on NaPA-treated nanoparticles. Likewise, Figure 2.18 shows the spectra before and after using Method #3 on silane-treated nanoparticles.

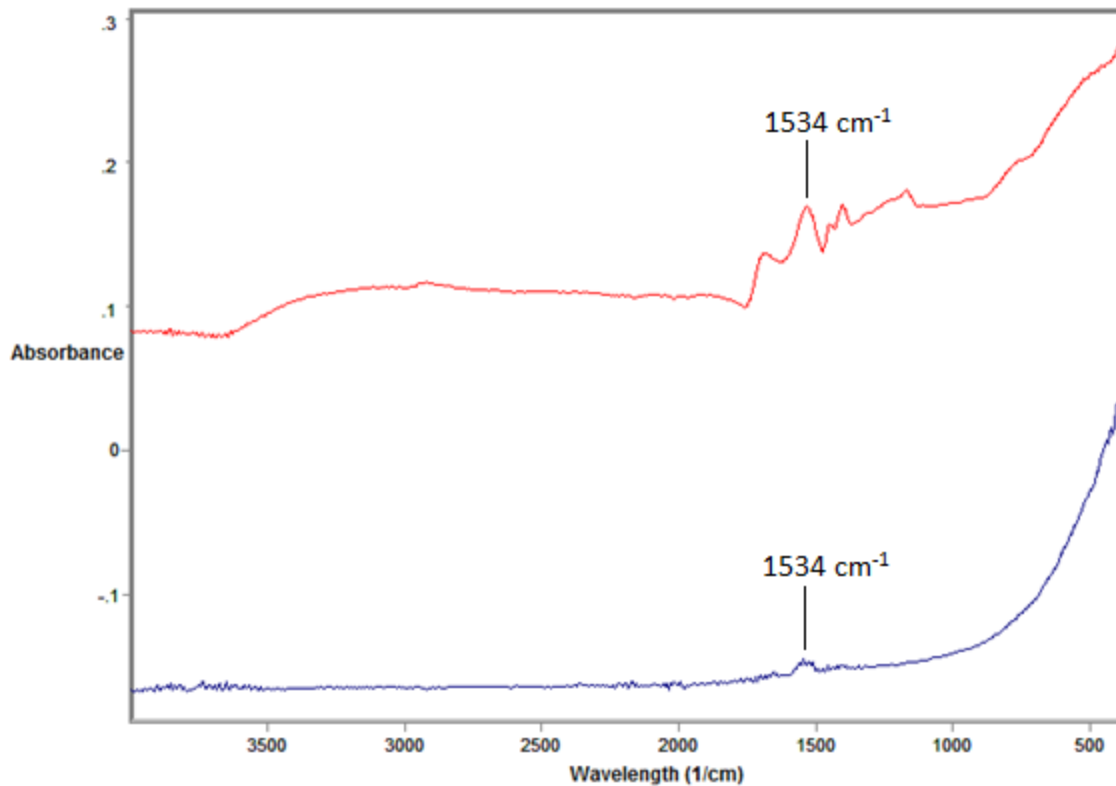


Figure 2.17. ATR-IR spectra before and after using Method #3 for DFB derivatization on NaPA-treated Co-C nanoparticles. The top spectrum was taken before derivatization while the bottom spectrum was taken after.

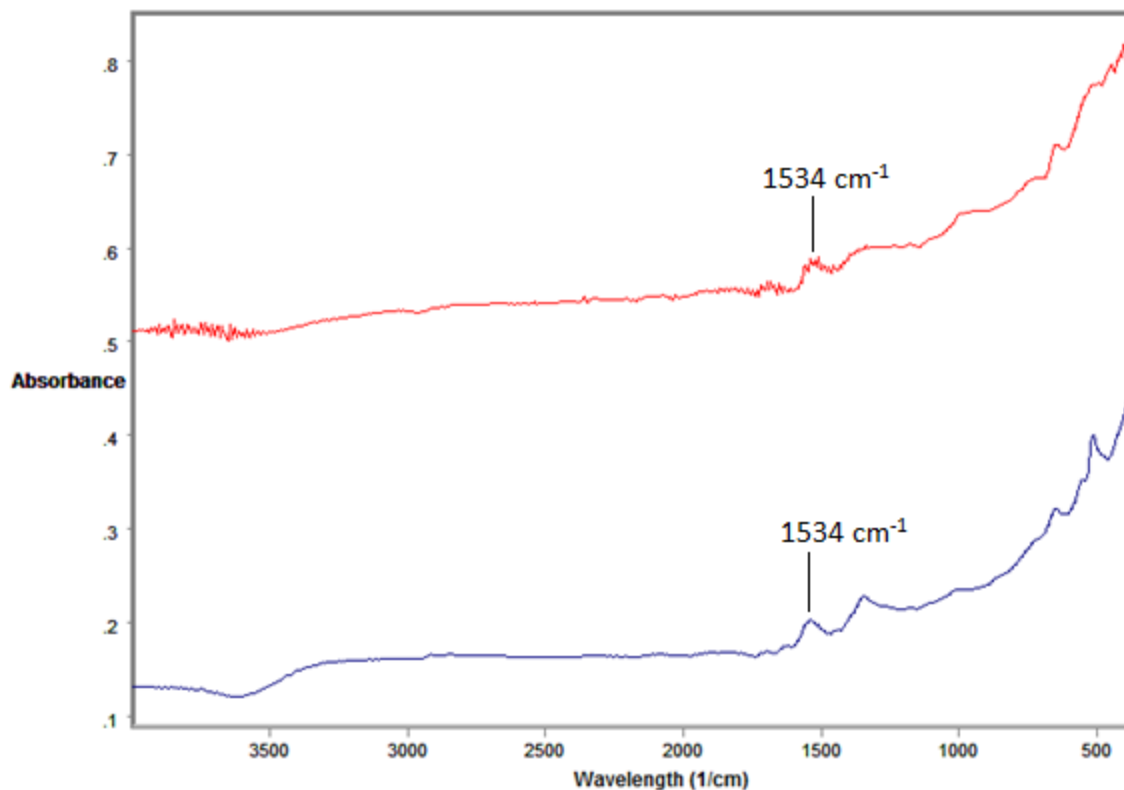


Figure 2.18. ATR-IR spectra before and after using Method #3 for DFB derivatization on silane-treated Co-C nanoparticles. The top spectrum was taken before derivatization while the bottom spectrum was taken after.

Before the reaction, both the NaPA- and silane-treated samples have peaks at 1534 cm^{-1} . In both cases, this peak is still present in the spectrum after the DFB derivatization was attempted. Moreover, neither spectrum taken after this reaction has a peak near 1650 cm^{-1} , which is comparable in size to the 1534 cm^{-1} peak. Therefore, it is reasonable to conclude that in these cases, as well as when using Method #2 for DFB derivatization, no amide linkage was formed and DFB was not covalently linked to the surface of the particles.

2.3.4. Iron (III) Uptake & Removal with Oxalate from DFB-Derivatized Co-C

The EDX data (see Table 2.3) shows that there was iron on the surface of the NaPA- and silane-treated particles after using Method #1 for DFB derivatization. Thus, the next step was to remove this iron from the surface with oxalate at pH 1.5. Table 2.4 shows the results of this experiment – the amount of iron (III) recovered in each oxalate wash from the particles. The amount of iron (III) removed decreased with each successive wash for both particle samples. In total, 16.6 μmol iron (III) was removed from the NaPA-treated particles, and 7.7 μmol iron (III) was removed from the silane-treated particles. However, even after the sixth wash, iron was still eluting off of the particles. Therefore, it is likely that even after washing the particles six times with oxalate (the last wash involving stirring the particles for 18 hours), some iron still remained on the particles.

Table 2.4. DFB-Fe Absorbance Measurements in Oxalate Washes

Sample	Wash Number	Fe ⁺³ Amount (μmol)
NaPA-Treated Co-C Nanoparticles	1	11.7
	2	3.4
	3	0.9
	4	0.3
	5	0.2
	6	0.1
Silane-Treated Co-C Nanoparticles	1	3.1
	2	1.4
	3	0.9
	4	0.6
	5	0.8
	6	0.9

Nonetheless, another experiment was performed to see if these particles would take iron (III) out of solution. To do this, each particle sample, along with some unmodified Co-C nanoparticles, was put into a solution containing iron (III). After stirring the particles in the solution, the amount of iron (III) left in the solution was measured using UV-Vis. The results of this experiment (the amount of iron (III) in the FeCl₃ solutions before and after shaking with the particles) are shown in Table 2.5.

Table 2.5. DFB-Fe Absorbance Measurements in Iron (III) Supernatants

Sample Tested	Amount Fe ⁺³ in 20 mL (μmol)
Fresh FeCl ₃ Solution (not exposed to nanoparticles)	22.6
Untreated Co-C Nanoparticles	0
NaPA-Treated Co-C Nanoparticles	22.6
Silane-Treated Co-C Nanoparticles	22.9

Table 2.5 shows that the same amount of iron (III) was present in 20 mL of the fresh solution as was present in 20 mL after stirring with either of the treated nanoparticle samples. It is concluded that these particles did not remove any iron (III) from solution. This is not surprising, as it was shown that there may have still been iron on the particles at the start of this experiment. Because of that, it is possible that the particles may not have been able to take up more iron (III).

What is surprising about these results was what occurred on the untreated Co-C nanoparticles. More specifically, there was no iron (III) left in the solution after these

particles were stirred in it, meaning that it must have adsorbed onto the particles. In other words, the untreated particles are able to take iron (III) out of solution. This is due to non-specific binding with the carbon-coated surface.

2.4. Conclusions

First, thermogravimetric analysis was done on the carboxylic acid-treated Co-C nanoparticles to determine if either method, using NaPA or the silane, worked to put carboxylic acid onto the surface. These experiments showed that both the NaPA and silane treatments of Co-C particles resulted in successful surface treatment. However, the ATR-IR evidence suggests that despite attempting different methods to derivatize the NaPA- and silane-treated Co-C nanoparticles with DFB, derivatization was unsuccessful.

It was also shown that untreated Co-C nanoparticles are able to take iron (III) out of solution. This result led to the pursuit of two different directions for investigation. The first direction was an attempt to take advantage of this property. In other words: could Co-C nanoparticles be used, without modification, to take iron (III) out of solution? Subsequently, could it then be removed from the particles with DFB and then measured as DFB-Fe in that solution using UV-Vis? These questions were explored in the work described in Chapter 3.

The second direction (see Chapter 4) was to first coat the underlying surface, then modify this coating with DFB. It was thought that if the particles could not be used unmodified to remove iron from solution, that they should be blocked from doing so.

This prevents any potential competing reactions when adding or removing iron (III) from the surface, which could potentially make the process less effective overall. In order to do this, it was thought that the same method used by Roy *et. al.* to derivatize silicon wafers with DFB⁸ could be used for this goal. In that instance, silicon wafers were first coated with silica, which was then derivatized with carboxylic acid functional groups. The amine group on DFB could be covalently-linked via a reaction with the carboxylic groups to form an amide linkage.

2.5. References

1. Helm, Z. Determining Oceanic Iron Concentrations Using a Siderophore Based Sensor. University of Maine, 2013, M.S. Thesis; Tripp, C. P.; Hair, M. L., Kinetics of the Adsorption of a Polystyrene-Poly(Ethylene Oxide) Block Copolymer on Silica: A Study of the Time Dependence in Surface/Segment Interactions. *Langmuir* **1996**, *12* (16), 3952-3956.
2. Gammana, M. A UV-Vis. Spectroscopic Based Method for Iron Detection in Aqueous Solutions by Using DFB Tethered to Membranes. University of Maine, 2014, Ph.D Thesis.
3. Kanan, S. A.; Tze, W. T. Y.; Tripp, C. P., Method to Double the Surface Concentration and Control the Orientation of Adsorbed (3-

aminopropyl)dimethylethoxysilane on Silica Powders and Glass Slides. *Langmuir* **2002**, *18* (17), 6623-6627.

4. Lei, Q. P.; Lamb, D. H.; Heller, R. K.; Shannon, A. G.; Ryall, R.; Cash, P., Kinetic Studies on the Rate of Hydrolysis of N-Ethyl-N'-(Dimethylaminopropyl)carbodiimide in Aqueous Solutions Using Mass Spectrometry and Capillary Electrophoresis. *Analytical Biochemistry* **2002**, *310* (1), 122-124.
5. Owusu-Nkwantabisah, S. Polymer Adsorption on Solid Surfaces: Layer-By-Layer Studies and Development of an Iron (III) Sensor. University of Maine, 2014, Ph.D Thesis; Hansen, K. Detection of Iron (III) Using Agarose Beads Derivatized with Desferrioxamine B. University of Maine, 2014, B.S. Thesis.
6. Garcia-Gonzalez, C. A.; Fraile, J.; Lopez-Periago, A.; Domingo, C., Preparation of Silane-Coated TiO₂ Nanoparticles in Supercritical CO₂. *Journal of Colloid and Interface Science* **2009**, *338* (2), 491-499.
7. Witucki, G. L., A Silane Primer - Chemistry and Applications of Alkoxy Silanes. *Journal of Coatings Technology* **1993**, *65* (822), 57-60.

8. Roy, E. G.; Jiang, C. H.; Wells, M. L.; Tripp, C., Determining Subnanomolar Iron Concentrations in Oceanic Seawater Using a Siderophore-Modified Film Analyzed by Infrared Spectroscopy. *Analytical Chemistry* **2008**, *80* (12), 4689-4695.

CHAPTER 3: IRON UPTAKE WITH UNMODIFIED, CARBON-COATED COBALT NANOPARTICLES

3.1. Introduction

In Chapter 2, we showed that the bare Co-C nanoparticles are capable of drawing iron (III) out of solution. Therefore, it was thought that these particles could be used without DFB attached to the surface to extract iron (III) from solution. Once the particles had gathered iron (III) from a solution, they could be removed from the supernatant using a magnet. The key would be to develop a strategy to remove the captured iron (III) from the particles. Because there is no DFB on the surface in this case, it was thought that a DFB solution could be used to remove iron (III) from the surface. By using a smaller volume of DFB than the original solution, the iron (III) would be concentrated and measured directly via UV-Vis to determine the amount of iron (III). This scheme is illustrated in Figure 3.1. The work presented herein was done to explore the possibility of using this scheme to concentrate iron (III) from a solution for measurement with UV-Vis spectroscopy.

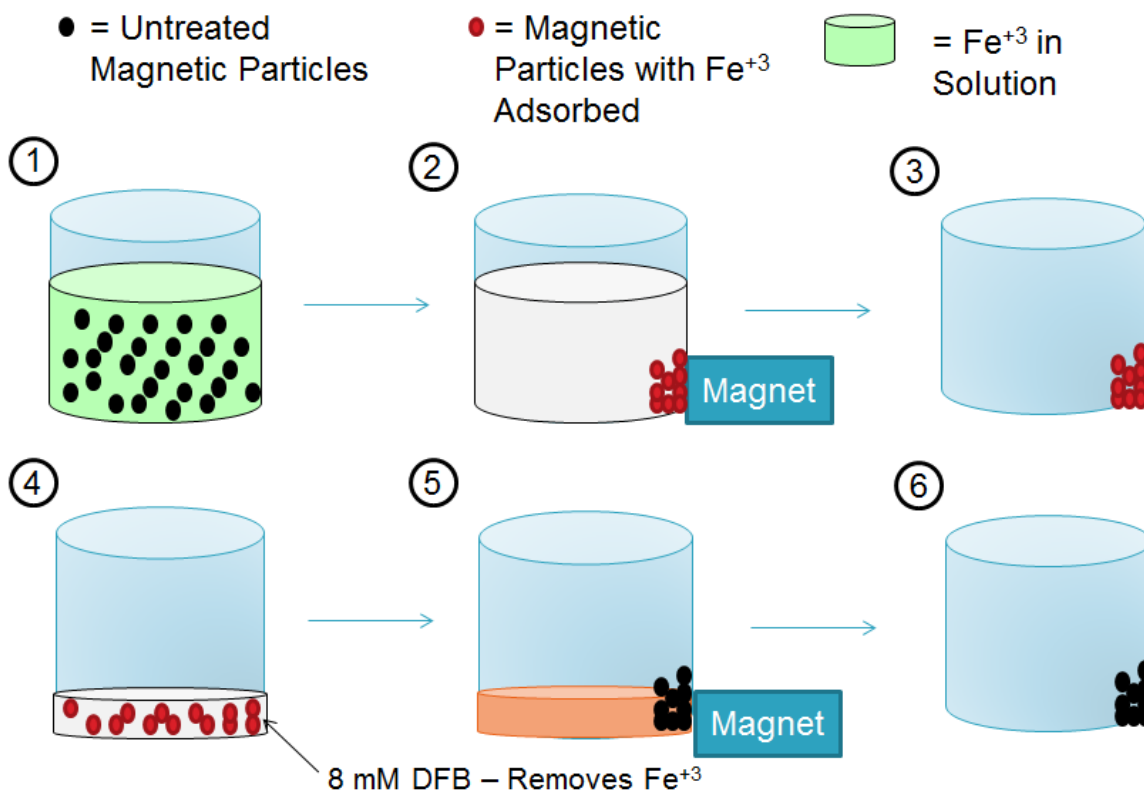


Figure 3.1. Steps to remove and concentrate iron (III) using unmodified Co-C nanoparticles. 1) Bare Co-C nanoparticles are dispersed in a solution of FeCl_3 . 2) Co-C particles remove iron (III) from solution and are drawn to a magnet. 3) Supernatant is removed. 4) Co-C particles are dispersed in a DFB solution (smaller volume than original FeCl_3 solution). 5) DFB removes iron (III) from Co-C particles, forming a DFB-Fe solution. 6) DFB-Fe solution is removed so that a UV-Vis spectrum can be recorded.

3.2. Experimental

3.2.1. Materials

The following materials were obtained from Sigma-Aldrich: carbon-coated magnetic cobalt nanopowder (Co-C), deferoxamine mesylate salt (DFB), and iron (III) chloride (FeCl_3). Sodium hydroxide and hydrochloric acid were purchased from Fisher

Scientific. The sodium hydroxide and hydrochloric acid were diluted as necessary to make pH adjustments to the solutions.

The FeCl_3 was received as a powder. First, a 1 mM stock solution was made by dissolving the solid material in DI water (16.2 mg per 100 mL). Then, the pH was adjusted to between 2.5 and 2.8 with concentrated HCl to prevent the formation of iron hydroxides in solution. In most cases, a lower concentration used, in which case 1 to 2 mL of the 1 mM FeCl_3 was diluted to 100 mL with DI water. The pH of the diluted solution was immediately adjusted to between 2.5 and 2.8 with concentrated HCl.

The DFB was also received as a powder and frozen when not in use. Solutions of DFB were prepared in concentrations of 2 mM and 8 mM by dissolving the appropriate amount of the DFB powder in the desired volume of DI water. For a 2 mM solution, this required 0.1314 g DFB per 100 mL; for an 8 mM solution, this required 0.1314 g DFB per 25 mL. The pH of the 8 mM solutions was controlled with HCl and NaOH solutions. The Co-C nanoparticles were used as received.

All UV-Vis spectra were recorded on an Ocean Optics USB 2000 UV-Vis spectrometer with SpectraSuite software. A 1 cm cuvette was used unless otherwise noted. For background and absorbance spectra, each scan took 2 minutes. Mass was recorded on a Mettler Toledo AG245 analytical balance. Mechanical shaking was performed using a Vibramax 100 from Heidolph.

3.2.2. Washing the Particles

Washing was performed by adding the desired solvent (usually DI water unless otherwise noted), mixing for 2 seconds, drawing the particles to the side of the container using an external magnet, and then decanting the wash liquid or extracting the liquid with a pipette.

3.2.3. The Effect of NaCl on Bare Co-C Particles' Uptake of Iron (III) from Solution

Two samples were prepared containing unmodified Co-C particles and an iron (III) solution. One contained 9.0 mg Co-C, 10 mL DI water, and 10 mL 1 mM FeCl₃ (i.e. 0.5 mM FeCl₃). The other contained 12.5 mg Co-C, 10 mL 1 M NaCl, and 10 mL 1 mM FeCl₃ (i.e. 0.5 mM FeCl₃/0.5 M NaCl). Each was sonicated for 30 minutes and then mechanically shaken with a Vibramax 100 for 2.5 hours. Next, the supernatant was removed from each solution.

In preparation to determine the amount of iron (III) left in the supernatant, 1000 µL of each supernatant was combined with 500 µL 2 mM DFB. The pH of each mixture was adjusted to be between 8 and 10 using dilute NaOH. This was done because DFB is fully deprotonated at this pH, and as such has a higher affinity for cations such as iron (III). (This was determined to be unnecessary for subsequent experiments because there were no competing ligands for iron (III).) The volume of NaOH added for the pH adjustment was recorded, as stated in Table 3.1. The iron (III) contents of 0.5 mM FeCl₃ and 0.5 mM FeCl₃/0.5 M NaCl were also measured in this same manner. This was done

to determine the amount of iron (III) present in these solutions before exposure to the particles.

Table 3.1. Amounts of NaOH Added for pH Adjustments – Measuring Iron (III) in FeCl₃ Solutions

Sample	NaOH (+ any HCl) Added to Sample/DFB Mixture (μL)
FeCl ₃ Solution in DI Water	110
FeCl ₃ Solution in NaCl	115
FeCl ₃ Solution in DI Water – Exposed to Particles	40
FeCl ₃ Solution in NaCl – Exposed to Particles	40

Note: When the pH of the oxalate/DFB mixture went over 9, some HCl was added to bring the pH to between 8 and 9.

3.2.4. Removing Iron (III) from Bare Co-C Nanoparticles with DFB – Initial Attempt

The target concentration of the FeCl₃ solution to be used in this experiment was 20 μM; therefore, when making the solution, 2 mL 1 mM FeCl₃ was diluted to 100 mL. The exact concentration of the FeCl₃ solution was measured in the following manner. First, 2000 μL of the solution was added to a cuvette. The background spectrum was recorded through the solution. Then, 200 μL 2 mM DFB was added and an absorbance spectrum was recorded. See Section 2.2.11 for details on how the concentration of iron (III) in the solution was calculated from measuring the UV-Vis spectrum.

Next, 20 mL FeCl₃ was added to 0.0511 g (51.1 mg) Co-C nanoparticles. This suspension was sonicated for 30 minutes and then mechanically shaken at 600 rpm with a Vibramax 100 for 30 minutes. The particles were separated from the supernatant with

a magnet and the supernatant was removed. The particles were washed 3 times with DI water. Then, using the same procedure described in the previous paragraph, the iron (III) content of the supernatant was measured by recording a UV-Vis spectrum.

A 8 mM DFB solution was made as described in Section 3.2.1 and the pH adjusted to 1.88 with HCl. To remove the iron (III) from the particles after their exposure to FeCl₃, 5000 µL 8 mM DFB (pH 1.88) was added to the particles. The pH of the DFB solution was adjusted below 2 to ensure that the iron (III) would not form oxyhydroxides prior to chelation with DFB. This suspension was shaken at 600 rpm in 5-minute intervals. After each 5-minute interval, the particles were separated from the supernatant with a magnet and 2000 µL of the supernatant was added to a cuvette and a UV-Vis spectrum was recorded. The background spectrum was recorded using a fresh aliquot of 8 mM DFB solution. The portion of supernatant in the cuvette was then added back into the rest of the sample before the next interval of shaking. The particles were shaken for a total of 40 minutes (eight 5-minute intervals).

3.2.5. Removing Iron (III) from Bare Co-C Nanoparticles with DFB: Varying DFB pH

The procedure to measure the iron (III) concentration of the FeCl₃ used in this experiment, as well as the procedure to add iron (III) to the Co-C particles, was the same as described in Section 3.2.4. This was used on four different samples of Co-C at different DFB solution pH. The mass of Co-C nanoparticles and corresponding DFB solution pH for each experiment are reported in Table 3.2.

To remove iron (III) from the particles with DFB, the following procedure was used. First, four separate 5000 μL samples of 8 mM DFB were prepared. Each was adjusted to a different pH and added to a different Co-C particle sample as stated in Table 3.2. Each suspension was shaken with a Vibramax 100 at 600 rpm for 1 hour. After that hour, 2000 μL of the supernatant was added to a cuvette and a UV-Vis spectrum was recorded. The portion in the cuvette was added back into the rest of the sample. The suspension was shaken at 600 rpm for another hour. Again, 2000 μL of the supernatant was added to a cuvette and a UV-Vis spectrum was recorded.

Table 3.2. pH of DFB Used with Each Sample; Mass of Each Sample

Sample Label	Mass of Co-C Particles (mg)	pH of DFB Used
A	50.8	2.06
B	48.5	3.98
C	55.5	6.23
D	54.8	8.08

3.2.6. Removing Iron (III) from Bare Co-C Nanoparticles with DFB – Adding NaCl

The procedure used in this experiment was the same as in Section 3.2.4, except that the FeCl_3 and 8 mM DFB solutions contained 1 M NaCl. The pH of the 8 mM DFB solution was 1.34.

3.2.7. Investigation of Particles' Interference in UV-Vis Spectra

The motivation for this experiment is discussed in Section 3.3.5.

Two suspensions were made. In one case, 0.0488 g Co-C nanoparticles were suspended in 20 mL DI water. In the other case, 0.0542 g Co-C nanoparticles were suspended in 20 mL of an HCl solution at a pH of 2.08. These two suspensions were sonicated for 30 minutes, followed by shaking at 600 rpm for 30 minutes; these two steps of sonication and shaking were repeated twice more, in that order. After each sonication/shaking cycle, a UV-Vis spectrum of the supernatant was recorded. Fresh supernatant (DI or the HCl) was added after any time a UV-Vis spectrum indicated the presence of particles in suspension (see Section 3.3.6 for more details). The background for the UV-Vis spectra was DI water.

The sonication of the large aggregated particles resulted in the production of a small fraction of fine particles that would remain in suspension and not be extracted by the magnet. A follow-up experiment was done in an attempt to remove the fine particles from the suspension. A suspension of 0.0544 g Co-C in 20 mL DI water was sonicated for 30 minutes. The particles were separated out with a magnet and a UV-Vis spectrum of the supernatant was recorded; the background was DI water. The suspension was then shaken at 600 rpm with a Vibramax 100 for 1 hour, after which a UV-Vis spectrum of the supernatant was recorded. At this point, the supernatant was removed entirely and the particles were washed 5 times with DI water. A fresh 20 mL DI water was added to the particles. The particles were then shaken at 600 rpm for a total

of 2 hours, with a UV-Vis spectrum of the supernatant recorded every 30 minutes. One week later, the particles were washed 3 times with DI water. In a fresh 20 mL DI water supernatant, the previous step was repeated.

The results of these experiments led to changes in the general procedure for adding FeCl_3 solutions to Co-C particles and removal of iron (III) from the particles with DFB. These procedural changes are described in Sections 3.2.8 and 3.2.9.

3.2.8. Removing Iron (III) from Bare Co-C Nanoparticles with DFB – Substituting DI Water with pH 2 HCl

First, a solution of HCl at a pH of 2.00 was prepared. Then, 0.0545 g Co-C nanoparticles was suspended in 5000 μL of the pH-2 HCl. This suspension was sonicated for 30 minutes. The particles were then separated from the supernatant with a magnet and the supernatant was removed. The particles were washed 3 times with the pH-2 HCl.

The target concentration of FeCl_3 solution was approximately 20 μM ; therefore, when making the solution, 2 mL 1 mM FeCl_3 was diluted to 100 mL. The actual concentration of the FeCl_3 solution was measured using the following manner. First, 2000 μL of the solution was added to a cuvette. The background spectrum was recorded through the solution. Then, 200 μL 2 mM DFB was added and an absorbance spectrum was recorded.

Next, 20 mL of that FeCl_3 solution was added to the particles. This suspension was shaken at 450 rpm with a Vibramax 100 for 1 hour. The particles were separated

from the supernatant with a magnet and the supernatant was removed. The particles were washed 3 times with the pH-2 HCl. Then, using the same procedure described in the previous paragraph, the iron (III) content of the supernatant was measured.

An 8 mM DFB solution was prepared and the pH adjusted to 1.74 with HCl. To remove the iron (III) from the particles after their exposure to FeCl_3 , 5000 μL 8 mM DFB (pH 1.74) was added to the particles. This suspension was shaken at 450 rpm in 5-minute intervals. After each 5-minute interval, the particles were separated from the supernatant with a magnet and 2000 μL of the supernatant was added to a cuvette so that a UV-Vis spectrum was recorded. The background used was fresh 8 mM DFB solution. The portion of supernatant in the cuvette was then added back into the rest of the sample before the next interval of shaking. The particles were shaken for a total of 40 minutes (eight 5-minute intervals).

3.2.9. Removing Iron (III) from Bare Co-C Particles – Concentrating Iron (III) from $<10 \mu\text{M}$ FeCl_3

Two separate experiments were performed using lower concentrations of FeCl_3 solutions which were measured to be $<10 \mu\text{M}$ FeCl_3 . They will be discussed together.

The procedure for the first experiment was the same as described in Section 3.2.8 with two exceptions. First, where an HCl solution at pH 2 was used, DI water was used instead. Second, when making the FeCl_3 solution, 1 mL of $\sim 1 \text{ mM}$ FeCl_3 was diluted to 100 mL. As discussed in Section 3.3.8, the concentration of the FeCl_3 solution was measured to be $9.1 \mu\text{M}$. The pH of the 8 mM DFB used was 1.74.

The second experiment was designed to be a repeat of the first experiment on several samples. When making the FeCl₃ solution, 900 μL 1 mM FeCl₃ was diluted to 100 mL. The exact concentration of the FeCl₃ solution was measured in the following manner. First, 5000 μL of the solution was added to a 5 cm cuvette. (A larger path length cuvette was used to increase the signal, thereby making it easier to measure lower concentrations of iron (III).) The background spectrum was recorded through the solution. Then, 1000 μL 2 mM DFB was added and an absorbance spectrum was recorded.

Four samples of Co-C nanoparticles were prepared (the masses were all 50 mg ± 3 mg). Each sample was suspended in approximately 10 mL DI water. These suspensions were sonicated for 30 minutes. The particles were then separated from the supernatant with a magnet and the supernatant was removed. The particles were washed 3 times with DI water.

Next, 20 mL of that FeCl₃ solution was added to each of these samples. This suspension was shaken at 450 rpm with a Vibramax 100 for 1 hour. The particles were separated from the supernatant with a magnet and the supernatant was removed. The particles were washed 3 times with DI water. Then, using the same procedure described in the previous paragraph, the iron (III) content of the supernatant was measured.

For reasons discussed in Section 3.3.8, no attempt was made to remove the iron (III) from the particles with DFB in this case.

3.2.10. Calculation of Amount of Iron (III)

To calculate the amount of iron (III) in a solution based on the DFB-Fe absorbance, Equations 2.1 – 2.3 (see Chapter 2) were used.

3.2.11. Detection Limits and Error Bars

In most cases, when a background UV-Vis spectrum was recorded, 5 absorbance spectra were recorded through the solution used to record the background spectrum. These were termed the baseline spectra. These baseline spectra were then used to determine the detection limit. To do this, the noise level in each baseline spectrum was determined. The standard deviation of this noise was calculated. Unless otherwise noted, one standard deviation of the baseline noise level was defined as the error in measurement. Three times the standard deviation of this noise level was defined as the detection limit.

3.3. Results and Discussion

3.3.1. The Effect of NaCl on Bare Co-C Particles' Uptake of Iron (III) from Solution

The purpose of this experiment was to see if increasing the ionic strength of the iron (III) solution would have any effect on the Co-C particles' ability to take iron (III) out of the solution. This was done because, if this technique were to be used on real samples, the ionic strength would be higher due to all of the salts present in oceanic water. Therefore, it was desirable to know the ionic strength dependence of iron (III) uptake.

The top spectrum in Figure 3.2 was recorded for the supernatant containing FeCl_3 in DI water after shaking with the particles, while the bottom spectrum shows a similar spectrum for the supernatant containing FeCl_3 in the NaCl solution. While neither baseline is flat, there are no peaks due to the DFB-Fe complex in the spectrum. There is, however, an increasing absorbance with decreasing wavelength, indicative of light scattering. This scattering is due to the presence of small particulates.

The absence of a DFB-Fe peak in the supernatant indicates that there was no iron (III) left in the supernatant after each solution was shaken with the particles. In turn, this means that in both cases, the iron (III) in solution adsorbed onto the particles. Note that due to the signal-to-noise ratio, and also the level of scattering present, one cannot say with 100% certainty that there is no iron (III). The detection limit was calculated to be an absorbance of 0.0014, which translates to an iron (III) concentration of 1.1×10^{-6} M in the supernatant. This means that in each 20 mL supernatant studied in this experiment, there was no more than 0.02 μmol of iron (III) remaining. This is roughly 5% of the amount of iron (III) measured in each of the original solutions.

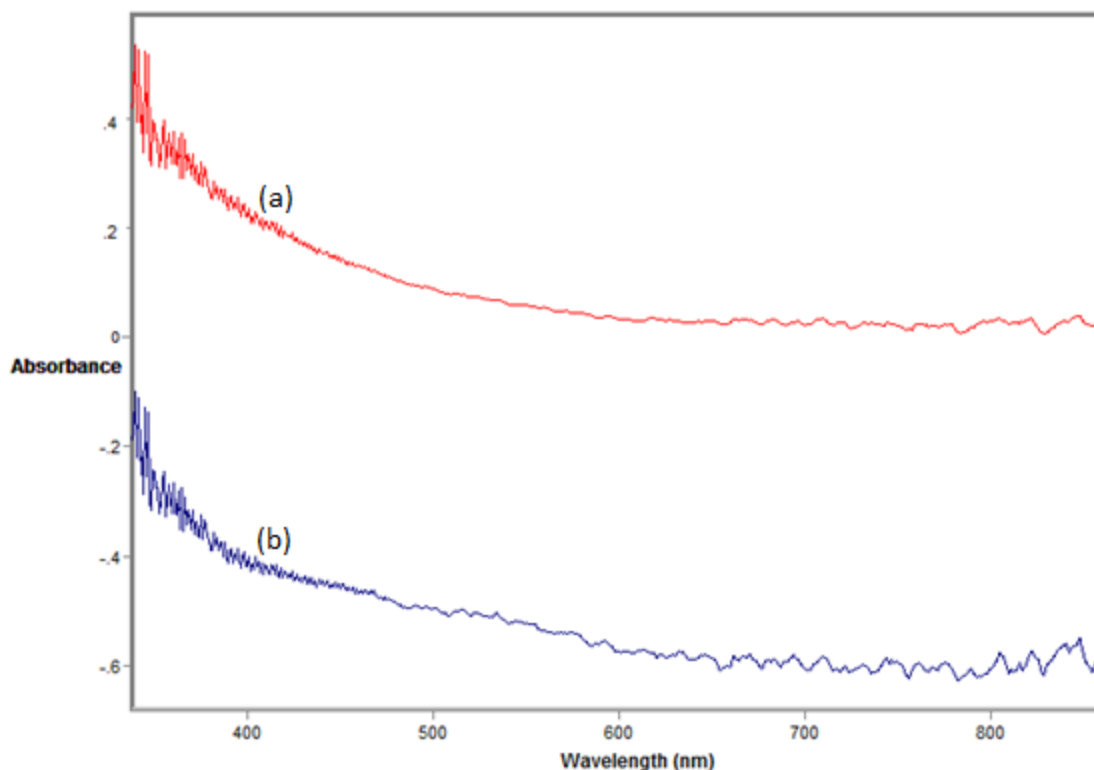


Figure 3.2. UV-Vis absorbance spectra of FeCl_3 -containing supernatants after being stirred with Co-C nanoparticles for 3 hours. a) Spectrum of the supernatant in DI water. b) Spectrum of the supernatant in 0.5 M NaCl. DFB is present in both cases.

In contrast, when the concentrations of iron (III) in the original solutions were measured, a clear DFB-Fe peak ($\lambda_{\text{max}} = 430 \text{ nm}$) could be seen in the UV-Vis spectrum. These are shown in Figure 3.3. For the supernatant containing no NaCl, the concentration was calculated to be $0.35 \pm 0.03 \text{ mM}$ iron (III). The concentration in the supernatant containing 0.5 M NaCl was calculated to be $0.43 \pm 0.03 \text{ mM}$ iron (III). Here, the error represents half the total absorbance of the noise at the top of each peak, because as one can see in Figure 3.3, the noise at the top of the peaks was quite substantial in these spectra. The noise is greater at the top of the peaks due to the relative signal-to-noise levels at different wavelengths. The detector measures light that

is not absorbed, so at wavelengths which are strongly absorbed, there is less signal getting to the detector. In turn, this makes the signal-to-noise ratio lower, resulting in a greater amount of noise at high absorbance values.

Overall, because there was iron (III) present in the solutions before stirring them with the particles, and no detectable iron (III) after, it can be said that in both cases, the particles were able to remove all of the iron (III) out of solution. Thus, it can be concluded that the presence of NaCl in solution did not hinder uptake of iron (III) by the particles.

The key to why iron (III) can adsorb onto the particles is their carbon coating, which consists of a few layers of graphene.¹ The coating may not be pure graphene – instead, there may be some graphite oxide functionality on the surface. Graphite oxide is an oxidized form of graphite; a sample structure of graphite oxide is shown in Figure 3.4. Among the basic graphite structure of interlocking benzene rings are epoxides, hydroxides, and carbonyls such as carboxylic acid.² These groups are able to chelate a variety of metals such as iron (III). Additionally, depending on the pH, some of these functionalities may become deprotonated, causing a negative charge on the surface. This negative charge may attract the positively-charged iron (III) ions (Fe^{+3}).

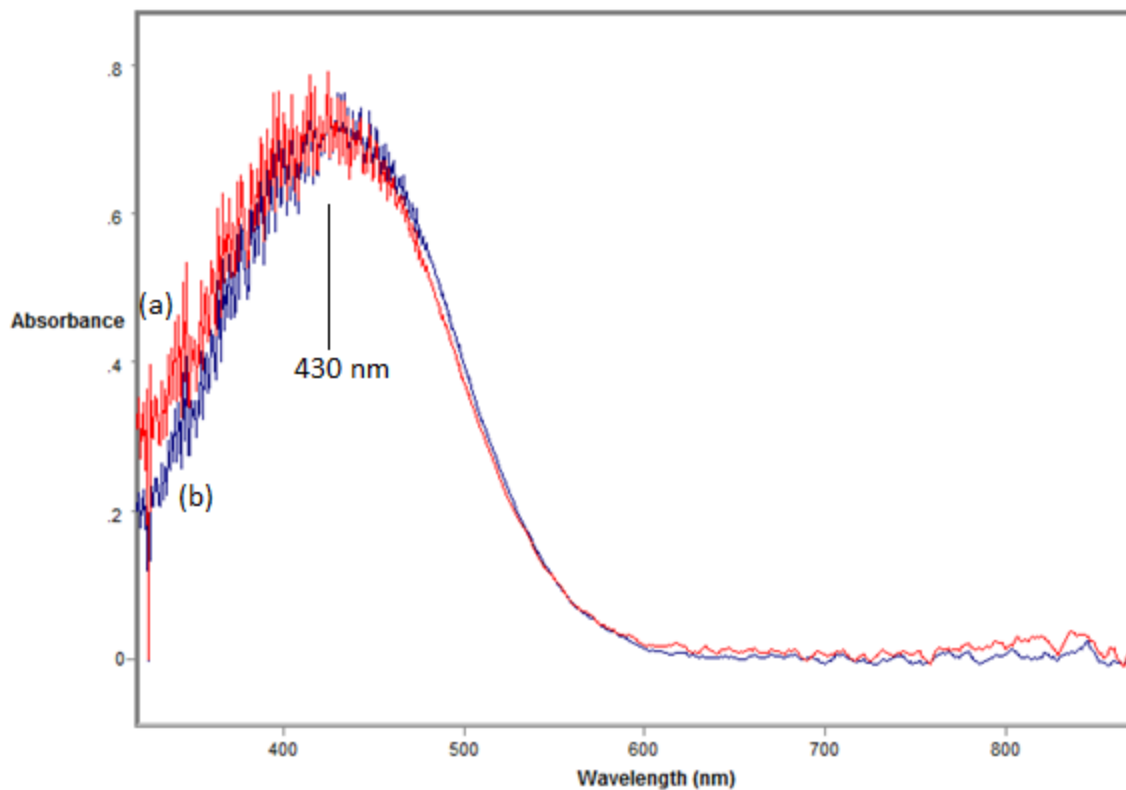


Figure 3.3. UV-Vis spectra of FeCl_3 solutions prior to stirring with particles. Both supernatants have had DFB added to them. a) Solutions in DI water; b) Solutions in 0.5 M NaCl.

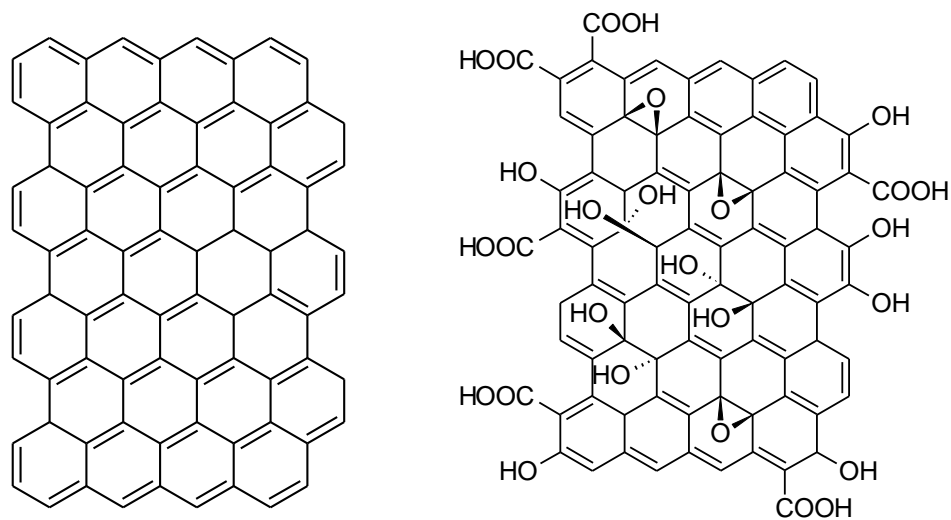


Figure 3.4. Sample structures of graphite and graphite oxide. The left structure is graphite while the right structure is graphite oxide.

3.3.2. Removing Iron (III) from Bare Co-C Nanoparticles with DFB – Initial Attempt

In this experiment, iron (III) was first removed from 20 mL of a solution of FeCl₃ using unmodified Co-C particles. Then, the particles were stirred with 5 mL 8 mM DFB (pH 1.88) in an attempt to remove iron (III) from the surface. Table 3.3 shows the amounts of iron (III) extracted as a function of time stirred.

Table 3.3. Amount of Iron (III) in the FeCl₃ Solution, FeCl₃ Supernatant, and DFB Supernatants (pH 1.88) as a Function of Time Stirred

Sample	Amount of Fe ⁺³ (μmol) in 20 mL
Original Solution (28.5 μM)	0.570
FeCl ₃ From Particles	0
DFB at t = 5 min.	0.160
DFB at t = 10 min.	0.234
DFB at t = 15 min.	0.266
DFB at t = 20 min.	0.262
DFB at t = 25 min.	0.232
DFB at t = 30 min.	0.231
DFB at t = 35 min.	0.230
DFB at t = 40 min.	0.214

The total amount of iron (III) added to the particles was 0.570 μmol. Table 3.3 also shows that after stirring the particles with the FeCl₃ solution, no DFB-Fe absorbance peak (and hence, no iron (III)) was measured in the supernatant, showing that all the iron (III) adsorbed onto the particles. The detection limit was calculated to be an absorbance of 0.0018, which is equivalent to 0.016 μmol in 20 mL. Therefore, no more than 0.016 μmol iron (III) was left in the solution after stirring it with the particles for 1 hour.

After that, the amount of iron (III) present in the DFB supernatant was measured as a function of total stirring time of the DFB solution at pH 1.88 with the particles. Figure 3.5 is a graph of the amount of iron (III) extracted in that supernatant as a function of stirring time with the particles. The DFB reaches a maximum in iron (III) extracted at about 15 minutes of stirring and at this point, 47% of the iron (III) in the original solution was recovered.

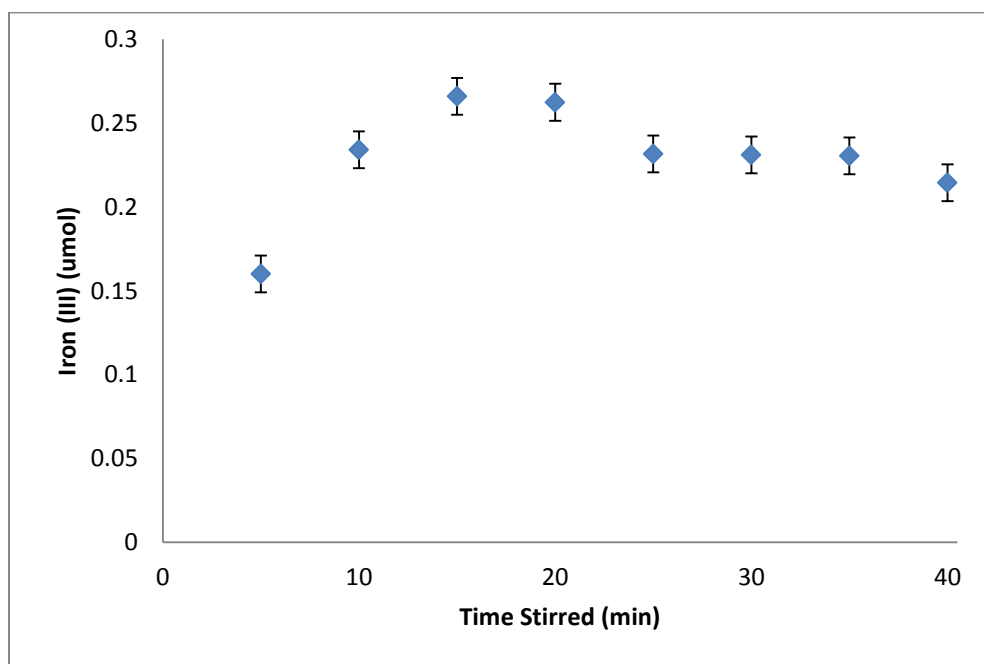


Figure 3.5. The amount of iron (III) measured in the DFB supernatant as a function of the amount of time spent stirring with the particles. The error bars represent 1 standard deviation in the baseline noise level.

Figure 3.5 shows a slight drop in the amount of iron (III) recovered after the 20-minute mark. It is possible that a small amount of the iron (III) was re-adsorbed by the particles as the stirring time was increased. Additionally, the UV-Vis spectra at later points in the stirring process showed more scattering (an increase in absorbance with

decreasing wavelength). This scattering profile partially obscured and overlapped with the peak at 430 nm, making selection of the baseline points difficult to estimate. This led to a measurement of the peak's intensity to be lower in value. The scattering is likely due to an increase in the amount of fine particulates in solution with stirring time.

3.3.3. Removing Iron (III) from Bare Co-C Nanoparticles with DFB: Varying DFB pH

In this experiment, four separate samples of Co-C nanoparticles were exposed to 20 mL FeCl₃. The concentration of the FeCl₃ solution used was measured to be 26.6 μM. The amount of iron (III) left in each supernatant after an hour of stirring with the particles was measured. Then, DFB was used to remove the iron from the particles. For each sample, the DFB used was adjusted to a different pH, to determine if this pH had an effect on the amount of iron (III) which could be removed from the particles. Depending on the pH, the DFB can lose up to 3 protons, giving it a charge of -3. Thus, the higher the pH, the more negatively-charged DFB can become.³ Increasing the negative charge on DFB will in turn increase the binding constant of DFB for iron (III) because the iron (III) is positively-charged.

Table 3.2 shows the different pH of the DFB solutions used. The amount of iron (III) detected as a function of stirring time is shown in Table 3.4. The detection limit for each case is also shown, because in many cases, there was no DFB-Fe peak in the spectrum.

The only sample in which the DFB appeared to acquire iron (III) was Supernatant A (where the DFB was adjusted to a pH of 2.06). In this case, after 2 hours, 0.206 μmol

iron (III) was found in the supernatant. This was 39% of the iron (III) in the 20 mL of FeCl₃ solution which was added to this particular sample of particles. In the initial experiment performed to remove iron (III) from Co-C nanoparticles, (Section 3.3.2), 47% of the iron (III) could be recovered from the particles, but after an increased time stirring, the amount in the supernatant appeared to decrease. In this experiment, the particles were stirred for a total of 2 hours. This is longer than the total stirring time of the experiment in Section 3.3.2, where the particles were only stirred for 40 minutes. It is possible that the amount of iron (III) collected was somewhat lower because of the longer stirring time.

Table 3.4. Amounts of Iron (III) in FeCl₃ Solution, FeCl₃ Supernatant, and DFB Supernatants

Sample	Amount of Fe ⁺³ (μmol) in 20 mL	Detection Limit (μmol)
Original FeCl ₃ Solution	0.532	0.031
FeCl ₃ Supernatant A	0	0.059
FeCl ₃ Supernatant B	0	0.041
FeCl ₃ Supernatant C	0	0.027
FeCl ₃ Supernatant D	0	0.023
DFB A (pH 2.06) at 1 hr	0.181	0.015
DFB B (pH 3.98) at 1 hr	0*	0.015
DFB C (pH 6.23) at 1 hr	0*	0.015
DFB D (pH 8.08) at 1 hr	0*	0.015
DFB A (pH 2.06) at 2 hr	0.206	0.015
DFB B (pH 3.98) at 2 hr	0*	0.015
DFB C (pH 6.23) at 2 hr	0*	0.015
DFB D (pH 8.08) at 2 hr	0*	0.015

*In these cases, the spectra were not flat. They had a scattering profile (increasing absorbance with decreasing wavelength) and/or a peak centered at 508 nm. Because there did not appear to be a peak in the normal range which DFB-Fe appears, the amount of DFB-Fe should be stated to be 0. However, because of these interfering features, it is difficult to say with certainty that there was no DFB-Fe in these samples.

In all cases, the spectra had a feature which significantly interfered with the ability to distinguish a DFB-Fe peak. In the spectra of DFB from samples B, C, and D after 1 hour, all had a peak centered at 508 nm. While the DFB-Fe peak may shift somewhat from its typical 430 nm absorbance, a shift greater than 70 nm seems unlikely. This is especially true given that these DFB supernatants appeared pink in color, while the DFB-Fe complex is more orange in color. Thus, this peak is due to another source. After 2 hours, some spectra still had this peak, while others only showed a large scattering curve (increasing absorbance with decreasing wavelength, in a $1/\lambda^4$ relationship).

The source of such interference (the peak at wavelengths above 500 nm and the scattering) was explored in Section 3.3.6. Nevertheless, from this experiment the efficiency of iron (III) extracted increased when the pH of the DFB used for extraction was adjusted to a pH of 2 or less. Even in this case, the yield of the iron (III) extraction was below 50%.

As discussed further in Section 3.3.7, iron (III) can form iron hydroxides in solutions of higher pH. This is why the iron (III) solutions are all adjusted to a pH between 2.5 and 2.8. Therefore, if the pH of the DFB solution was above 3 (as was the case with 3 of the 4 samples in this experiment), iron hydroxides could have formed before the DFB had a chance to react with the iron (III). For the sample exposed to DFB at a pH of 2, this would not have been a problem, because the low pH should have prevented the formation of iron hydroxides. However, this experiment still did not reveal why less than 50% of the iron (III) was recovered in this case.

3.3.4. Removing Iron (III) from Bare Co-C Nanoparticles with DFB – Adding NaCl

In this experiment, 50.7 mg Co-C nanoparticles were exposed to a solution of iron (III) in 1 M NaCl. An attempt was made to remove the iron (III) from the particles with a DFB solution, also made in 1 M NaCl. The ionic strength of the iron (III) solution was increased in order to repeat the results in Section 3.3.1, which indicated that the particles still took up iron (III) from such a solution. The DFB solution was made in 1 M NaCl because it was thought that it may prevent particles from becoming stable in solution. This is helpful because such an occurrence may be responsible for interference in UV-Vis spectra, such as scattering or the shifted peak seen in the experiment in Section 3.3.3.

Table 3.5 shows the amount of iron (III) in each sample measured. There was no DFB-Fe peak seen in the FeCl_3 supernatant after it had been allowed to stir with the particles. The detection limit in this case was an absorbance of 0.0038. This is equivalent to 0.033 μmol in 20 mL – thus, this is the maximum possible amount of iron (III) which could have been left in the supernatant after shaking with the particles. Also, note that the concentration of iron (III) in the original $\text{FeCl}_3/\text{NaCl}$ solution was measured to be 19.0 μM .

Figure 3.6 better shows the trend of iron (III) retrieval by the DFB/NaCl solution from the Co-C particles. Similar to the experiment done with no NaCl (Section 3.3.2), it appears that the maximum amount of iron (III) was removed from the particles after 15 minutes of stirring.

Table 3.5. Amounts of Iron (III) in FeCl₃ Solution, FeCl₃ Supernatant, and DFB Supernatants

Sample	Amount of Fe ⁺³ (μmol) in 20 mL
Original Solution (FeCl ₃ /1 M NaCl)	0.380
FeCl ₃ From Particles	0
DFB at t = 5 min.	0.117
DFB at t = 10 min.	0.208
DFB at t = 15 min.	0.274
DFB at t = 20 min.	0.274
DFB at t = 25 min.	0.272
DFB at t = 30 min.	0.283
DFB at t = 35 min.	0.267
DFB at t = 40 min.	0.262

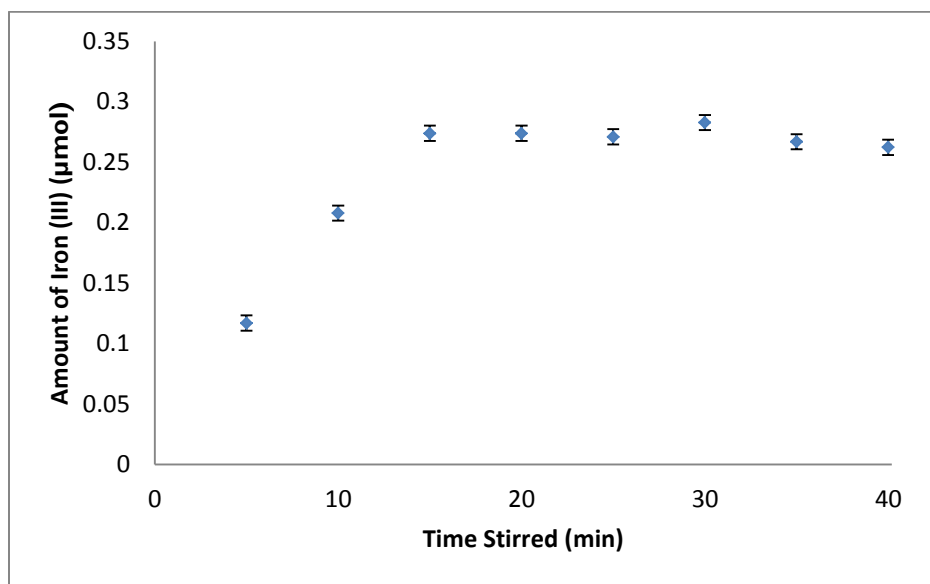


Figure 3.6. The amount of iron (III) measured in the DFB/NaCl supernatant as a function of the amount of time spent stirring with the particles. The error bars represent 1 standard deviation in the baseline noise level.

The error bars on all data points at 15 minutes and later overlap in Figure 3.6, indicating that these amounts of iron (III) are likely the same. Therefore, the amount of iron (III) is not decreasing. This is unlike what was seen in the experiment done with no

NaCl (Section 3.3.2), where the amount of iron (III) appeared to decrease somewhat after peaking at 15 minutes.

As to the relative amount of iron (III) recovered from the particles in the DFB, in this experiment, about 72% of the iron (III) found in 20 mL of the original solution was recovered by the DFB/NaCl solution. At first glance, this appears to be an improvement over the amount recovered in the experiment performed without NaCl present (Section 3.3.2). In that case, 47% of the iron (III) in the original solution was recovered. However, in this experiment, the FeCl₃ solution used had a lower concentration, so a higher percentage does not necessarily mean more iron (III) was recovered. In fact, in both cases, about 0.27 μmol of iron (III) was recovered – the higher percentage in this case is just due to the fact that there was less iron (III).

Because of these results, it was thought that perhaps the only reason not all the iron (III) could be recovered is that 0.27 μmol is the maximum amount of iron (III) which can be recovered by the DFB from Co-C nanoparticles. Theoretically, this should not be the case, because 5 mL of 8 mM DFB contains 40 μmol DFB, which is more than 100 times the amount of iron (III) present. Nonetheless, 0.27 μmol was the maximum amount which could be recovered. Therefore, the next step was to perform a similar experiment wherein less than 0.27 μmol of iron (III) was captured by the particles.

3.3.5. Removing Iron (III) from Bare Co-C Nanoparticles with DFB – Interference of Particles

The procedure described in Section 3.2.4 was repeated, but with a lower concentration of FeCl_3 . More specifically, the goal was to make a solution around $10\ \mu\text{M}$, so 1 mL of a 1 mM FeCl_3 solution was diluted to 100 mL. This experiment was performed twice.

In both attempts, a significant shift in the DFB-Fe peak was seen in the DFB supernatant. Figure 3.7 shows the UV-Vis spectrum of the FeCl_3 solution used in these experiments, compared to a UV-Vis spectrum of the DFB supernatant after attempting to remove iron (III) from the particles.

Spectrum (a) in Figure 3.7 is an example of a spectrum recorded through a solution of FeCl_3 with DFB added. This peak is centered at 430 nm. In contrast, when measuring the DFB-Fe peak in a DFB solution used to remove iron (III) from Co-C nanoparticles, the result was spectrum (b) in Figure 3.7. This peak is centered at 497 nm. Additionally, the shape of the peak is asymmetric toward higher wavelengths. This indicates that the peak seen in the DFB supernatant may not be entirely, or at all, due to the presence of DFB-Fe.

In any case, this problem (which also occurred when studying the effect of the DFB pH on these experiments in Section 3.3.3) had to be investigated before going further with this project. It was suspected that the shift in the peak may be due to a

small amount of the Co-C particles becoming stable in solution. To determine if this might be the case, the experiments described in Section 3.3.6 were performed.

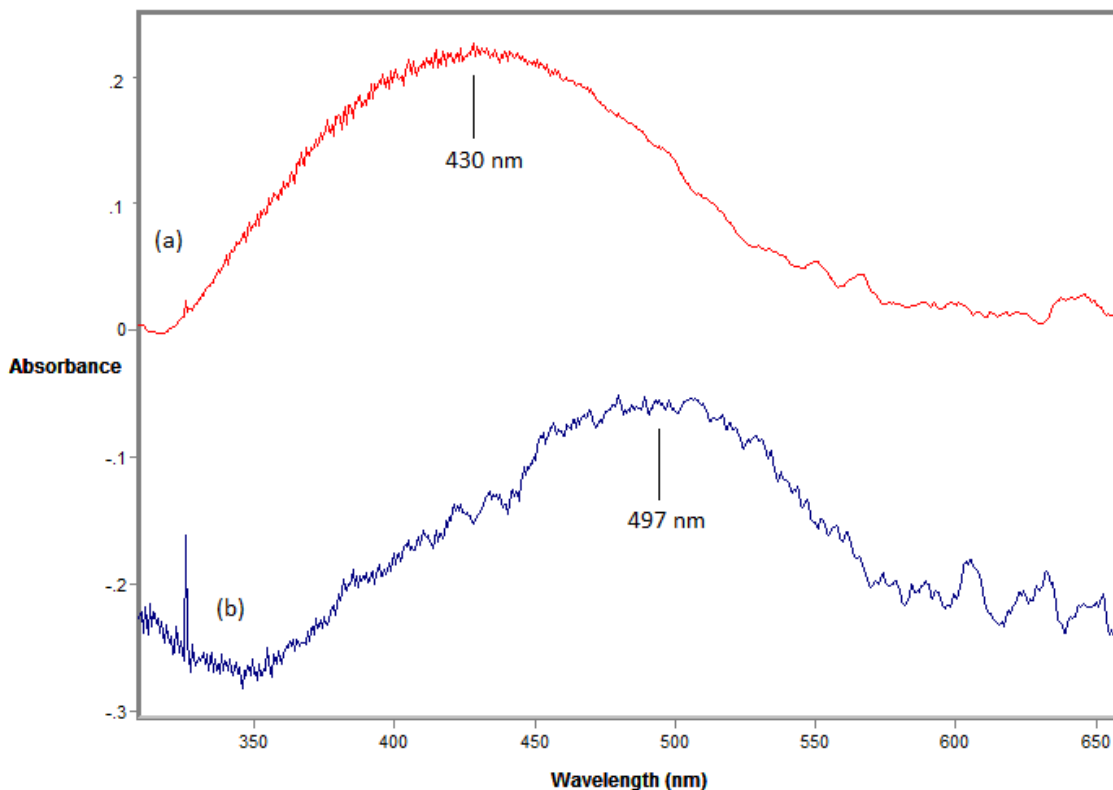


Figure 3.7. Absorbance UV-Vis spectra of a FeCl_3 solution with DFB added and a DFB solution used to remove iron (III) from Co-C nanoparticles. a) FeCl_3 with DFB added. b) DFB solution used to remove iron (III) from Co-C nanoparticles. Note: these spectra are not on the same absorbance scale; they were made to be of comparable size to easily see the differences between the two spectra.

3.3.6. Investigation of Particles' Interference in UV-Vis Spectra

To investigate whether particles becoming stable in solution could interfere with the UV-Vis spectrum, bare Co-C particles were sonicated and stirred in DI water and in water adjusted to pH 2. UV-Vis spectra of the supernatants were recorded.

Table 3.6 gives a description of observations (both spectral and otherwise) at various points in this experiment. In general, the pH 2 water supernatants showed a peak at around 510 nm after being sonicated, then shaken with Co-C nanoparticles. Additionally, the DI water supernatants showed a peak at around 410 nm after the same treatment. Whenever a peak appeared, the supernatant generally appeared to have a pinkish/orange color.

Table 3.6. Observations and Spectral Features of Supernatants Sonicated/Shaken with Co-C Nanoparticles

Sample/Point in Experiment	Features in UV-Vis Spectrum	Observations About Supernatant Color
DI Water Supernatant #1 – 1 cycle sonication/stirring	Flat	Clear
pH 2.08 Water Supernatant #1 – after sonication/stirring	Peak ~510 nm	Slightly Colored
DI Water Supernatant #1 – 2 cycles sonication/stirring	Peak ~410 nm	Slightly Colored
pH 2.08 Water Supernatant #2 – after sonication/stirring	Peak ~510 nm	Slightly Colored
DI Water Supernatant #2 – after sonication	Flat	Clear
pH 2.08 Water Supernatant #3 – after sonication	Maybe slight peak ~520 nm	Clear
DI Water Supernatant #2 – after stirring	Peak ~410 nm	Slightly colored
pH 2.08 Water Supernatant #3 – after stirring	Peak ~515 nm	Colored (pinkish)

It is important to remember that in this experiment, the only components present are the water (either DI water or water acidified to pH 2 with HCl) and the Co-C nanoparticles. Therefore, the peaks are most likely due to fine particles which dislodge from aggregates of nanoparticles, forming a stable suspension. The particles in the stable suspension are resistant to removal by the magnet. Neither water nor HCl absorb any wavelengths in the UV-Vis region of the electromagnetic spectrum and the pink colorization of the particles appears only after prolonged stirring of the particles (at least 5 minutes).

Additionally, the wavelength at which these peaks appear varied, depending on whether the supernatant was DI water or HCl. The color of nanoparticle suspensions is known to depend on the particle size, shape, and concentration in suspension. The size of nanoparticle aggregates which form can also have an effect.⁴ The size of aggregates and the distance between them is going to depend on the Debye length of the particles, which is the distance over which a charged species can have an electrostatic effect on its surroundings.⁵

The Debye length is affected by the surface charge, which in turn will be affected by the solution pH.⁵ The DI water's pH was not controlled, whereas the HCl was adjusted to a pH of 2. Therefore, the particles' surface charges are going to be different, depending on what solution they are in. Additionally, the HCl will have more charged species in solution, causing some charge screening, which will also affect the Debye length. Ultimately, because the solution pH affects the surface charge of the particles,

particles in different pH solutions will have different Debye lengths. The Debye length will affect the size of aggregates which form, so different Debye lengths will result in differently-sized aggregates. This will in turn affect the color of the suspension.

After obtaining the results in Table 3.6, we investigated possible solutions to the presence of fine particles in suspension. We examined if it was possible to “pre-screen” the particles. That is, before the addition of iron (III), particles would be sonicated in a supernatant, then washed, to remove any smaller, fine particles. During the addition of iron (III), only mechanical shaking would be used (not sonication) to avoid the additional formation of fine particulates.

Co-C particles were sonicated, shaken, then washed. They were shaken again in fresh DI water for 2 hours. UV-Vis spectra were recorded through the DI water supernatant every 30 minutes. For the first 60 minutes, the UV-Vis spectra remained flat. A peak appeared after 2 hours of shaking. Then, the particles were once again washed, added to fresh DI water, and shaken for 2 hours. Again, UV-Vis spectra were recorded through the DI water supernatant every 30 minutes. In this instance, a peak appeared in the UV-Vis spectrum after 90 minutes of shaking.

Therefore, it was determined that the maximum amount of time the particles should be stirred in any supernatant is 1 hour. Additionally, before using the particles in an experiment, they should be sonicated, and then washed with DI water. During the experiment, they should not be sonicated, only shaken. This was implemented in experiments performed throughout the remainder of the chapter.

3.3.7. Removing Iron (III) from Bare Co-C Nanoparticles with DFB – Using pH 2 HCl for Washes

Thus far, while the particles have been able to remove all of the iron (III) from a solution, recovery of iron (III) from the particles using a DFB solution has remained below 50%. While the iron (III) solution and, in most cases, the DFB solution are kept at a low pH, the water used to wash the particles between steps was just DI water. The reason pH is relevant is that, in solutions at a higher pH, iron (III) can form iron hydroxides and precipitate out of solution. Therefore, it was possible that by exposing the iron-covered particles to DI water, it could cause some iron (III) on the surface to precipitate and become inaccessible to the DFB.

Therefore, in the next experiment, rather than washing the particles with DI water, they were washed with an HCl solution at pH 2. Additionally, changes were made to the procedure in order to prevent fine particles from entering the solution phase (see Section 3.2.8). Other than that, the procedure for adding iron (III) to the particles and then removing them with DFB was the same as for the experiment described in Section 3.3.2. Table 3.7 shows the amount of iron (III) in the original solution, in the solution after stirring it with the Co-C nanoparticles, and in the DFB added post-iron (III) exposure at varying lengths of stirring time. Note that the iron (III) concentration of the original solution was found to be 27.4 mM.

Table 3.7. Iron (III) in FeCl₃ Solution, Supernatant, and DFB after Shaking with Co-C

Sample	Amount of Fe ⁺³ (μmol) in 20 mL
Original Solution	0.431
FeCl ₃ From Particles	0
DFB at t = 5 min.	0.0583
DFB at t = 10 min.	0.0961
DFB at t = 15 min.	0.105
DFB at t = 20 min.	0.105
DFB at t = 25 min.	0.115
DFB at t = 30 min.	0.119
DFB at t = 35 min.	0.118
DFB at t = 40 min.	0.122

Figure 3.8 also shows the amount of iron (III) recovered by the DFB from the particles as a function of stirring time. As with all previous experiments, there was no DFB-Fe peak detected in the iron (III) solution after it was allowed to stir with the particles. The detection limit was found to be an absorbance of 0.013, which translates to a measurement of 0.012 μmol iron (III) in 20 mL. Therefore, that is the maximum amount of iron (III) which could be left in solution.

The maximum amount of iron (III) recovered by the DFB appears to have been achieved after about 30 minutes of stirring time. Although a slightly larger amount was found in the DFB after 40 minutes, the error bars on the last three data points appear to overlap, indicating that these measurements are approximately the same number – about 0.12 μmol. In 20 mL of the original solution, there was 0.431 μmol, so the 0.12 μmol of iron (III) recovered is 28% of the iron (III) in solution. Therefore, washing the particles with a dilute HCl solution instead of DI water, between adding the iron (III)

and attempting to remove it, did not improve the amount of iron (III) recovered in the DFB solution. In fact, a lower percentage of iron (III) was recovered – in the other experiments discussed thus far in this chapter, the amount of iron (III) recovered was above 30%.

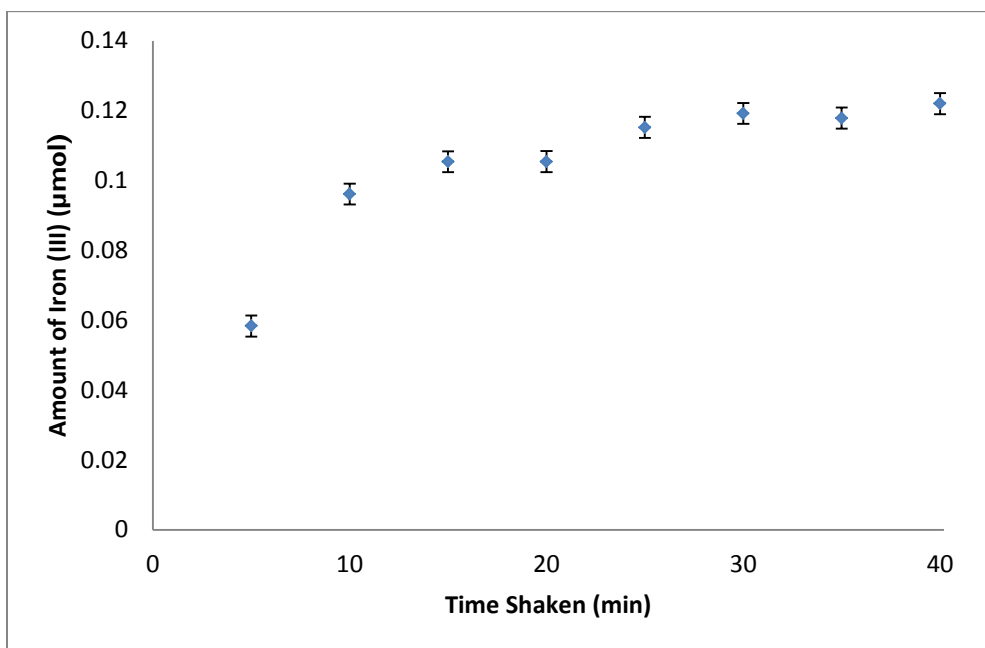


Figure 3.8. Amount of iron (III) in DFB as a function of time shaken. The error bars represent one standard deviation of the noise level in the baseline.

3.3.8. Removing Iron (III) from Bare Co-C Particles – Concentrating Iron (III) from <10 µM FeCl₃

After determining a potential way to avoid interference in the UV-Vis spectrum from particles becoming stable in solution, two experiments were done to determine if decreasing the FeCl₃ concentration would ultimately allow DFB to remove a larger portion of iron (III) captured by the particles.

In the first experiment, the concentration of iron (III) in the original solution was measured to be 9.1 μM . The results of this experiment are displayed in Table 3.8.

Note that there was once again no DFB-Fe peak in the UV-Vis spectrum of the iron (III) solution after it was stirred with the particles. The detection limit was found to be an absorbance of 0.0016, which translates to a measurement of 0.014 μmol iron (III) in 20 mL. Therefore, this is the maximum amount of iron (III) which could have been left in solution.

Table 3.8. Amounts of Iron (III) in FeCl_3 Solution, FeCl_3 Supernatant, and DFB Supernatants

Sample	Amount of Fe^{+3} (μmol) in 20 mL
Original Solution (FeCl_3 , 9.1 μM)	0.183
FeCl_3 From Particles	0
DFB at t = 5 min.	0.0819
DFB at t = 10 min.	0.149
DFB at t = 15 min.	0.171
DFB at t = 20 min.	0.183
DFB at t = 25 min.	0.188
DFB at t = 30 min.	0.177
DFB at t = 35 min.	0.187
DFB at t = 40 min.	0.190

The trend in the amount of iron (III) collected by the DFB with respect to the amount of time it was stirred with the particles is shown in graphical form in Figure 3.9. Interestingly, the maximum amount of iron (III) measured was technically 0.190 μmol . This is 104% of the iron (III) in the original solution. However, if the error is assumed to be 1 standard deviation of the noise in the baseline, this means each measurement was

$\pm 0.005 \mu\text{mol}$. The total amount of iron (III) measured in 20 mL of the original solution was $0.183 \mu\text{mol}$. Given an error of $\pm 0.005 \mu\text{mol}$, the difference between these two numbers is not significant.

Therefore, this experiment indicates that all of the iron (III) present in 20 mL of the $9.1 \mu\text{M FeCl}_3$ solution was captured by the Co-C nanoparticles and subsequently, taken off by the DFB solution. The results of this experiment were promising, indicating that if a relatively small amount of iron (III) is captured by the particles (in this case, below $0.2 \mu\text{mol}$), then an 8 mM DFB solution can remove it from the particles, concentrating it.

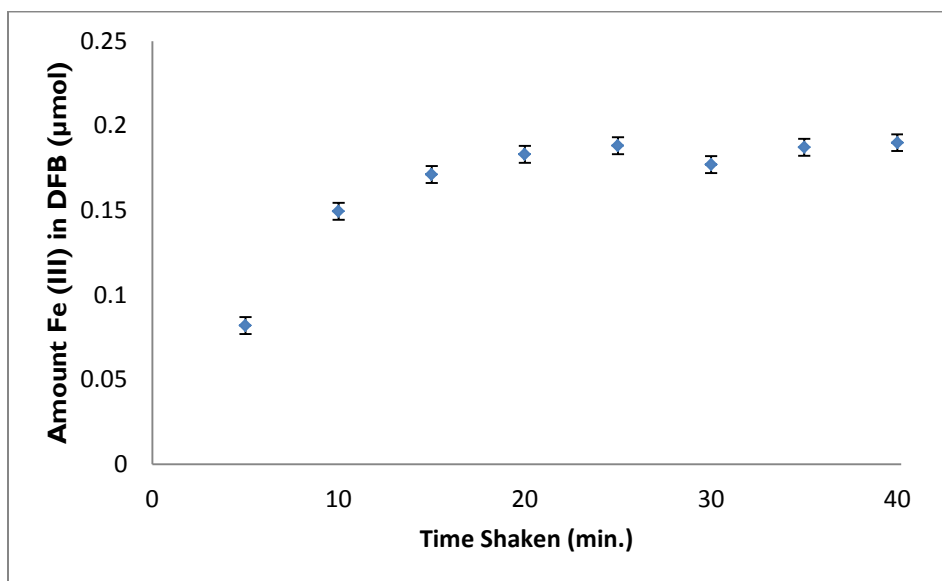


Figure 3.9. The amount of iron (III) measured in the DFB supernatant from Co-C nanoparticles as a function of the amount of time spent stirring with the particles. In this experiment, iron (III) was drawn from $9.1 \mu\text{M FeCl}_3$. The error bars represent 1 standard deviation in the baseline noise level.

These promising results prompted a second experiment to show repeatability in the measurement. In this case, the FeCl_3 solution used had a concentration of $7.1 \mu\text{M}$. The experiment was performed on 4 separate samples of Co-C nanoparticles. However, unlike all previous experiments discussed in this chapter, the evidence showed that none of the nanoparticle samples took any iron (III) out of solution. This data is shown in Table 3.9.

Unfortunately, for this experiment, only 1 baseline spectrum was recorded for each of the supernatant samples, so the error in these numbers cannot be determined in the same manner which it has been done throughout the chapter (see Section 3.2.11 for more details). Nonetheless, the fact that a DFB-Fe peak could still be detected in the FeCl_3 solution after shaking with the particles indicates that there is still iron (III) in the solution. After an FeCl_3 solution was stirred with the particles, about the same amount of iron (III) was detected as in the solution before exposure to the particles. In other words, this time, the particles did not take iron out of solution – there was not even a decrease in the amount of iron (III) present in solution.

Table 3.9. Amounts of Iron (III) in FeCl_3 Solution, FeCl_3 Supernatant

Sample	Amount of Fe^{+3} (μmol) in 20 mL
Original Solution (FeCl_3 , $7.1 \mu\text{M}$)	0.142
FeCl_3 from Particle Sample A	0.143
FeCl_3 from Particle Sample B	0.142
FeCl_3 from Particle Sample C	0.151
FeCl_3 from Particle Sample D	0.158

The DFB and water used in these experiments were not found to be contaminated with iron (III), so that does not explain the discrepancy. Other sources of contamination are unlikely, because the amounts of iron (III) detected fell within 0.02 μmol of each other.

It is not clear why, if contamination was not a factor, iron (III) could not be removed from the 7.1 μM FeCl_3 solution. Every other experiment described in this chapter shows that 100% of the iron (III) was removed from a FeCl_3 solution after stirring with the Co-C nanoparticles. This experiment would have to be repeated to determine if this were a true result. However, this portion of the project was halted here for reasons discussed in Section 3.4.

3.4. Conclusion

In all but one case, it was shown that the unmodified Co-C nanoparticles are capable of taking iron (III) out of a solution. This was attributed to the presence of graphite oxide functionalities on the surface which were capable of chelating metals such as iron (III). In the instances where this was not shown, it is possible that the experiment suffered from contamination. This experiment would need to be repeated in order to determine if it were a true result.

It was found that the iron (III) could not consistently be removed from the Co-C particles with a DFB solution. Only in one instance was 100% of the iron (III) adsorbed onto the particles recovered in a DFB solution, and that result could not be repeated. In most cases, less than 50% of the iron (III) was recovered.

It is possible that iron (III) cannot be completely recovered due the reaction of iron (III) with oxygen in the air. Between the addition of iron (III) to the particles and the addition of DFB to the particles, the particles are exposed to air. Although the exposure is less than a minute, the amount of iron (III) on any given sample of Co-C particles is less than 1 μmol and present as a very thin layer of iron (III) on the surface. Therefore, the small amount of iron (III) present could react to form oxyhydroxides when exposed to air. This would make the iron (III) inaccessible to the DFB, resulting in an incomplete recovery. To prevent this from happening when changing supernatants, the supernatant would have to be flushed out with a new solution to prevent the particles from becoming exposed to air. This would not be feasible to do in our lab without purchasing new equipment.

It was determined that the capture and concentration of iron (III) with untreated Co-C nanoparticles could no longer be pursued. The inconsistency in the amount of iron (III) which could be recovered from the particles made this scheme impractical. Additionally, allowing the particles to be exposed to air after becoming exposed to iron (III) may cause the formation of iron oxyhydroxides. This problem could not be fixed with the current available equipment. Therefore, for the remainder of the project, the focus was put on the work in Chapter 4.

3.5. References

1. Grass, R. N.; Athanassiou, E. K.; Stark, W. J., Covalently Functionalized Cobalt Nanoparticles as a Platform for Magnetic Separations in Organic Synthesis. *Angewandte Chemie-International Edition* **2007**, *46* (26), 4909-4912.
2. He, H. Y.; Klinowski, J.; Forster, M.; Lerf, A., A New Structural Model for Graphite Oxide. *Chemical Physics Letters* **1998**, *287* (1-2), 53-56.
3. Helm, Z. Determining Oceanic Iron Concentrations Using a Siderophore Based Sensor. University of Maine, 2013, M.S. Thesis.
4. Quinten, M., The Color of Finely Dispersed Nanoparticles. *Applied Physics B-Lasers and Optics* **2001**, *73* (4), 317-326.
5. Lebovka, N. I., Aggregation of Charged Colloidal Particles. In *Polyelectrolyte Complexes in the Dispersed and Solid State I: Principles and Theory*, Muller, M., Ed. Springer-Verlag Berlin: Berlin, 2014; Vol. 255, pp 57-96.

CHAPTER 4: IRON UPTAKE WITH SILICA-COATED, DESFERRIOXAMINE B-TREATED MAGNETIC NANOPARTICLES

4.1. Introduction

In the work of Roy *et. al.*, they derivatized a silicon wafer with DFB, which provided a means to quantitatively extract iron (III) from seawater at the low ppt level.¹ The wafer was first coated with a mesoporous silica, then functionalized with carboxylic acid groups using an alkoxysilane. The amine tail of DFB was reacted with the carboxylic acid groups to form an amide linkage, effectively attaching DFB to the surface. These wafers were then able to collect iron (III) out of a sample. Thus, a potential solution to the hurdles described in Chapters 2 and 3 is to coat the magnetic particles with a silica layer and then attach DFB, following the same protocols outlined by Roy *et. al.*

Initially, work in this chapter was done to coat the Co-C nanoparticles in silica, and then use Roy *et. al.*'s method to derivatize the surface with DFB. Other types of magnetic nanoparticles were also used in this chapter, primarily nickel nanoparticles and TurboBeads Silica™, and to a lesser degree, iron (II, III) oxide particles. The TurboBeads Silica™ are commercially available Co-C particles supplied with a silica coating.

4.2. Experimental

4.2.1. Materials

The following materials were obtained from Sigma-Aldrich: carbon-coated magnetic cobalt nanopowder (Co-C), deferoxamine mesylate salt (DFB), iron (III) chloride (FeCl_3), tetraethyl orthosilicate (TEOS), triethylamine, 1-ethyl-3-(3-dimethylaminopropyl)carbodiimide (EDC), 2-(N-morpholino)ethanesulfonic acid (MES) hydrate, TurboBeads Silica™ (Co-C-Silica), nickel nanopowder (Ni), iron (II, III) oxide (Fe_3O_4) nanopowder, oxalic acid dihydrate, sodium oxalate, nickel (II) chloride hexahydrate, and toluene. Ammonium hydroxide, sodium hydroxide, hydrochloric acid, and absolute/anhydrous ethanol were all purchased from Fisher Scientific. The potassium bromide (KBr) used was either from Sigma-Aldrich or Fisher Scientific. The 3-(triethoxysilyl)propylsuccinic anhydride (anhydride silane) came from Gelest, Inc.

The sodium hydroxide and hydrochloric acid were diluted as necessary and used to make pH adjustments to solutions. The MES hydrate was used to make buffers at a pH of 5. To do this, 0.195 g solid MES hydrate was added to 90 mL of DI water. The pH was adjusted to 5.0 with NaOH, and the volume was topped off to 100 mL. This made a 0.01 M MES buffer.

The FeCl_3 was received as a powder. To make a solution of FeCl_3 , first a 1 mM solution was made by dissolving the solid material in DI water (16.2 mg per 100 mL). The pH was adjusted to between 2.5 and 2.8 with concentrated HCl to prevent the formation of iron hydroxides in solution. Generally, a concentration close to 20 μM was

desired, so 2 mL of the 1 mM FeCl₃ was diluted to 100 mL with DI water. The pH of the diluted solution was immediately adjusted to between 2.5 and 2.8 with concentrated HCl to prevent the formation of iron hydroxides in solution. Solutions older than 1 week were discarded.

A Toyopearl® column derivatized with DFB was provided by Dr. Whitney King at Colby College. This column was used to remove iron (III) from 0.1 M solutions of oxalate. First, a 0.1 M solution of oxalate was prepared with sodium oxalate in DI water (1.34 g per 100 mL DI water) and adjusted to a pH of 8 using NaOH. This solution was run through the Toyopearl® column. The column was cleaned with an oxalic acid solution at a pH of 1.5. This solution was prepared with oxalic acid dihydrate in DI water (1.26 g per 100 mL DI water) and adjusted to a pH of 1.5.

A 0.1 M NiCl₂ solution was made by combining 2.3833 g NiCl₂ hexahydrate and 100 mL DI water in a 150 mL beaker.

All other materials listed above were used as received. The DFB and EDC were stored at -50 °C when not in use. The nickel nanopowder and anhydride silane were stored under nitrogen.

All UV-Vis spectra were recorded on an Ocean Optics USB 2000 UV-Vis spectrometer with SpectraSuite software. In general, after a background UV-Vis spectrum was recorded, 5 absorbance spectra were recorded through the solution used for the background. These were known as the baseline spectra. A 5 cm cuvette was used

unless otherwise noted. For background and absorbance spectra, each scan took 2 minutes.

Diffuse reflectance infrared spectra were recorded using an ABB-Bomem FTLA 2000 spectrometer at a resolution of 8 cm^{-1} . For diffuse reflectance spectra, 500 scans were used, taking a total time of approximately 6.5 minutes.

XPS measurements were recorded using a SPeCS instrument equipped with a VG Microtech Ltd dual Al anode x-ray source and a SPeCS HAS 3000 Plus x-ray analyzer.

Mass was recorded on a Mettler Toledo AG245 analytical balance. Mechanical shaking was performed using a Vibramax 100 from Heidolph. TEM images were recorded using a Philips CM10 instrument. The propeller stirrer used was an Arrow 1750. Calcination was performed in a Barnstead | Thermolyne 48000 furnace.

4.2.2. Washing the Particles

Washing was performed by adding the desired solvent (usually DI water, unless otherwise noted), mixing for about 2 seconds, drawing the particles to the side of the container using an external magnet, and then decanting the wash liquid or extracting the liquid with a pipette.

4.2.3. Treatment of Co-C Particles with Silica, Anhydride Silane, and DFB

This procedure was performed in an effort to acquire DFB-derivatized Co-C particles wherein the underlying graphene-like surface was completely coated with silica. The first step was to coat the surface of the particles in silica. To do this, 40 mL

ethanol, 10 mL DI water, and 1200 μ L ammonium hydroxide were combined with 0.1129 g Co-C nanoparticles in a 250 mL beaker. This mixture was sonicated for 1 hour (two 30-minute increments). Then, the mixture was moved to a propeller stirred beaker. As it was stirred vigorously, 395 μ L tetraethyl orthosilicate (TEOS) was added dropwise. The mixture was allowed to stir vigorously for 2 hours. Then, the supernatant was removed from the particles and the particles were washed 3 times with ethanol, then placed into a 10 mL beaker. The particles were dried under vacuum for 1 hour at 50 – 60 $^{\circ}$ C. (Note: it was only discovered after the fact that the typical procedure involves calcination at 500 $^{\circ}$ C.) A small portion was set aside for later characterization.

The remainder of this procedure was adopted from Eric Roy's method of derivatizing silica-coated wafers with DFB.¹ The particles were first functionalized with carboxylic acid using 3-(triethoxysilyl)propylsuccinic anhydride. The particles were added to a mixture of 50 mL toluene and 1000 μ L triethylamine in a 250 mL beaker. The beaker was shaken on a Vibramax 100 for about 10 minutes at 450 rpm. The supernatant was removed from the particles, then the particles themselves were washed with toluene and added to a fresh 50 mL aliquot of toluene in a 125-mL Erlenmeyer flask. The flask was stoppered with a rubber septum. N_2 gas was added to the flask through a syringe needle inserted into the septum.

Next, 2 mL of 3-(triethoxysilyl)propylsuccinic anhydride was added to the flask via a syringe. The syringe was rinsed into the flask three times with 5 mL toluene. The flask was shaken on a Vibramax 100 at 600 rpm for 1 hour. After shaking for an hour the

particles were removed from the supernatant and washed 3 times with DI water. To convert the anhydride functionality to a dicarboxylic acid, the particles were shaken in 10 mL DI water on a Vibramax 100 at 450 rpm for 15 minutes. A small portion was set aside for later characterization.

The necessary solution to derivatize the particles with DFB was mixed in the following procedure. First, approximately 10 mL of a 10 mg/mL solution of EDC/0.01 M MES buffer was made. Then, 0.1637 g deferoxamine mesylate salt was added to this solution. Next, 0.0360 g FeCl_3 (90% of the number of moles required to form 100% DFB-Fe) was added. This solution was added to the silica and carboxylic acid-derivatized particles, and the resulting mixture was allowed to shake for 3 hours at 450 rpm. After shaking, the supernatant was removed and the particles were washed 3 times with DI water. A portion was removed and dried for further characterization.

Each of the portions set aside for characterization was analyzed with diffuse reflectance FT-IR (DRIFT). For each, a 1% mixture of the sample in KBr was mixed using a mortar and pestle. A spectrum of each mixture was recorded against a background of pure KBr powder.

4.2.4. Iron Uptake of Silica- and DFB-Treated Co-C Particles

The DFB used during the derivatization was 90% bound with iron (III). To remove the iron (III) bound to the DFB, the particles were washed 7 times with 0.1 M oxalate. To perform each wash, 5000 μL 0.1 M oxalate was added to the particles. For the first wash, the pH of the oxalate was at 4, while for subsequent washes, it was at a pH of 1.5.

The mixture was shaken on a Vibramax 100 for 5 minutes at 450 rpm before the supernatant was removed. To measure the amount of iron (III) extracted into the oxalate supernatant, 4000 μL of the supernatant was combined with 1000 μL 2 mM DFB. This mixture was adjusted to a pH between 8 and 9 using NaOH. The exact volume of the NaOH added was recorded, as stated in Table 4.1. A UV-Vis spectrum of this mixture was recorded against a background of DI water.

Table 4.1. Amounts of NaOH Added for pH Adjustments – Measuring Iron (III) in Oxalate Supernatants

Oxalate Wash Number	NaOH (+ any HCl) Added to Oxalate/DFB Mixture (μL)
1	305
2	700
3	1220
4	850
5	850
6	650
7	800

Note: When the pH of the oxalate/DFB mixture exceeded 9, HCl was added to lower the pH to between 8 and 9. Also, the NaOH solution used was diluted, as needed, in an attempt to avoid adjusting the pH over 9. These two factors resulted in a varying amount of liquid added to make the necessary pH adjustment.

Next, the iron (III) uptake on these particles was measured. To do this, 20 mL of a solution of FeCl_3 (17.9 μM) was added to the Co-C-Silica-DFB particles. This mixture was shaken on a Vibramax 100 at 450 rpm for 1 hour before the supernatant was removed.

The iron (III) content of the original solution and this supernatant were each measured in the following way, using UV-Vis spectroscopy. First, 5000 μL of the solution to be measured for iron (III) content was added to a 5 cm cuvette. A background

spectrum was recorded through the solution, and then 500 μL 2 mM DFB was added to the cuvette and another spectrum was recorded.

4.2.5. Treatment of Fe_3O_4 , Ni Nanoparticles with Silica

This method of coating the surface of these nanoparticles with silica was based upon one used by Yue, *et. al.* on Fe_3O_4 particles.² To do this, 0.25 g of the nickel or Fe_3O_4 was added to a mixture of 100 mL ethanol, 25 mL DI water, and 3000 μL ammonium hydroxide. This mixture was sonicated for 1 hour and then transferred to a propeller stirred beaker. As the mixture was stirred vigorously, 875 μL TEOS was added dropwise. This was stirred for 2 hours before the supernatant was removed. The particles were washed 3 times with water. This was the last step performed to coat the nickel particles in silica.

After coating the Fe_3O_4 particles in silica, they were calcined in an oven. The oven was set to increase to 500 $^\circ\text{C}$ at 5 $^\circ\text{C}/\text{min}$, hold at 500 $^\circ\text{C}$ for 2 hours, then cool back down to room temperature at a rate of 5 $^\circ\text{C}/\text{min}$. The particles were analyzed with DRIFT spectroscopy.

4.2.6. Transmission Electron Microscopy (TEM) Of Silica-Treated Nanoparticles

TEM images were recorded of the following samples: nickel nanoparticles, silica-treated nickel nanoparticles, and TurboBeads Silica™. In each case, a small amount of the particles was dispersed in water by sonicating for 1 to 2 minutes. A drop of this

dispersion was applied to a sample grid and allowed to dry under a lamp. Once the grid was dry, TEM images were recorded.

4.2.7. Derivatizing TurboBeads Silica™ and Ni-SiO₂ with DFB

Once the particles were coated in silica, a similar procedure as the one used to treat silica-coated Co-C with anhydride silane and DFB was used on TurboBeads Silica™ and silica-treated Ni (see Section 4.2.3). The main difference was that the particles were shaken on a Vibramax 100 with the anhydride silane for about 18 hours instead of 1 hour to attempt to maximize the carboxylic acid groups on the surface. Also, one sample each of TurboBeads Silica™ and silica-treated Ni was derivatized, using DFB which had not first been reacted with iron (III). This was done in addition to treatment of samples with 90% DFB-Fe (as described in Section 4.2.3).

TurboBeads Silica™ treated with DFB will be referred to as Co-SiO₂-DFB, while TurboBeads Silica™ treated with DFB-Fe will be referred to as Co-SiO₂-FB. Nickel nanoparticles treated with DFB will be referred to as Ni-SiO₂-DFB, while nickel nanoparticles treated with DFB-Fe will be referred to as Ni-SiO₂-FB.

4.2.8. Characterization of Silica- and DFB-Treated Magnetic Nanoparticles

IR spectra of coated particles were measured by DRIFT. A 1% mixture (by weight) of the sample was prepared using a mortar and pestle. A spectrum of this mixture was recorded against a background of pure KBr powder.

XPS analysis of the particles was performed on the following samples: TurboBeads Silica, silica-treated Ni (Ni-SiO₂), TurboBeads Silica treated with DFB, TurboBeads Silica treated with 90% DFB-Fe, Ni-SiO₂ treated with DFB, and Ni-SiO₂ treated with 90% DFB-Fe. In each case, the sample was dried and spread onto a piece of double-sided carbon tape stuck to the sample holder. The sample was placed in the XPS, which was evacuated.

4.2.9. Iron (III) Uptake of Ni-SiO₂

This experiment was performed on 5 different 50 mg (\pm 4 mg) samples, each of which came from one of two batches of Ni-SiO₂.

As a control experiment, the iron (III) uptake of silica-coated Ni nanoparticles was measured. To do this, 20 mL of a 20 μ M solution of FeCl₃ was added to the particles. This mixture was shaken on a Vibramax 100 at 450 rpm for 1 hour. After that, the supernatant was removed. The iron (III) content of the original solution and this supernatant were each tested in the following way using UV-Vis spectroscopy. First, 5000 μ L of the solution to be tested was added to a 5 cm cuvette. A background spectrum was recorded through the solution, and then 1000 μ L 2 mM DFB was added to the cuvette and another spectrum was recorded.

4.2.10. Iron (III) Uptake of Ni-SiO₂-DFB

The procedure described in Section 4.2.9 was also performed on the Ni-SiO₂-DFB. In this case, DFB (not DFB-Fe) was reacted with the Ni-SiO₂ particles derivatized with the anhydride silane.

4.2.11. Iron (III) Uptake of Ni-SiO₂-FB; Removal of Iron (III) from Particles

Removal of iron (III) from the Ni-SiO₂-FB particles was done by washing with oxalate solutions. To do this, 0.1 M oxalate at pH 1.5 was added to the particles. This suspension was shaken on a Vibramax 100 for 5 minutes, after which the supernatant was removed from the particles. Then, 4000 µL of this supernatant was mixed with 1000 µL 2 mM DFB. This mixture was adjusted to a pH between 8 and 9 using NaOH. The exact volume of the NaOH added was recorded, as stated in Table 4.2. Also, a UV-Vis spectrum of this mixture was recorded against a background of DI water unless otherwise noted.

To add iron (III) to the particles, the procedure from Section 4.2.9 was used.

An outline of the order and number of times the above procedures were performed on the Ni-SiO₂-FB particles is presented in the list below, with any changes noted. In between each addition of oxalate or FeCl₃, the particles were washed 3 times with DI water.

- Step 1: Remove Iron (III) by Washing with 0.1 M Oxalate at pH 1.5
 - Wash with 5000 µL for 5 Minutes

- Repeat
- Step 2: Add Iron (III) by Stirring with 20 mL 32.0 μM FeCl_3 for 1 Hour
- Step 3: Remove Iron (III) by Washing with 0.1 M Oxalate at pH 1.5
 - Wash with 10 mL for 5 Minutes
 - Repeat, but with 5000 μL oxalate
 - Note: the background for these measurements was a mixture of 4000 μL from the 10 mL wash and 1500 μL DI water.
- Step 4: Add Iron (III) by Stirring with 20 mL 17.2 μM FeCl_3 for 1 Hour
- Step 5: Remove Iron (III) by Washing with 0.1 M Oxalate at pH 1.5
 - Wash with 5000 μL for 5 Minutes
 - Repeat
- Step 6: Add Iron (III) by Stirring with 20 mL 17.5 μM FeCl_3 for 1 Hour

Table 4.2. Amounts of NaOH Added for pH Adjustments – Measuring Iron (III) in Oxalate Supernatants from Ni-SiO₂-FB

Oxalate Wash	NaOH (+ any HCl) Added to Oxalate/DFB Mixture (μL)
Step 1 – Wash #1	505
Step 1 – Wash #2	500
Step 3 – Wash #1	495
Step 3 – Wash #2	495
Step 5 – Wash #1	500
Step 5 – Wash #2	600

Note: When the pH of the oxalate/DFB mixture exceeded 9, some HCl was added to lower the pH to between 8 and 9.

4.2.12. UV-Vis Spectra of 0.1 M NiCl₂, Product of Oxalic Acid and Ni Nanoparticles

First, 0.0290 g of nickel nanoparticles were added to a 50 mL plastic centrifuge tube. Then, 5000 μ L 0.1 M oxalate, at a pH of 1.6, was added to the particles. This suspension was shaken on a Vibramax 100 at 450 rpm for 15 minutes. After 15 minutes, the supernatant was removed and added to a 5 cm cuvette. A UV-Vis spectrum of this supernatant was recorded. A UV-Vis spectrum of a 0.1 M NiCl₂ solution in a 1 cm cuvette was also recorded. In both cases, the background was DI water.

4.2.13. Iron (III) Uptake of TurboBeads Silica™

The procedure for this experiment was the same as that in Section 4.2.9, but performed on TurboBeads Silica™. A total of five 50 mg (\pm 4 mg) samples of TurboBeads Silica™ were tested.

4.2.14. Iron (III) Uptake of Co-SiO₂-DFB

It should be noted that a new sample of Co-SiO₂-DFB had to be prepared after XPS was performed, because the XPS measurements consumed the entirety of the original sample. The same procedure was used, as described in Section 4.2.7.

First, iron (III) was added to the particles, using the same procedure as described in Section 4.2.9 (iron (III) uptake of Ni-SiO₂). Next, the Co-SiO₂-DFB particles were washed with oxalate to remove iron (III). To do this, 0.1 M oxalate at pH 1.5 was added to the particles. This suspension was shaken on a Vibramax 100, after which the supernatant was removed from the particles. Then, to measure the amount of iron (III)

captured by the oxalate, 4000 μL of the oxalate supernatant was mixed with 1000 μL 2 mM DFB. This mixture was adjusted to a pH between 8 and 9 using NaOH. The exact volume of the NaOH added was recorded, as stated in Table 4.3. A UV-Vis spectrum of this mixture was recorded against a background of DI water, unless otherwise noted.

The procedure to wash the particles with oxalate was repeated 6 times on this sample. For the first three washes, the particles were shaken on a Vibramax 100 for 5 minutes. For the fourth and fifth washes, the suspension was shaken for 15 minutes; for the sixth wash, it was shaken for 20 minutes.

Table 4.3. Amounts of NaOH Added for pH Adjustments – Measuring Iron (III) in Oxalate Supernatants from Co-SiO₂-DFB

Oxalate Wash	NaOH (+ any HCl) Added to Oxalate/DFB Mixture (μL)
1	580
2	570
3	500
4	520
5	550
6	570

Note: When the pH of the oxalate/DFB mixture exceeded 9, some HCl was added to lower the pH to between 8 and 9.

In between the addition of iron (III) and the first addition of oxalate, as well as between each subsequent addition of oxalate, the particles were washed 3 times with DI water.

4.2.15. Iron (III) Uptake of Co-SiO₂-FB

It should be noted that a new sample of Co-SiO₂-FB had to be prepared after XPS analysis because the XPS measurements consumed the entirety of the original sample. The procedure described in Section 4.2.7 was used in preparing a new batch.

First, the procedure described in Section 4.2.14, to remove iron (III) from the particles with oxalate, was performed on the Co-SiO₂-FB to remove any iron (III) which might be present. Two oxalate washes were performed. Then, as described in Section 4.2.9, iron (III) was added to the particles. After that, two more oxalate washes were performed, again using the same procedure as in Section 4.2.14. The amounts of NaOH added to mixtures of oxalate and DFB for pH adjustments are stated in Table 4.4.

Table 4.4. Amounts of NaOH Added for pH Adjustments – Measuring Iron (III) in Oxalate Supernatants from Co-SiO₂-FB

Oxalate Wash	NaOH (+ any HCl) Added to Oxalate/DFB Mixture (μL)
Wash #1 (Before adding FeCl ₃)	520
Wash #2 (Before adding FeCl ₃)	550
Wash #1 (After adding FeCl ₃)	470
Wash #2 (After adding FeCl ₃)	470

Note: When the pH of the oxalate/DFB mixture exceeded 9, some HCl was added to lower the pH to between 8 and 9.

4.2.16. Calculations

Equations 2.1 – 2.3 (See Chapter 2) were used again to calculate the amount of iron (III) from the absorbance of a DFB-Fe UV-Vis peak. Additionally, the error in this measurement was determined in the same manner as described in Section 3.2.11.

4.3. Results and Discussion

4.3.1. Characterization of Co-C Particles Treated with Silica and DFB

In order to determine if Co-C particles were successfully treated with silica, then carboxylic acid, and then finally DFB, DRIFT spectra were recorded. The spectra recorded after each of these steps were performed are shown in Figure 4.1. Not shown, for simplicity, is the spectrum of unmodified Co-C particles. The only feature in such a spectrum is a low-intensity broad peak centered at 1400 cm^{-1} . This band is due to the aromatic C=C stretching of the graphene carbon coating.

After treatment of the Co-C particles with silica, the IR spectrum (Figure 4.1 (a)) shows a new broad peak at 1130 cm^{-1} , which is characteristic of the Si-O stretching mode of silica. Therefore, the presence of this peak indicates that the particles were coated with silica.

After the derivatization with the anhydride silane followed by exposure to water, the IR spectrum in Figure 4.1 (b) shows bands at 1720 cm^{-1} and 1570 cm^{-1} . The 1720 cm^{-1} peak is a carbonyl peak, due to the C=O stretching of the carboxylic acid (COOH). The peak at 1570 cm^{-1} is assigned to a carboxylate (COO^-) mode. This shows that the surface was derivatized to contain carboxylic acid groups.

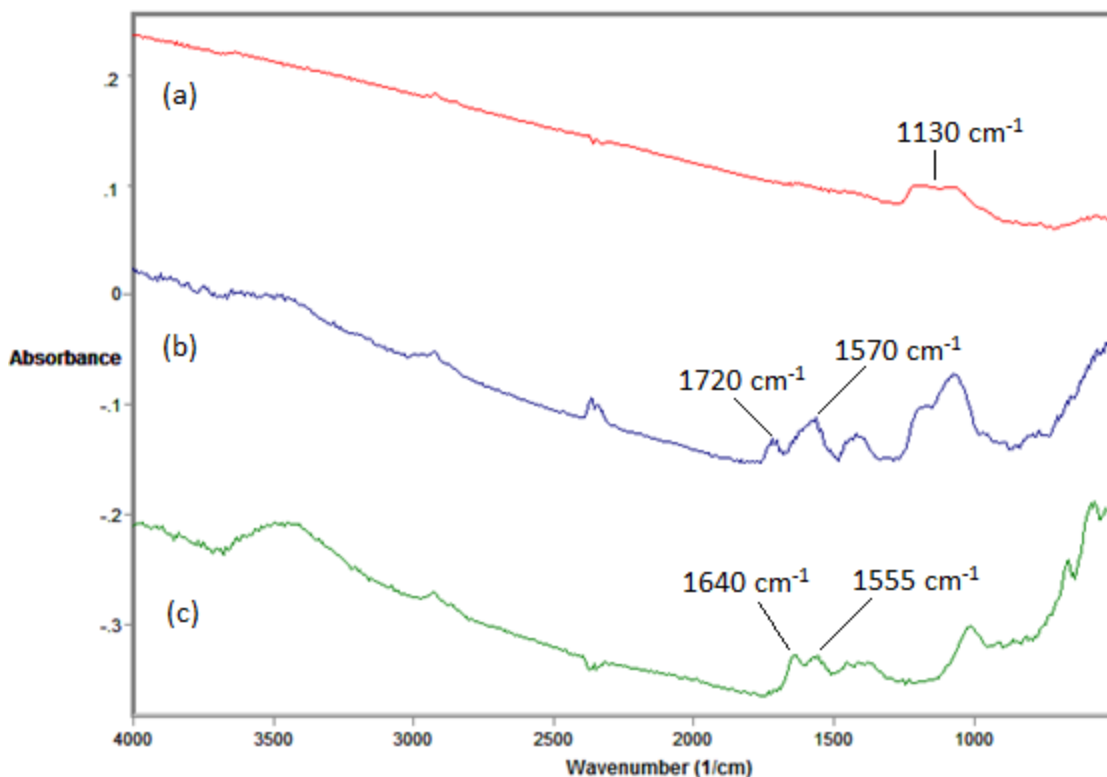


Figure 4.1. DRIFT spectra of Co-C particles. This was after a) treatment with silica, then b) treatment with anhydride silane, followed by exposure to water, and then c) treatment with 90% DFB-Fe.

Figure 4.1 (c) was obtained after treatment with DFB-Fe. The C=O band of the carboxylic acid is gone and two new bands appear at 1640 cm^{-1} and 1555 cm^{-1} . The reaction of carboxylic acid groups on the surface with the amine group of the DFB is expected to produce an amide linkage and two bands at 1650 cm^{-1} (amide I) and 1550 cm^{-1} (amide II) of equal intensity. The disappearance of the band at 1720 cm^{-1} in Figure 4.1 (b) shows that the carboxylic acid is involved in the reaction with the DFB-Fe. While the two bands at 1640 cm^{-1} and 1555 cm^{-1} coincide with the expected wavenumbers for amide formation, the 1640 cm^{-1} band is more intense than the one at

1555 cm^{-1} . This is because the 1640 cm^{-1} band contains a contribution from the bending mode of water. There is a broad peak at 3423 cm^{-1} due to the O-H stretching mode of water, showing that the surface contains adsorbed water. However, the intensity of the 3423 cm^{-1} peak (water stretching mode) should be at least twice as intense as the water bending mode at 1640 cm^{-1} . That is not the case here, so that peak at 1640 cm^{-1} has contributions from the bending mode of water and from the amide I mode. In other words, the amide linkage between the amine tail of DFB and the carboxylic acid on the surface was successfully formed.

4.3.2. Iron Uptake of Silica- and DFB-Treated Co-C Particles

Measurement of the iron (III) levels of the oxalate washes with DFB by recording UV-Vis spectra was not possible. The UV-Vis spectra showed peaks which interfered with the quantification of the DFB-Fe peak at 430 nm. For example, Figure 4.2 shows the UV-Vis spectrum of the second oxalate wash after adding DFB and adjusting the pH to 8.25. A broad feature, increasing in intensity, appears from 600 nm to 400 nm, obscuring detection of the DFB-Fe band at 430 nm. This is due to scattering of the light as it passes through the sample. It is possible that some particles have become stable in solution with the oxalate wash, which leads to scattering of the light. Additionally, it was observed that in some oxalate washes, the solution appeared to be slightly cloudy after stirring with the Co-C particles. This cloudiness is also indicative of particulates in solution. There is also a weak peak centered at 502 nm, which is 70 nm higher than the normal location for a DFB-Fe peak, appearing on top of the scattering curve.

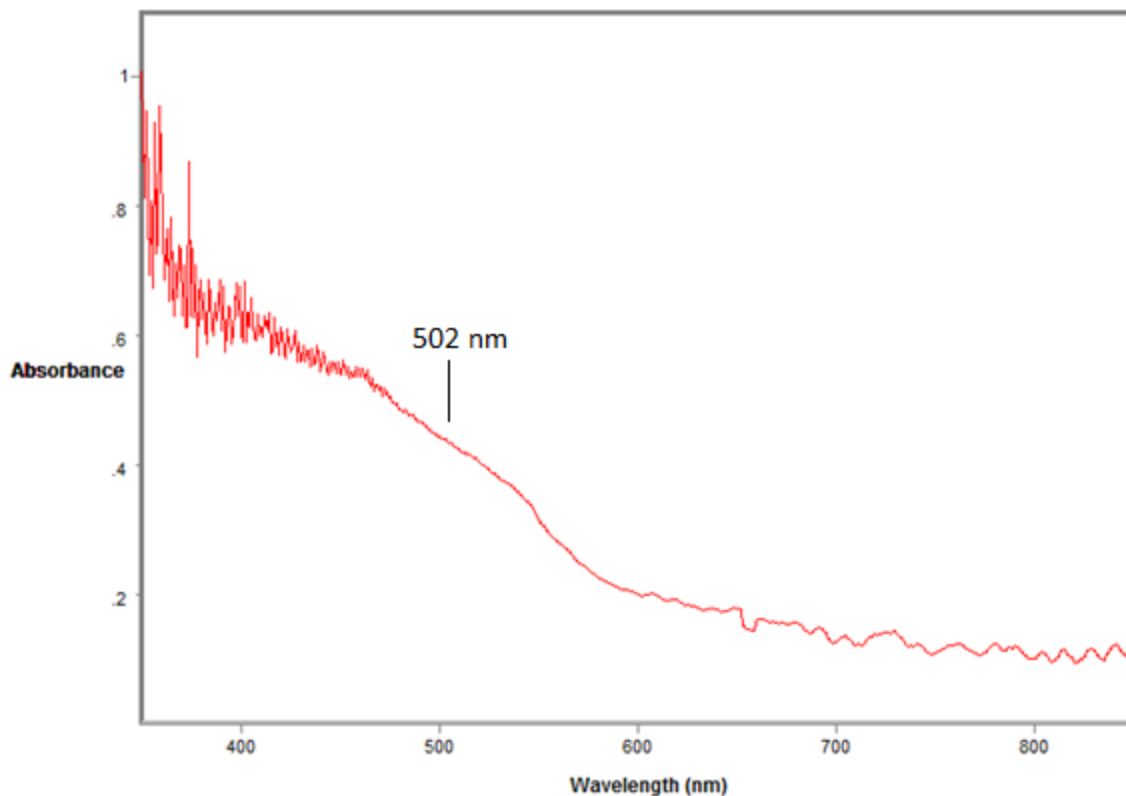


Figure 4.2. UV-Vis spectrum of the second oxalate wash of silica/DFB-treated Co-C nanoparticles.

Figure 4.3 shows the UV-Vis spectrum of the seventh and last oxalate wash performed on these particles. As with Figure 4.2, an increase in absorbance with a decreasing wavelength (scattering) can be seen. However, there is no sign of any other peaks, including a DFB-Fe peak. It was concluded that any iron (III) which could be removed from these particles had been removed by this point.

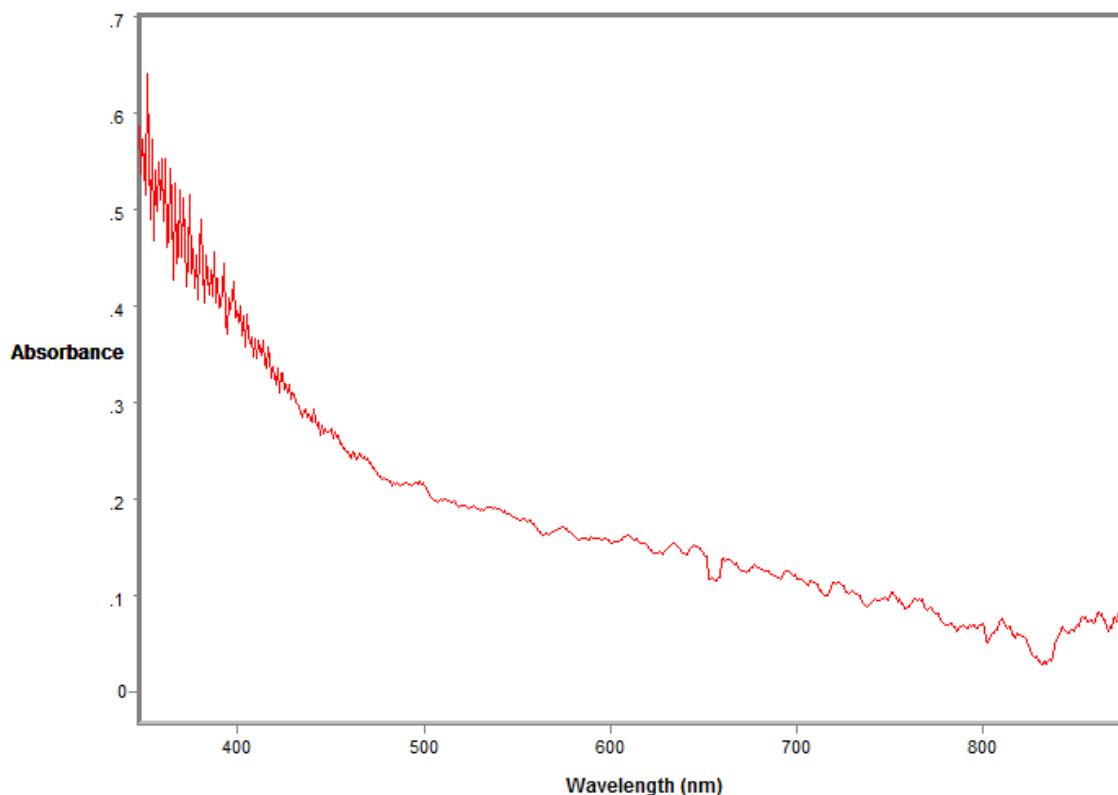


Figure 4.3. UV-Vis spectrum of the seventh oxalate wash of silica/DFB-treated Co-C nanoparticles.

The DFB-treated Co-C particles were exposed to solutions containing iron (III).

Table 4.5 shows the amount of iron (III) present in 20 mL of the FeCl_3 solution, before adding it to the particles, and in the supernatant, after this solution was stirred with the particles.

Table 4.5. Amount of Iron (III) in FeCl_3 Solution Before and After Stirring with Co-C/Silica/DFB Particles

Sample	Amount of Fe^{+3} (μmol) in 20 mL
Original Solution (FeCl_3 , 17.9 μM)	0.358 ± 0.003
FeCl_3 Solution from Particles	0.357 ± 0.002

The margins of error represent one standard deviation of noise in the baseline spectra of each measurement. In any case, the amount of iron (III) measured before and after stirring with the DFB-treated Co-C particles only differed by 0.001 μmol – well within the margins of error for both measurements. Therefore, the same amount of iron was present in solution before and after it was stirred with the DFB-treated particles. This means that, despite having DFB on the surface, these particles did not take iron (III) out of solution.

As discussed previously in this section, some of the oxalate supernatants from the oxalate washes (performed before adding iron) appeared cloudy. It is possible that this cloudiness was due to small amounts of silica coming off of the surface. Next, we recorded a DRIFT spectrum of the DFB-treated Co-C particles, after their exposure to iron (III) (which was also after their exposure to oxalate). This is shown in Figure 4.4 (b).

Figure 4.4 (a) shows the spectrum of the DFB-treated Co-C particles before their exposure to oxalate. This is the same spectrum as in Figure 4.1 (c). Figure 4.4 (b) is the spectrum of the DFB-treated Co-C particles again after their exposure to oxalate and FeCl_3 . After exposure to oxalate and FeCl_3 , a large peak at 1638 cm^{-1} and a pair of peaks at 1367 cm^{-1} and 1321 cm^{-1} are obtained. There is also no sign of a Si-O-Si stretching peak at 1000 to 1100 cm^{-1} , showing the absence of a silica coating. The peak at 1638 cm^{-1} is assigned to the carbonyl stretch of oxalate. The 1367 cm^{-1} and 1321 cm^{-1} peaks are also known to appear in oxalates³, which are attributed to the stretching of the C-O bond in oxalate.

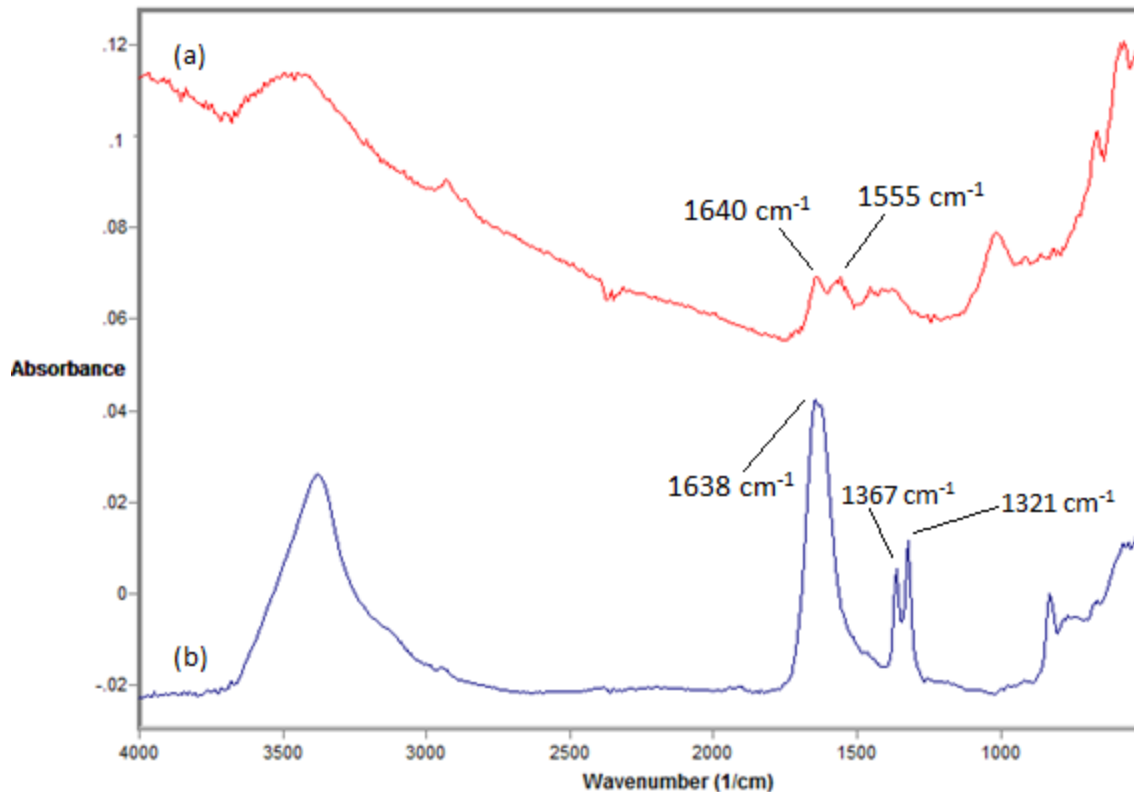


Figure 4.4. DRIFT spectra of silica- and DFB-treated Co-C nanoparticles. This was a) before exposure to oxalate and b) after exposure to oxalate and FeCl_3 solutions.

The presence of peaks which can be attributed to oxalate indicates that during the oxalate washes, oxalate adsorbed onto the surface of the particles. The lack of peaks due to silica suggests that the oxalate washes led to the removal of the silica coating (and hence, the attached DFB) from the Co-C nanoparticles. This would explain why the particles were not able to take iron (III) out of solution.

The cloudiness observed in the oxalate washes is consistent with the removal of silica from the particulate surface. It is possible that the carbon coating makes the Co-C particles a poor substrate for anchoring the silica coating. Because the carbon coating is

hydrophobic, it doesn't wet as well or form covalent linkages with the silica layer, as compared to the hydrophilic silicon layer used in Roy *et. al.*¹ For this reason, it was decided to try forming a silica substrate on a different magnetic material.

4.3.3. TEM Images of Silica-Coated Nanoparticles

After determining that Co-C particles were not reliably coated with silica, alternative materials for magnetic particulates to coat with silica were sought. TurboBeads Silica™, a version of the Co-C particles which comes pre-functionalized with silica, was bought for this purpose. Also purchased were nickel nanoparticles, which had to be coated with a layer of silica after purchase.

Before derivatization of these particles with DFB, TEM images of these particles were recorded in an attempt to determine the completeness of their coatings. Figure 4.5 shows the nickel nanoparticles, while Figure 4.6 shows these particles after being coated in silica.

The nickel nanoparticles were not uniform in shape and varied in diameter from about 10 to 25 nm. Figure 4.6 shows that when coating these particles with silica, the silica appeared to have polymerized around groups of nanoparticles, forming particulate clusters over 100 nm in size.

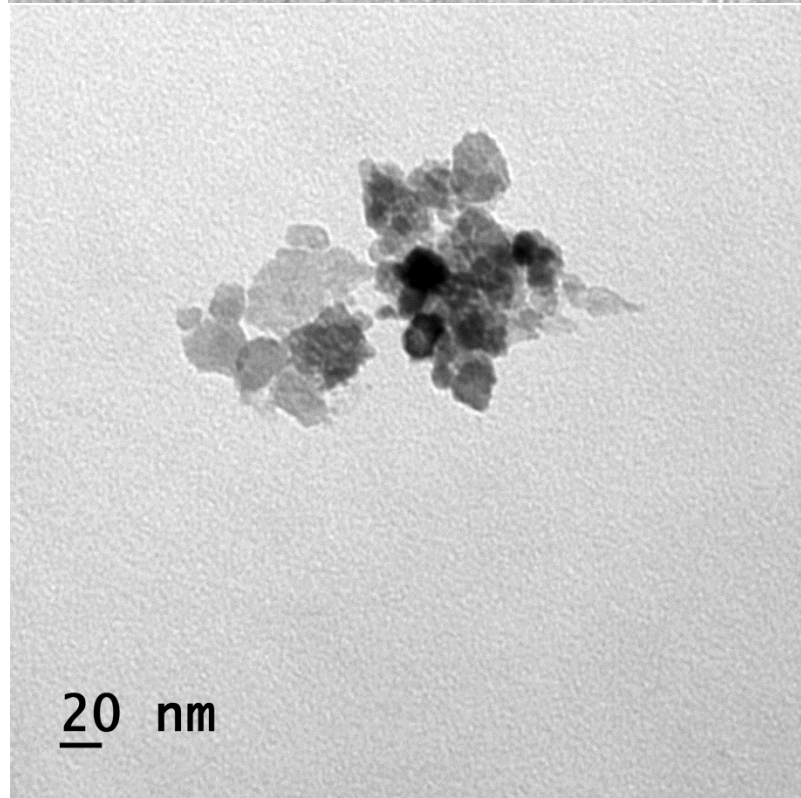
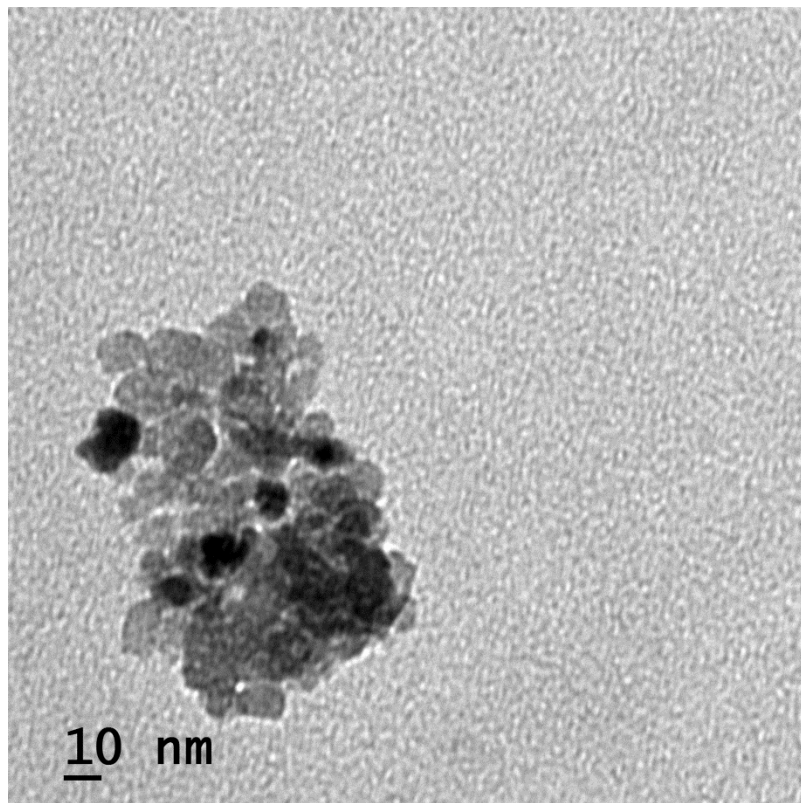


Figure 4.5. TEM images of nickel nanoparticles.

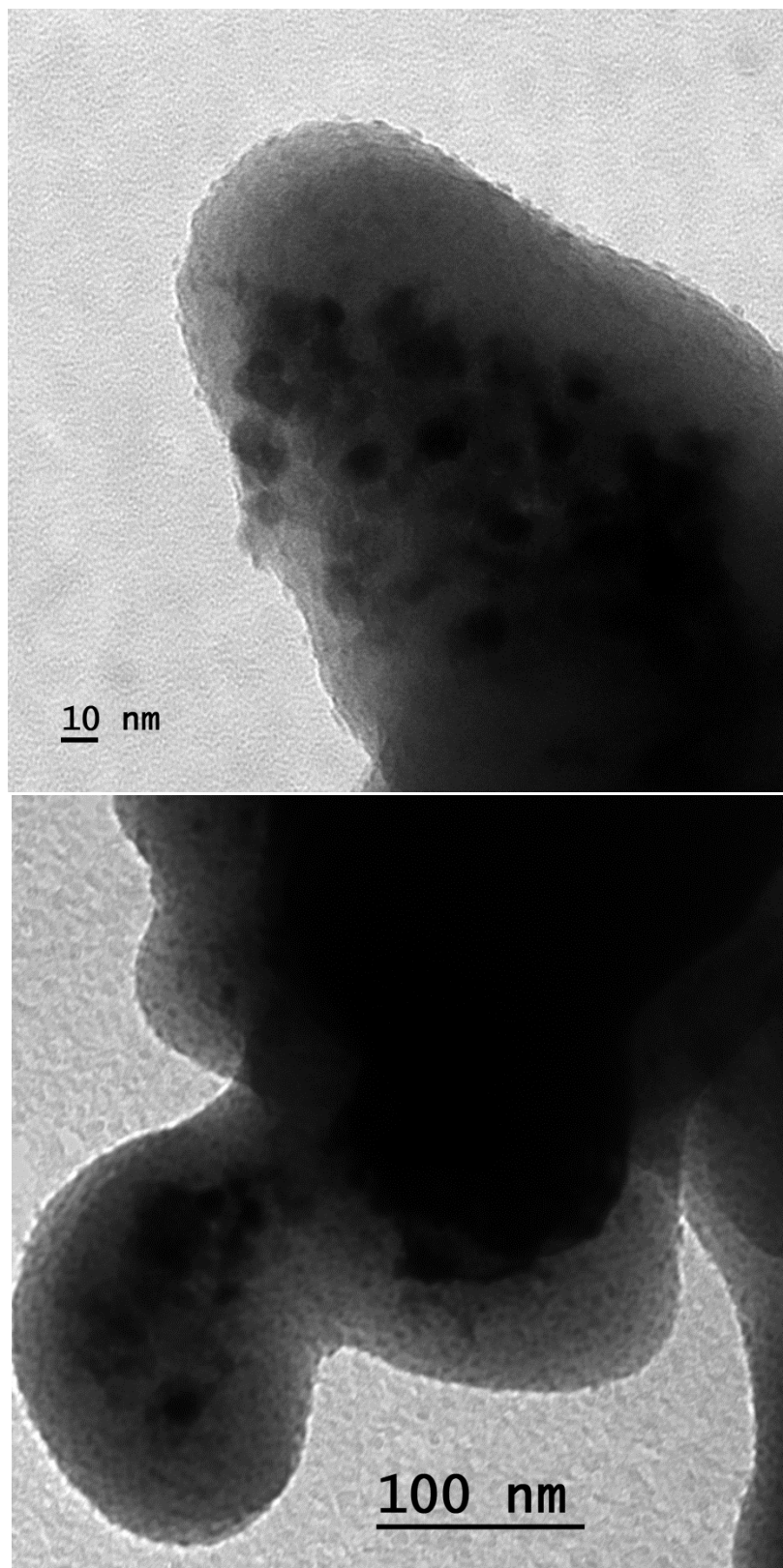


Figure 4.6. TEM images of silica-treated nickel nanoparticles.

Figure 4.7 shows a TEM image of Co-C particles taken by Grass *et. al.*⁴ This shows the graphene layers around the cobalt center (the thin lines which encompass the larger, darker circle), which is about 2 nm thick. Next, Figure 4.8 shows the recorded TEM images of the TurboBeads Silica™. There is evidence of a coating on the particles – a thin gray band around the particles about 5 nm thick. If this coating includes both the graphene layer and the silica layer, and the graphene layer is 2 nm thick, then the silica layer must be 3 nm thick.

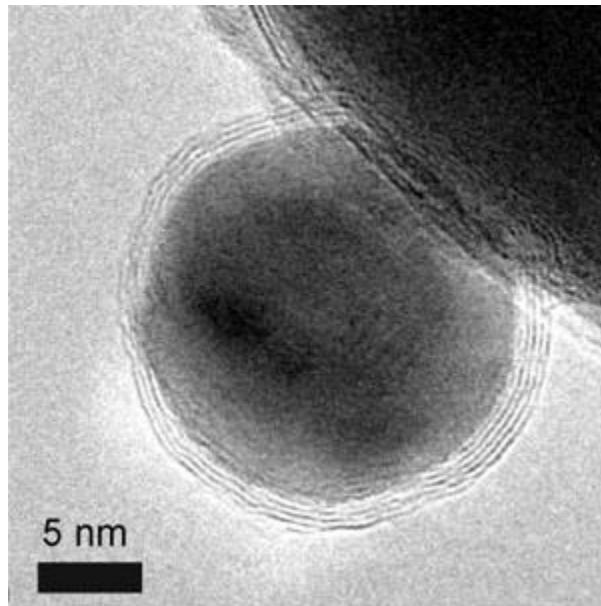


Figure 4.7. TEM image of a Co-C nanoparticle. Recorded by Grass *et. al.*⁴

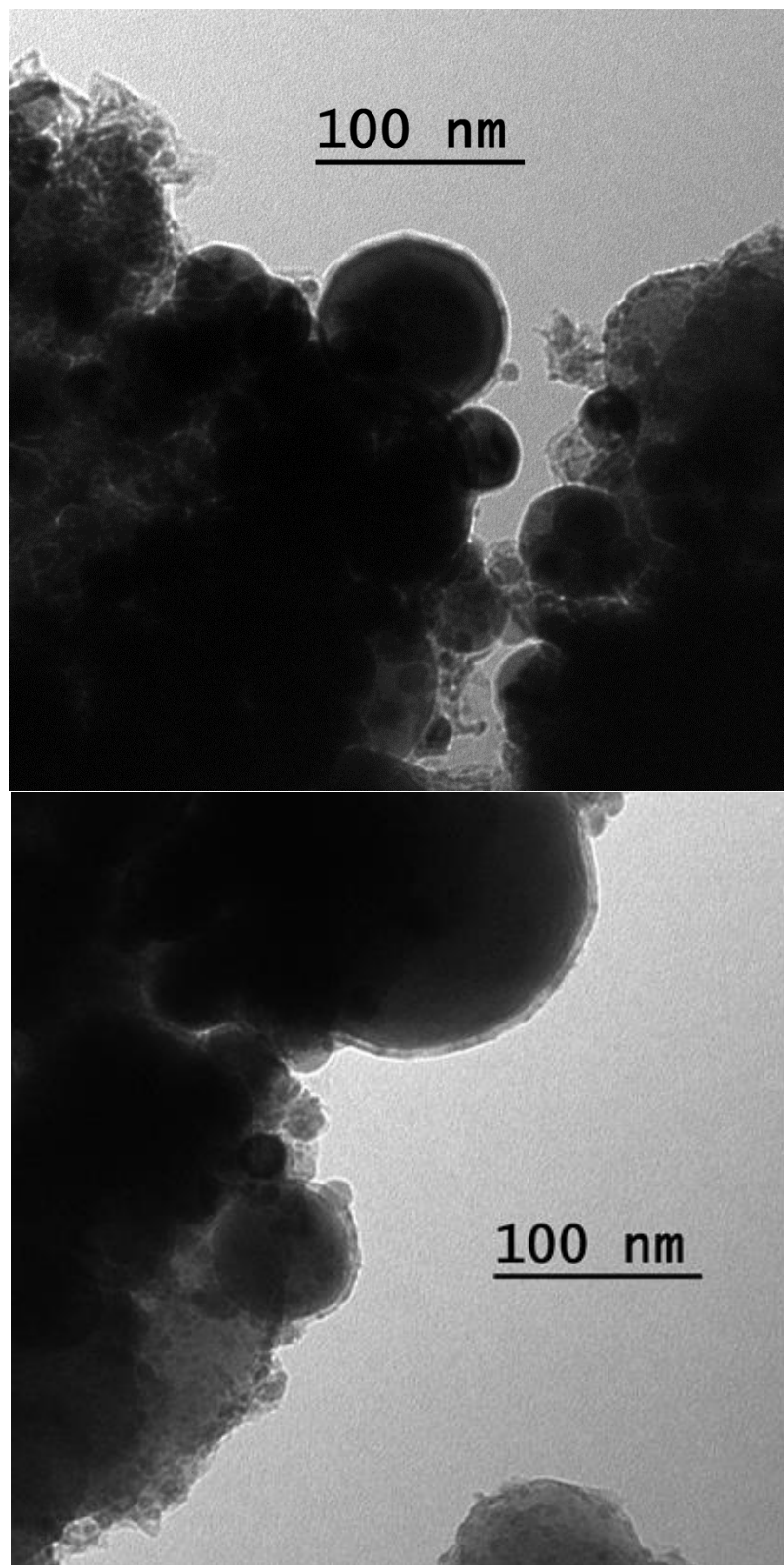


Figure 4.8. TEM images of TurboBeads Silica™.

4.3.4. Characterization of Silica-Treated, DFB-Treated Nanoparticles: IR Spectroscopy

Figure 4.9 shows the IR spectra of TurboBeads Silica™ before and after an addition of the anhydride silane – spectrum (a) and (b), respectively. The two spectra are similar. Both have a peak at 1666 cm^{-1} . Without knowing exactly how the silica was attached to the surface, it is difficult to say to what this peak may be due, because it is not a peak typically associated with silica. In both spectra, the largest feature is a peak at 1137 cm^{-1} . This is the Si-O-Si stretching peak due to the presence of silica.

One could argue that in the spectrum recorded after the reaction, there is a slight shoulder at 1713 cm^{-1} which is not present in the spectrum recorded before the reaction. This would be a sign of the carbonyl stretch of a carboxylic acid (COOH). However, it is difficult to say for certain that a peak is really there.

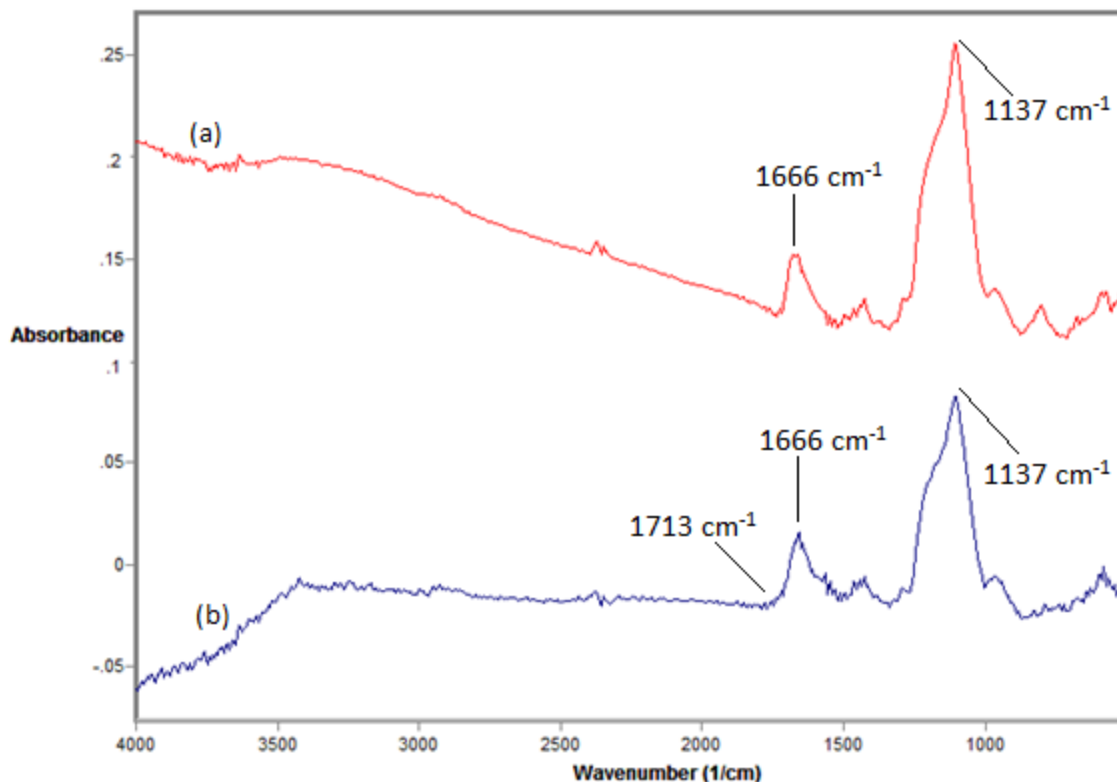


Figure 4.9. DRIFT spectra of TurboBeads Silica™ before and after addition of anhydride silane. a) TurboBeads Silica™ as purchased; b) TurboBeads Silica™ after the addition of anhydride silane.

Likewise, Figure 4.10 (a) and (b) shows the IR spectra of Ni-SiO₂ before and after addition of anhydride silane, respectively. While the two spectra are fairly similar, there is a small peak at 1714 cm⁻¹ in Figure 4.10 (b) which was not present in Figure 4.10 (a). This peak is due to the C=O stretch of a carboxylic acid, indicating a reaction between the silica and the anhydride silane.

The same reaction was performed on silica-treated Fe₃O₄ particles. The IR spectra of these particles, before and after reaction with the anhydride silane, are shown in Figure 4.11 (a) and (b), respectively. A peak at 1720 cm⁻¹ in Figure 4.11 (b) is

due to a carbonyl stretch (C=O), indicating the presence of carboxylic acid groups.

Because this reaction worked on the Fe₃O₄-Silica nanoparticles, it also worked on the TurboBeads Silica™ and Ni-SiO₂ particles. However, each of these samples had a large peak (1550 to 1700 cm⁻¹) near where a C=O stretching mode of a carboxylic acid appears, which made identification of a C=O band difficult.

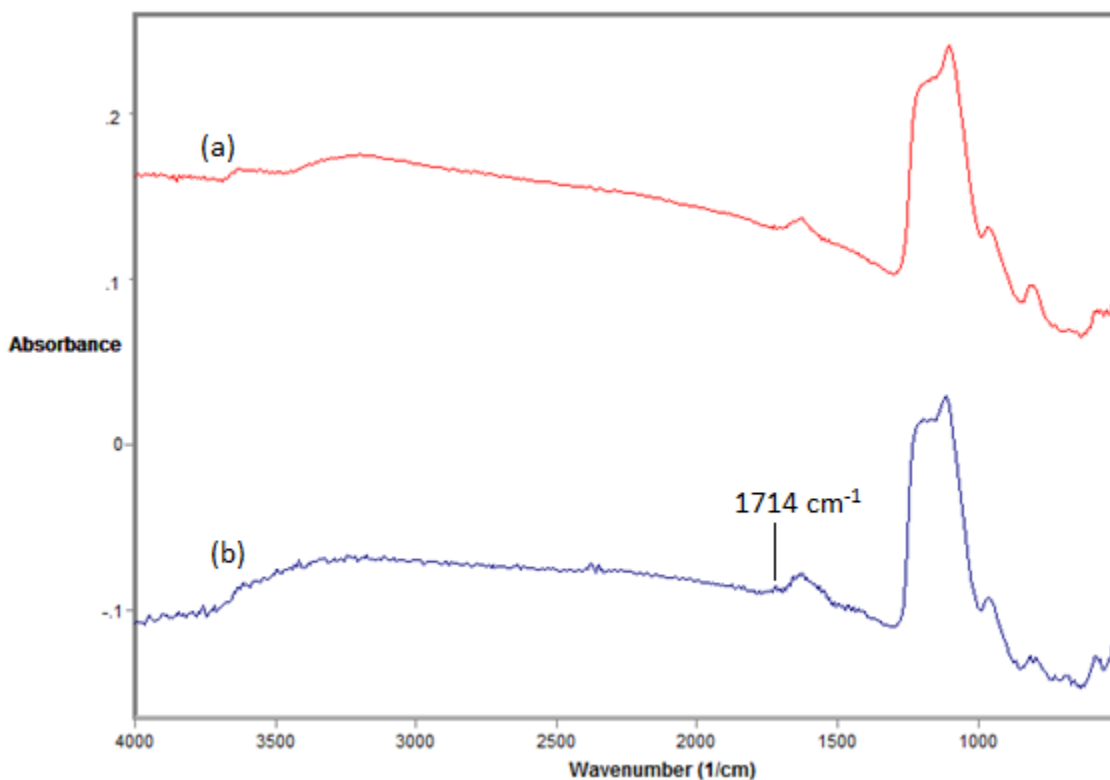


Figure 4.10. DRIFT spectra of Ni-SiO₂ before and after addition of anhydride silane. a) Ni-SiO₂; b) Ni-SiO₂ after the addition of anhydride silane.

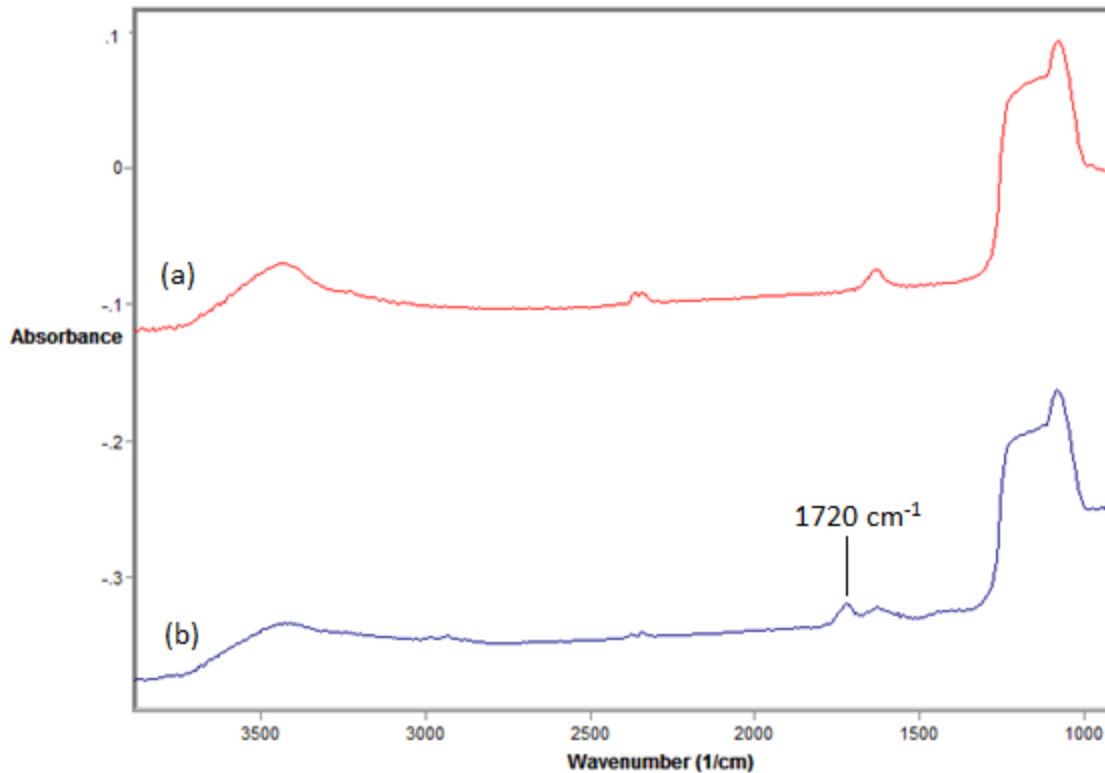


Figure 4.11. DRIFT spectra of $\text{Fe}_3\text{O}_4\text{-SiO}_2$ before and after addition of anhydride silane. a) $\text{Fe}_3\text{O}_4\text{-SiO}_2$; b) $\text{Fe}_3\text{O}_4\text{-SiO}_2$ after the addition of anhydride silane.

Thus, it was decided that the Ni-SiO₂ and TurboBeads Silica™ should be characterized in a different way, after undergoing the reaction with DFB. XPS was chosen as the technique to be used. It was thought that if DFB were successfully put on the surface, XPS should detect the presence of nitrogen, because there are 6 nitrogen atoms in each molecule of DFB. Before the reaction with DFB, there should not be any nitrogen present in the samples.

4.3.5. Characterization of Silica-Treated, DFB-Treated Nanoparticles: XPS

Figure 4.12 shows the XPS spectrum for Ni-SiO₂. Table 4.6 shows the atom percent, as determined by CasaXPS software, using the major peaks in Figure 4.12 for each element. Peaks due to oxygen and silicon are from silica coating. Nickel is detected at a low level, (1%). XPS detects to a depth of about 10 nm into the surface of a sample. This means that there is very little nickel within the top 10 nm of the sample and shows that the silica coating is uniformly covering the underlying nickel particle. Carbon is also present, partly due to the carbon tape which the sample is stuck on and partly due to normal hydrocarbon contamination from the environment. If nitrogen was present, it would have its major, 1s peak at 398 eV. There is no such peak in this spectrum.

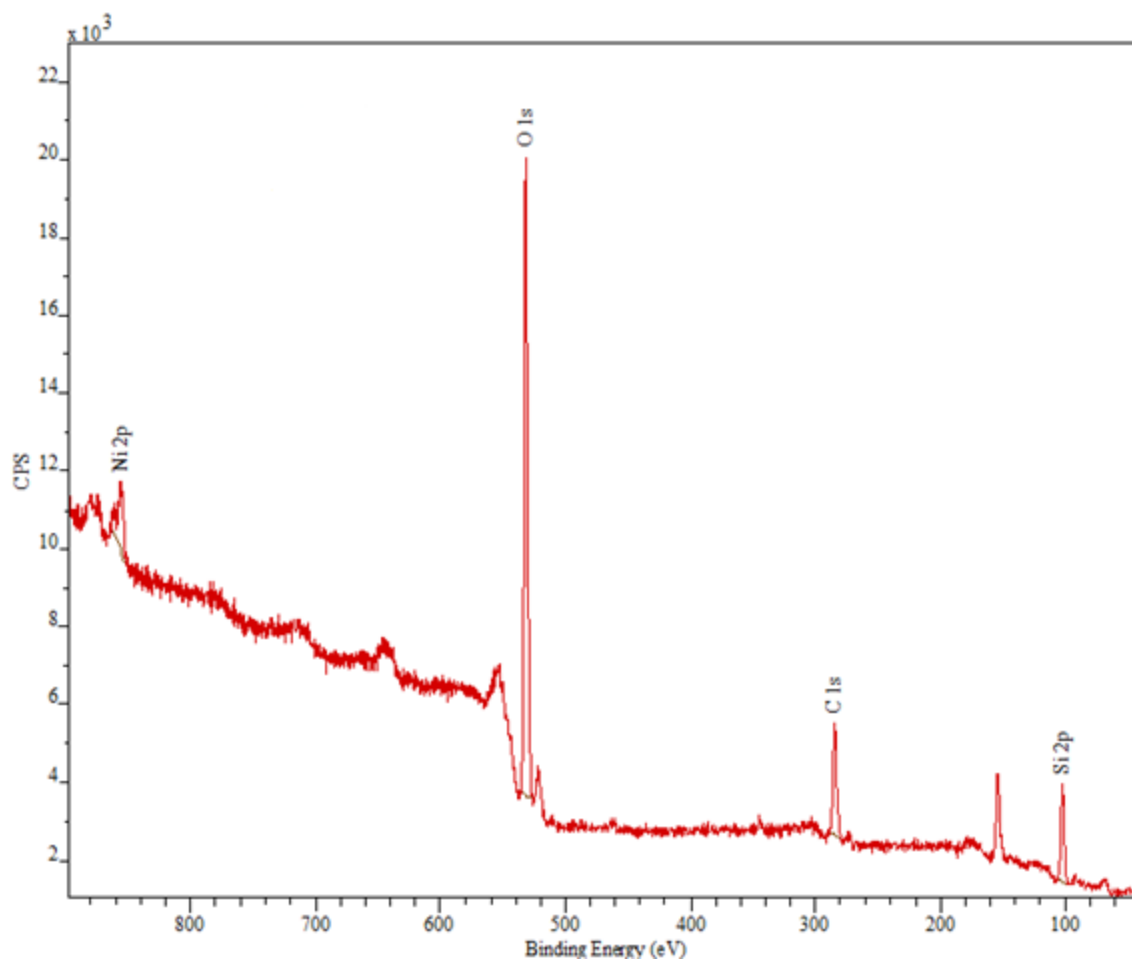


Figure 4.12. XPS spectrum of silica-treated nickel nanoparticles. It has been calibrated to the true value of the C 1s peak, 284 eV. The major peaks for each element present are labeled. Processed with CasaXPS software.

Table 4.6. Atom Percent of Elements in Ni-SiO₂ Sample

Element	Atom Percent
Oxygen	41 %
Carbon	27 %
Nickel	1 %
Silicon	31 %

Figure 4.13 shows the XPS spectrum of TurboBeads Silica™ and Table 4.7 provides the percentage of each element. Again, oxygen and silicon peaks indicate the presence of silica. Carbon is also present – there is hydrocarbon contamination and background signal due to the tape, in addition to the carbon coating beneath the silica. About 2% of the top 10 nm of the sample is cobalt. The TEM images of the TurboBeads Silica™ (see Figure 4.8) indicated that the coating (silica and carbon combined) was only 5 nm thick, so the XPS should be able to detect some material underneath it.

There is also a peak due to nitrogen in this sample. These TurboBeads Silica™ had not been exposed to DFB, so this was unexpected. The process by which the silica coating is applied to the carbon-coated particles is not stated by the manufacturer, so the source of nitrogen is not known. It is reasonable to conclude that the nitrogen signal is not due to contamination from the environment, since the Ni-SiO₂ particles did not contain nitrogen.

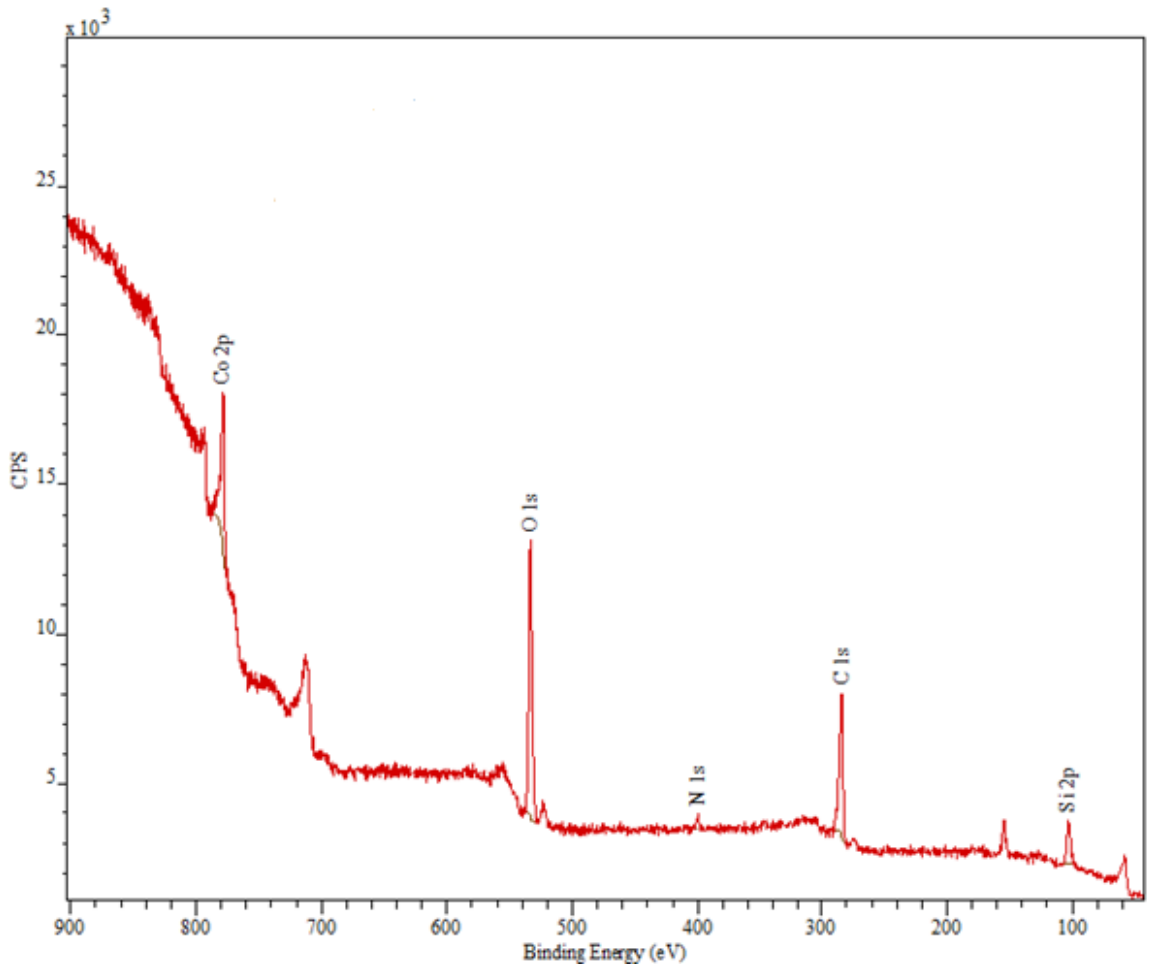


Figure 4.13. XPS spectrum of TurboBeads Silica™. It has been calibrated to the true value of the C 1s peak, 284 eV. The major peaks for each element present are labeled. Processed with CasaXPS software.

Table 4.7. Atom Percent of Elements in TurboBeads Silica™ Sample

Element	Atom Percent
Oxygen	25 %
Carbon	53 %
Cobalt	2 %
Silicon	19%
Nitrogen	1 %

Figure 4.14 shows the XPS spectrum of Ni-SiO₂-DFB and Table 4.8 shows the percentages of each element. The spectrum is similar to that of the spectrum of Ni-SiO₂ particles which were not exposed to DFB. In addition to peaks that were already present, there is also a small nitrogen peak at 398 eV, which shows the presence of DFB on the surface.

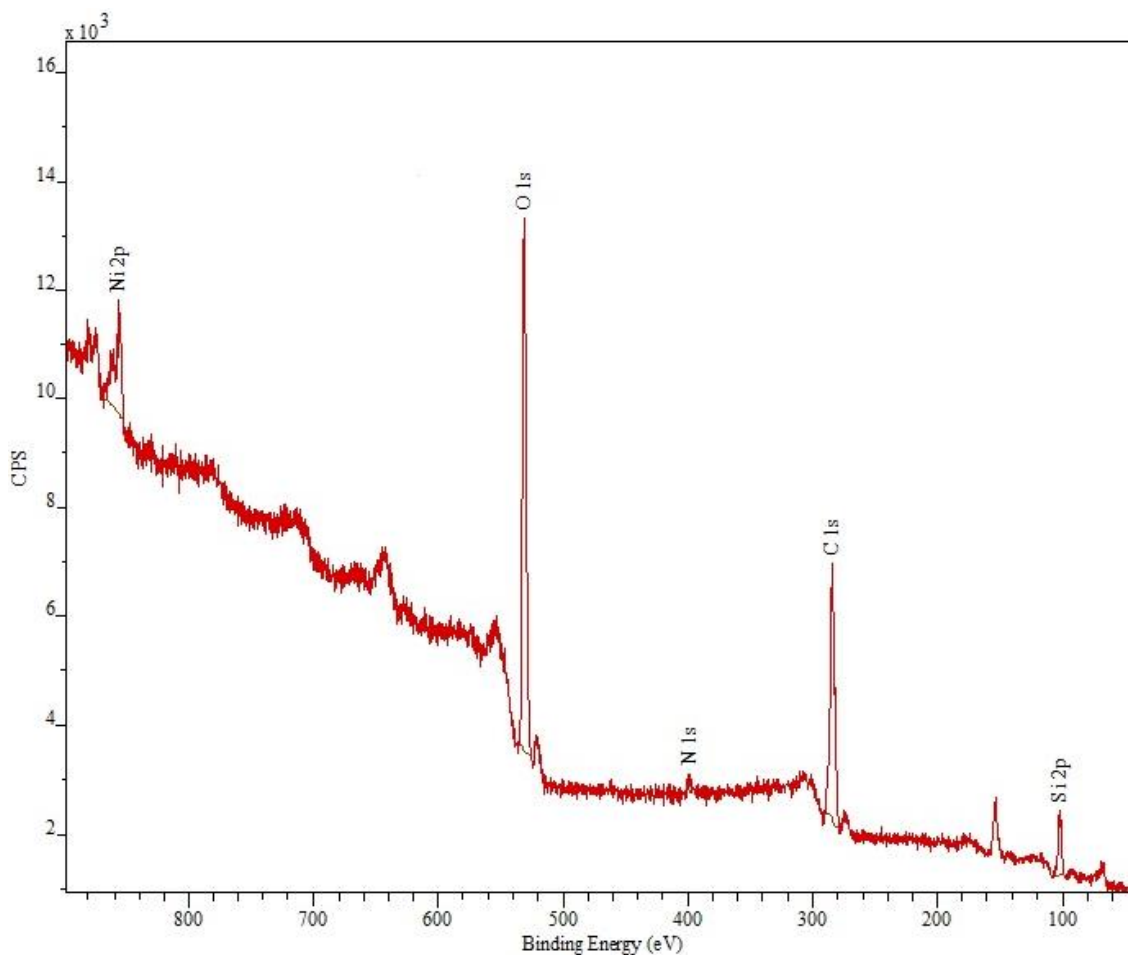


Figure 4.14. XPS spectrum of Ni-SiO₂-DFB. It has been calibrated to the true value of the C 1s peak, 284 eV. The major peaks for each element present are labeled. Processed with CasaXPS software.

Table 4.8. Atom Percent of Elements in Ni-SiO₂-DFB Sample

Element	Atom Percent
Oxygen	27 %
Carbon	56 %
Nickel	1 %
Silicon	15 %
Nitrogen	1 %

Figure 4.15 shows the XPS spectrum of Ni-SiO₂-FB. Again, a weak peak due to nitrogen is observed. Figure 4.16 is an expanded view of the nitrogen peak region. The presence of the nitrogen peak indicates that there is DFB on the surface, though it does not provide any information on the formation of an amide linkage to the surface.

The spectrum in Figure 4.15 is similar to the spectrum in Figure 4.14, except that there are an additional two small peaks overlapping with the broad peak at 712 eV. The 712 eV peak is an Auger peak from nickel. Auger XPS peaks are due to secondary emission of electrons from an atom, which occurs when electrons rearrange to fill gaps left by core electrons emitted upon x-ray incidence. The major peaks for iron (2p) typically occur at 707 and 720 eV, and so they can overlap with the nickel Auger peak mentioned. Indeed, in Figure 4.15 one can see the two peaks at 711 and 724 eV on top of the broader feature, which is likely due to the nickel Auger peak. This indicates that there is some iron in the sample, but because the peaks overlap, an accurate percentage of iron in the sample could not be calculated. Therefore, although the percentage of each element in this sample is displayed in Table 4.9, the amount of iron was not calculated.

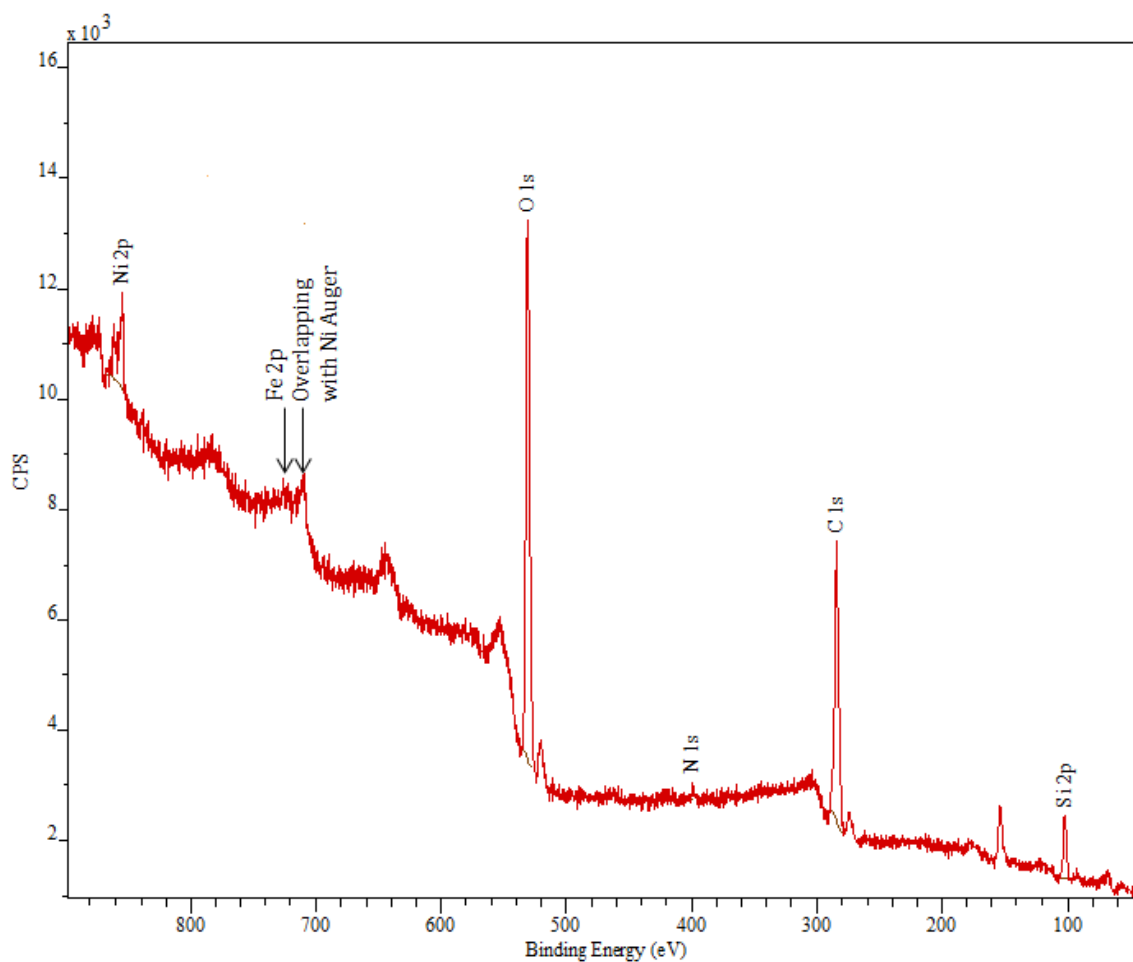


Figure 4.15. XPS spectrum of Ni-SiO₂-FB. It has been calibrated to the true value of the C 1s peak, 284 eV. The major peaks for each element present are labeled, including the two iron 2p peaks which are overlapping with a nickel Auger peak. Processed with CasaXPS software.

Table 4.9. Atom Percent of Elements in Ni-SiO₂-FB Sample, Excluding Fe

Element	Atom Percent
Oxygen	29 %
Carbon	57 %
Nickel	1 %
Silicon	13 %
Nitrogen	1 %
Iron	Peak overlaps – could not calculate.

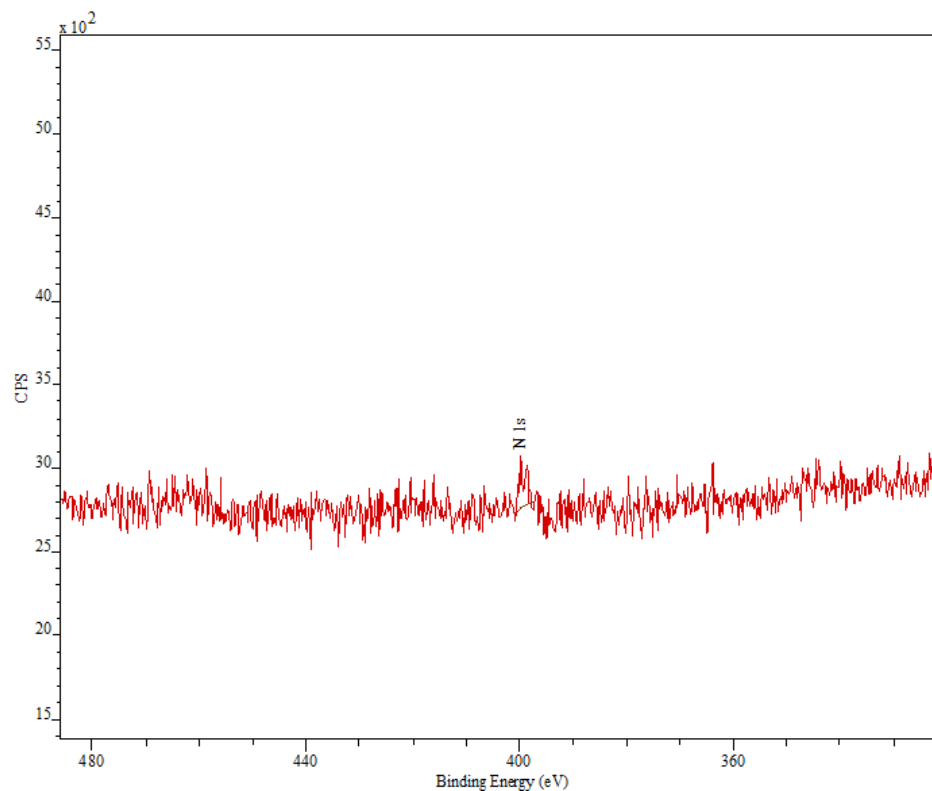


Figure 4.16. XPS spectrum of Ni-SiO₂-FB, showing the small nitrogen peak at 398 eV.

Figures 4.17 and 4.18 show the XPS of the Co-SiO₂-DFB and Co-SiO₂-FB samples, respectively. Tables 4.10 and 4.11 show the atom percent of elements present in the Co-SiO₂-DFB and Co-SiO₂-FB samples, respectively. The XPS spectra do not show any differences from the spectrum of TurboBeads Silica™ shown in Figure 4.13. Thus, there is no evidence that the DFB had bound to the TurboBeads Silica™ in either the Co-SiO₂-DFB or Co-SiO₂-FB samples.

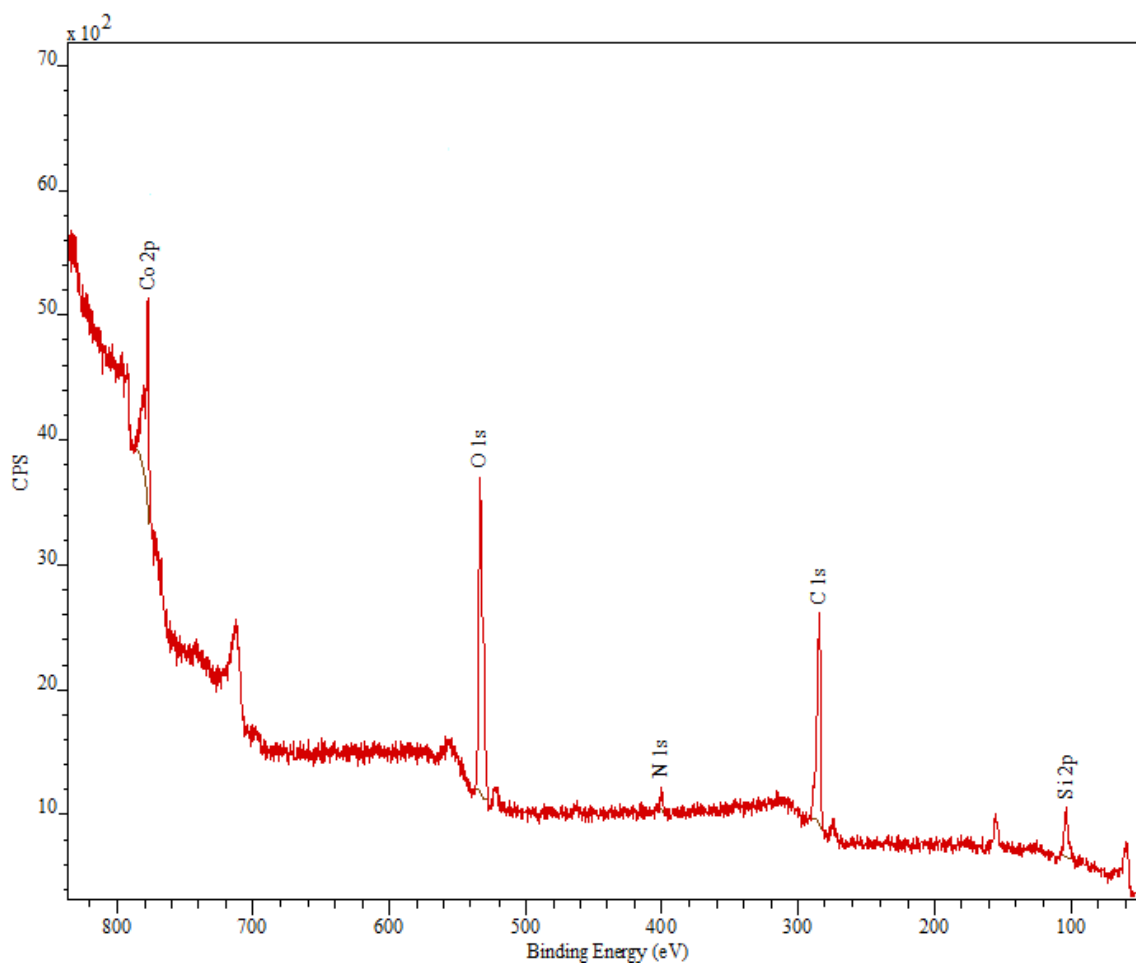


Figure 4.17. XPS spectrum of Co-SiO₂-DFB. It has been calibrated to the true value of the C 1s peak, 284 eV. The major peaks for each element present are labeled. Processed with CasaXPS software.

Table 4.10. Atom Percent of Elements in Co-SiO₂-DFB

Element	Atom Percent
Oxygen	22 %
Carbon	57 %
Cobalt	2 %
Silicon	17 %
Nitrogen	2 %

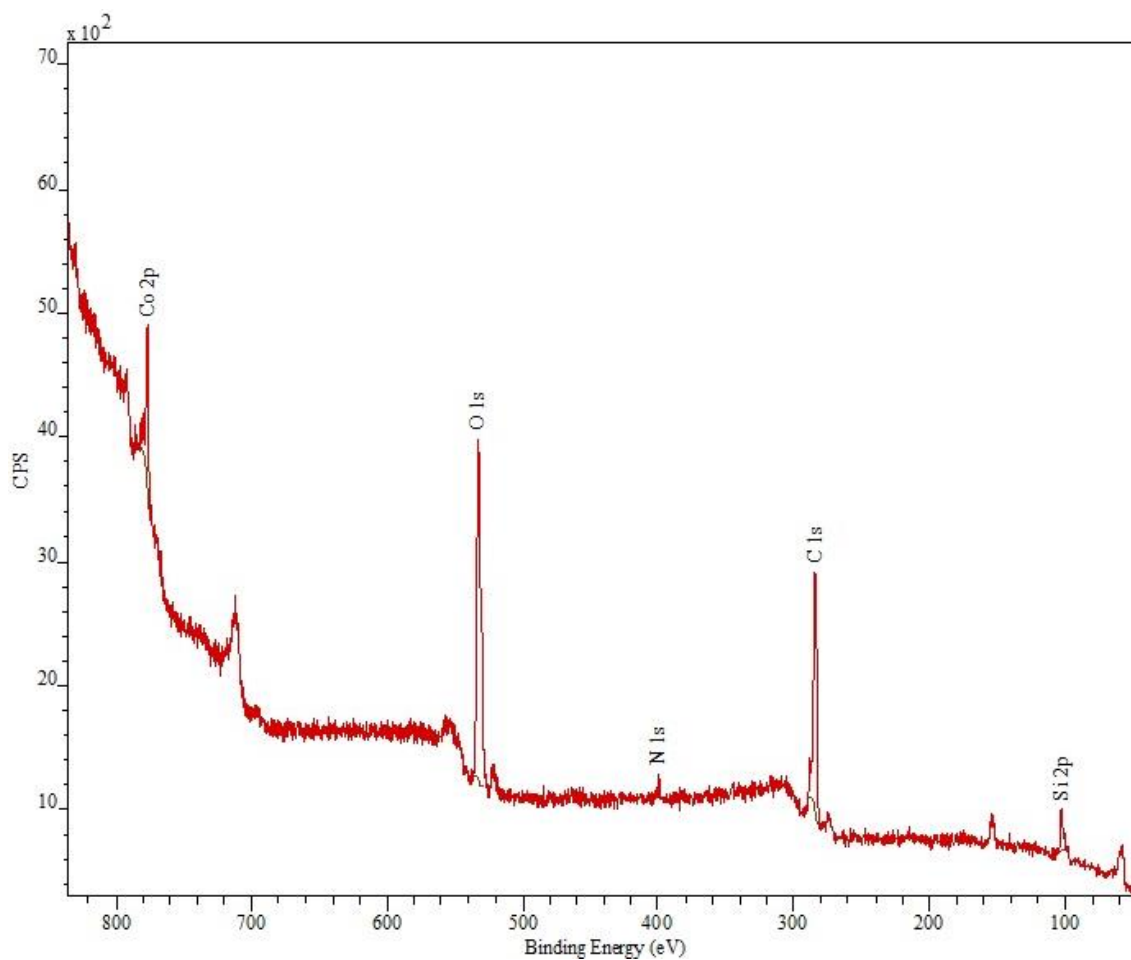


Figure 4.18. XPS spectrum of Co-SiO₂-FB. It has been calibrated to the true value of the C 1s peak, 284 eV. The major peaks for each element present are labeled. Processed with CasaXPS software.

Table 4.11. Atom Percent of Elements in Co-SiO₂-FB

Element	Atom Percent
Oxygen	23 %
Carbon	63 %
Cobalt	1 %
Silicon	11 %
Nitrogen	1 %

In summary, the XPS data shows that DFB is on the surface of both Ni-SiO₂-DFB and Ni-SiO₂-FB. This is evidenced by the presence of a nitrogen peak in the XPS spectrum of the DFB-treated material, which was not present in the XPS spectrum of Ni-SiO₂. For Ni-SiO₂-FB, iron was also detected. Because the XPS detected nitrogen in the native TurboBeads Silica™, it was not possible to determine if there was DFB on the surface. It should be noted that there did not appear to be any iron on the Co-SiO₂-FB, indicating that either there is no DFB on the surface or the portion which reacted was the non-iron-bound DFB.

4.3.6. Iron (III) Uptake of Ni-SiO₂ (Prior to DFB Exposure)

The amount of iron (III) in 20 mL of the iron (III) solutions added to each Ni-SiO₂ sample before and after stirring with the sample for 1 hour is provided in Table 4.12. The samples and solutions are numbered to indicate which sample received a particular FeCl₃ solution (e.g. Sample 1 received 20 mL of FeCl₃ Solution 1). Samples 1 and 2 are from one batch of Ni-SiO₂ and Samples 3, 4, and 5 are from another batch.

The margins of error represent one standard deviation of noise in the baseline spectra of each measurement. In all cases, the amount of iron (III) left in the supernatant, after shaking with the silica-treated nickel nanoparticles, was smaller than the amount present in 20 mL of the original solution. Table 4.13 lists the percentage of iron (III) lost from solution in each case. The largest amount lost in any particular sample was 12%. The difference is due to non-specific binding to the surface. Thus, the silica coating did not, in and of itself, prevent the adsorption of iron (III). Silica has an

isoelectric point at pH 2 and thus, has negatively charged sites even at low pH. These sites can electrostatically bind the iron (III) from solution. The origin of the negatively-charged sites is the deprotonation of surface Si-OH groups. These groups react with the anhydride silane, which is added before the addition of the DFB. Therefore, a DFB-treated silica may not have non-specific binding of iron (III).

Table 4.12. Amount of Iron (III) in FeCl₃ Solution Before and After Stirring with Ni-SiO₂

Sample	Amount of Fe ⁺³ (μmol) in 20 mL
FeCl ₃ Solution 1 (17.2 μM)	0.413 ± 0.002
FeCl ₃ Solution from Ni-SiO ₂ Sample 1	0.395 ± 0.003
FeCl ₃ Solution 2 (18.1 μM)	0.435 ± 0.005
FeCl ₃ Solution from Ni-SiO ₂ Sample 2	0.409 ± 0.001
FeCl ₃ Solution 3 (17.3 μM)	0.415 ± 0.003
FeCl ₃ Solution from Ni-SiO ₂ Sample 3	0.381 ± 0.004
FeCl ₃ Solution 4 (17.3 μM)	0.415 ± 0.003
FeCl ₃ Solution from Ni-SiO ₂ Sample 4	0.365 ± 0.003
FeCl ₃ Solution 5 (17.3 μM)	0.415 ± 0.003
FeCl ₃ Solution from Ni-SiO ₂ Sample 5	0.387 ± 0.004

Table 4.13. Amount of Iron (III) Adsorbed by Ni-SiO₂ Samples

Sample	Percent Iron (III) Adsorbed
1	4%
2	6%
3	8%
4	12%
5	7%

4.3.7. Iron (III) Uptake of Ni-SiO₂-DFB

Table 4.14 shows the amount of iron (III) measured in 20 mL of the FeCl₃ solution before and after it was allowed to stir with the Ni-SiO₂-DFB particles for 1 hour. The two measurements differ by 0.006 μmol, but the margins of error do overlap. This shows that there was no iron (III) uptake by this surface. Thus, while the DFB did prevent non-specific binding of iron (III), it was also inactive in taking up iron (III).

The XPS measurements performed on this sample indicated that it was likely that DFB was on the surface. However, that did not guarantee that the DFB would be accessible to iron (III). It is possible that DFB is on the surface, but it is unable to chelate iron. For instance, if the density of DFB on the surface was high enough, the molecules could be too crowded to form the hexadentate structure required to chelate iron (III) (see Figure 1.2). Also, the DFB could bind through multiple sites with the surface and hence, would not dislodge from the surface to form multiple bonds with an incoming iron (III) ion. Because the DFB-treated Ni-SiO₂ particles did not take up iron (III) from solution, no further work was done with them in this project.

Table 4.14. Amount of Iron (III) in FeCl₃ Solution Before and After Stirring with Ni-SiO₂-DFB

Sample	Amount of Fe ⁺³ (μmol) in 20 mL
FeCl ₃ Solution (30.4 μM)	0.729 ± 0.003
FeCl ₃ Supernatant from DFB-Treated Particles	0.723 ± 0.003

4.3.8. Iron (III) Uptake and Removal with Oxalate of Ni-SiO₂-FB Particles

The following list (reproduced from Section 4.2.11) describes the sequence of steps recorded to study the iron (III) uptake of the Ni-SiO₂-FB particles and subsequent removal of iron (III) from them.

- Step 1: Remove Iron (III) by Washing with 0.1 M Oxalate at pH 1.5 – Initial Oxalate Washes
 - Wash with 5000 μ L for 5 Minutes
 - Repeat
- Step 2: Add Iron (III) by Stirring with 20 mL FeCl₃ for 1 Hour – First Iron (III) Addition
- Step 3: Remove Iron (III) by Washing with 0.1 M Oxalate at pH 1.5 – Second Oxalate Washes
 - Wash with 10 mL for 5 Minutes
 - Repeat, but with 5000 μ L
 - Note: the background for these measurements was 4000 μ L from the 10 mL wash combined with 1500 μ L DI water.
- Step 4: Add Iron (III) by Stirring with 20 mL FeCl₃ for 1 Hour – Second Iron (III) Addition
- Step 5: Remove Iron (III) by Washing with 0.1 M Oxalate at pH 1.5 – Final Oxalate Washes
 - Wash with 5000 μ L for 5 Minutes

- Repeat
- Step 6: Add Iron (III) by Stirring with 20 mL FeCl_3 for 1 Hour – Third Iron (III)

Addition

Table 4.15 provides the values for the iron (III) measured at each step in this experiment; however, the amounts of iron (III) in the oxalate washes could not be measured accurately. This is because a second peak appeared at 386 nm that overlapped with the DFB-Fe peak at 430 nm (see Figure 4.19). Still, the absorbance of the DFB-Fe peak must be less than the total measured absorbance. Therefore, the total absorbance would put a “maximum” on the value for the amount of iron (III) extracted. It is this “maximum” value of iron (III) in a given oxalate wash which is stated in Table 4.15.

Table 4.16 shows the total amounts of iron (III) removed from (negative values) and added to (positive values) the Ni-SiO₂-FB particles during this experiment. The latter was calculated by subtracting the iron (III) measured in the supernatant after stirring with the particles from the amount measured in the original solution.

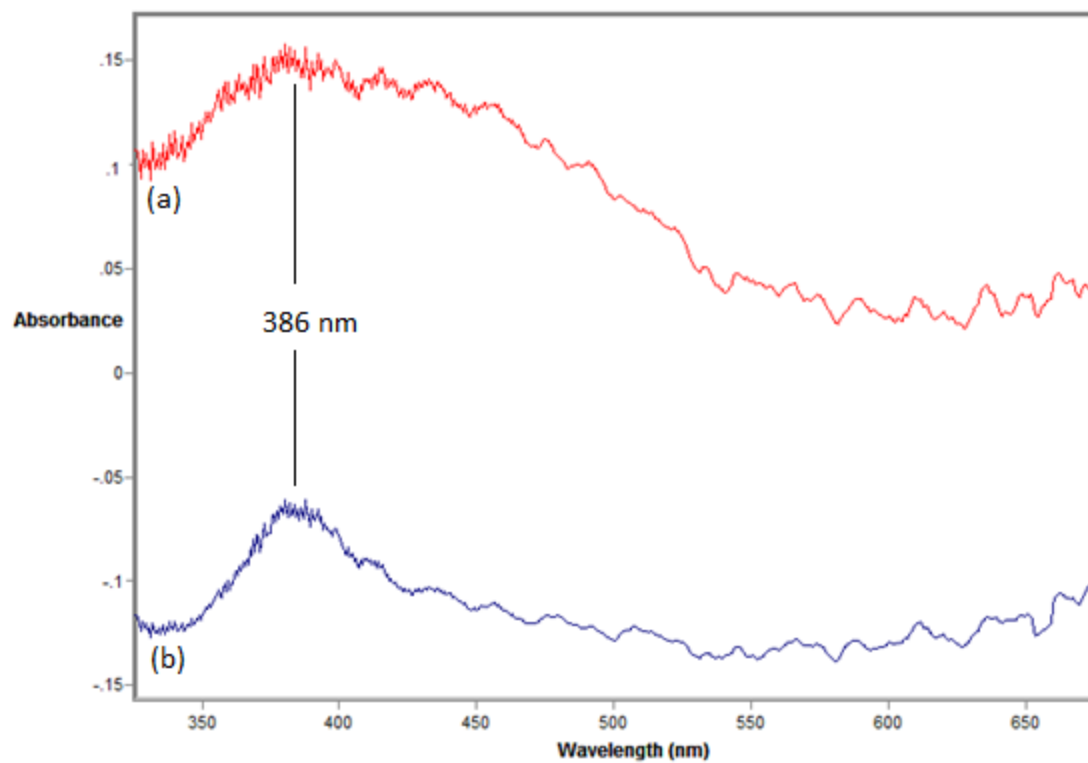


Figure 4.19. UV-Vis spectra of the final oxalate washes of DFB-Fe-treated Ni-SiO₂. a) The first of these washes has a DFB-Fe peak while b) the second does not.

Table 4.15. Amount of Iron (III) Measured in FeCl₃, Oxalate Samples from Ni-SiO₂-FB Particles

Sample	Sample Volume (mL)	Amount of Fe ⁺³ (μmol) in Sample Volume
Initial Oxalate Washes*	-	-
Wash #1	5	0.4
Wash #2	5	0
First FeCl₃ Addition	-	-
FeCl ₃ Solution (32.0 μM)	20	0.767 ± 0.003
FeCl ₃ Supernatant from Particles	20	0.624 ± 0.004
Second Oxalate Washes*	-	-
Wash #1	10	0.1
Wash #2	5	0
Second FeCl₃ Addition	-	-
FeCl ₃ Solution (17.2 μM)	20	0.413 ± 0.003
FeCl ₃ Supernatant from Particles	20	0.275 ± 0.004
Final Oxalate Washes*	-	-
Wash #1	5	0.08
Wash #2	5	0
Third FeCl₃ Addition	-	-
FeCl ₃ Solution (17.5 μM)	20	0.420 ± 0.003
FeCl ₃ Supernatant from Particles	20	0.346 ± 0.003

*The measurements made in oxalate washes are not accurate due to the interference of a second peak. The numbers quoted can be thought of as the maximum possible amount of iron (III) present. Errors are not included for these values.

Table 4.16. Amount of Iron (III) Measured for Each Step (Removed from Particles with Oxalate or Added to Ni-SiO₂-FB from FeCl₃ Solution)

Step (In Chronological Order)	Amount of Fe ⁺³ (μmol)
Iron (III) Removed from Particles with Oxalate (Initial Wash)	-0.4
Iron (III) Adsorbed onto Particles (First FeCl ₃ Addition)	+0.143
Iron (III) Removed from Particles with Oxalate (Second Wash)	-0.1
Iron (III) Adsorbed onto Particles (Second FeCl ₃ Addition)	+0.138
Iron (III) Removed from Particles with Oxalate (Final Wash)	-0.08
Iron (III) Adsorbed onto Particles (Third FeCl ₃ Addition)	+0.074

Note: In this table, negative values indicate iron (III) removed from the particles while positive values indicate iron (III) added to them.

The Ni-SiO₂-FB particles removed 0.143 μmol with the first addition of FeCl₃ solution. When these particles were washed with oxalate, a maximum of 0.1 μmol iron (III) was removed from the particles. This is 70% of the iron originally removed from the solution. When these Ni-SiO₂-FB particles were then added to a second FeCl₃ solution, the particles removed 0.138 μmol iron (III). Thus, the uptake of iron (III) is about the same value the second time in contact with a fresh iron (III) solution as the first time in contact with an iron (III) solution. When the Ni-SiO₂-FB particles were again washed with oxalate, only 0.06 μmol was found in the oxalate. This translates to about 43% of the iron (III) removed from the particles. That does not include any iron (III) which may be left on the particles from the particles' first exposure to FeCl₃. But in both

cases, not all of the iron (III) which the particles adsorbed from solution was removed from the particles with the subsequent oxalate wash.

4.3.9. UV-Vis Spectra of 0.1 M NiCl₂, Product of Oxalic Acid and Ni Nanoparticles

Experiments were performed to determine the source of the interfering peak at 386 nm, which appeared in UV-Vis spectra of oxalate exposed to nickel nanoparticles (see Figure 4.19). A sample containing 5 mL 0.1 M oxalate at pH 1.6 was shaken with unmodified nickel nanoparticles on a Vibramax 100 for 15 minutes. UV-Vis spectra of this supernatant and of 0.1 M NiCl₂ were also recorded (see Figure 4.20).

Both spectra have a peak at 394 nm. Given that this is seen in the spectrum of NiCl₂ as well as the spectrum of the oxalic acid exposed to nickel nanoparticles, it is likely that this peak is due to nickel (II). This means that the oxalic acid and nickel react, forming nickel (II) ions in solution.

One would expect the silica coating to protect the nickel inside from the oxalate. However, the peak in Figure 4.19 (the oxalate washes from the DFB-Fe-treated nickel nanoparticles) is at 386 nm, which is less than 10 nm from the wavelength of the peak in Figure 4.20. This indicates that the peak seen in Figure 4.19 is due to the oxalic acid reacting with exposed or leaked nickel from the particles. Thus, the use of nickel-based particles was not pursued any further.

While Ni-SiO₂-FB adsorbed iron (III), the formation of a band at 386 nm, due to a reaction between the oxalic acid and nickel, interferes with the band due to DFB-Fe.

Therefore, in order to use the nickel nanoparticles to detect iron (III), they would need a coating which can better protect them from the oxalate.

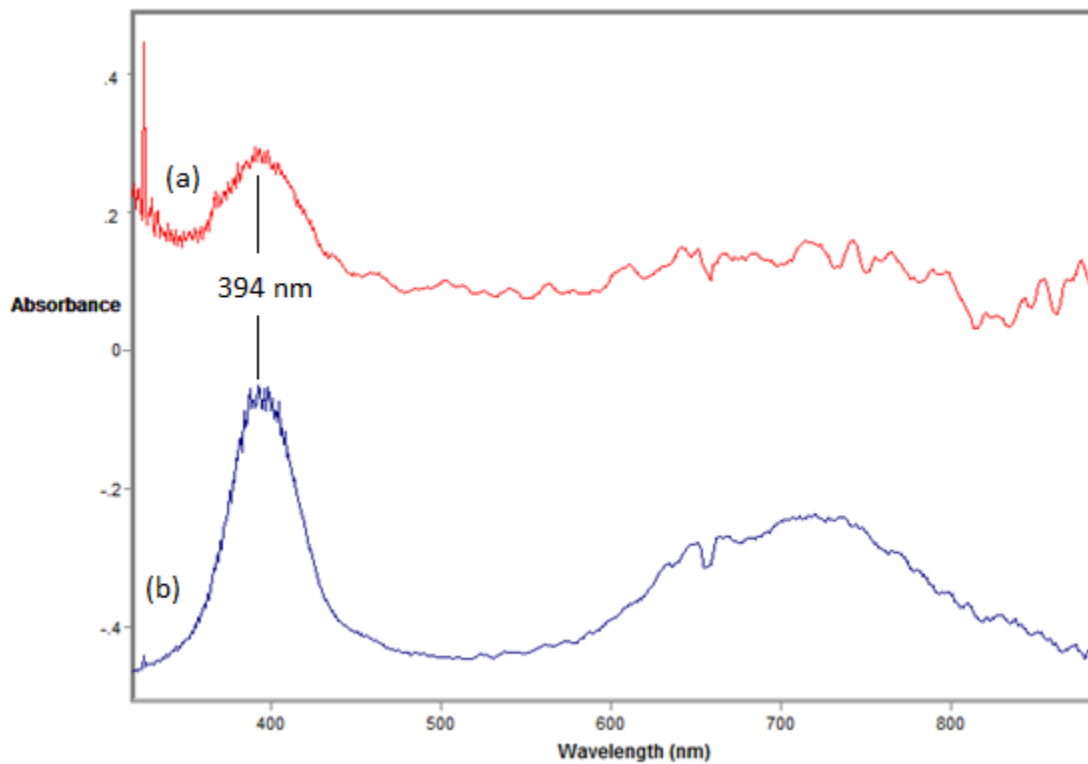


Figure 4.20. UV-Vis spectra for Section 4.3.9. a) Oxalic acid after shaking with nickel nanoparticles for 15 minutes; b) 0.1 M NiCl₂.

4.3.10. Iron (III) Uptake of TurboBeads Silica™

Table 4.17 shows the amount of iron (III) measured in FeCl₃ solutions before and after they were added to samples of TurboBeads Silica™ and stirred for 1 hour. The samples and solutions are numbered to indicate which sample received a particular FeCl₃ solution (e.g. Sample 1 received 20 mL of FeCl₃ Solution 1).

Table 4.17. Amount of Iron (III) in FeCl₃ Solution Before and After Stirring with TurboBeads Silica™

Sample	Amount of Fe ⁺³ (μmol) in 20 mL
FeCl ₃ Solution 1 (17.7 μM)	0.426 ± 0.002
Supernatant from Sample 1	0.363 ± 0.002
FeCl ₃ Solution 2 (17.8 μM)	0.428 ± 0.005
Supernatant from Sample 2	0.110 ± 0.004
FeCl ₃ Solution 3 (17.8 μM)	0.428 ± 0.005
Supernatant from Sample 3	0.065 ± 0.006
FeCl ₃ Solution 4 (17.8 μM)	0.428 ± 0.005
Supernatant from Sample 4	0.431 ± 0.003
FeCl ₃ Solution 5 (17.8 μM)	0.428 ± 0.005
Supernatant from Sample 5	0.430 ± 0.003

The results obtained from this experiment were not consistent. In two cases (Samples 4 and 5), the amounts of iron (III) measured in the solution were the same (within error) before and after stirring with the particles. This indicates that these samples did not take any iron (III) out of solution. In the other three cases, there was less iron (III) after stirring with the particles. This indicates that these samples took some iron (III) out of solution. Table 4.18 shows what percentage of the iron (III) in the original solution was lost in each sample. This was calculated by first taking the difference between the amounts of iron (III) measured in solution before and after exposing the solution to the particles. Then, this difference was converted to a percent of the amount of iron (III) in the original solution.

The values in Table 4.18 vary wildly, from 0% iron (III) adsorbed to 85% iron (III) adsorbed. Although the TEM images of the TurboBeads Silica™ show that the particles are coated (see Figure 4.8), it is difficult to establish the uniformity of the coating.

Section 4.3.6 showed that on Ni-SiO₂ particles, the amount of iron (III) lost was much more consistent than what was seen in this experiment – between 4% and 12% of the total iron (III) was lost from solution to the Ni-SiO₂ particles. This shows that the adsorption of iron (III) is reduced compared to the Co-C nanoparticles, where 100% iron (III) capture was obtained (see Sections 3.3.1 – 3.3.4 and 3.3.7). Therefore, it is likely that the TurboBeads Silica™ samples which adsorbed more iron (III) had some surface area not coated in silica, allowing the carbon coating to adsorb the iron (III).

Table 4.18. Amount of Iron (III) Adsorbed by TurboBeads Silica™ Samples

Sample	Percent Iron (III) Adsorbed
1	15%
2	74%
3	85%
4	0%
5	0%

4.3.11. Iron (III) Uptake of Co-SiO₂-DFB

Table 4.19 shows the iron (III) measured in an FeCl₃ before and after it was stirred with the Co-SiO₂-DFB for an hour. It also shows the amount of iron (III) measured in each of the oxalate washes performed on this sample after adding FeCl₃.

Table 4.19. Amount of Iron (III) in FeCl₃ Solution Before and After Stirring with Co-SiO₂-DFB, in Oxalate Washes

Sample	Volume of Sample (mL)	Amount of Fe ⁺³ (μmol) in Sample
FeCl ₃ Solution (17.8 μM)	20	0.427 ± 0.003
FeCl ₃ Supernatant	20	0 ± 0.003
Oxalate Wash #1	5	0.091 ± 0.001
Oxalate Wash #2	5	0.042 ± 0.001
Oxalate Wash #3	5	0.028 ± 0.001
Oxalate Wash #4	5	0.014 ± 0.001
Oxalate Wash #5	5	0 ± 0.002
Oxalate Wash #6	5	0 ± 0.002

All the iron (III) from the 20 mL of FeCl₃ solution added was adsorbed by these particles – that means a total of 0.427 μmol iron (III) was present on the Co-SiO₂-DFB. However, the oxalate washes only removed a total of 0.175 μmol iron (III). This is 41% of the iron (III) which the particles adsorbed. Therefore, while it can be measured, only some of the iron (III) captured could be recovered in the oxalate. Additionally, because some samples of TurboBeads Silica™ can adsorb iron (III) without being DFB-treated (see Section 4.3.10), one cannot claim that specific binding of the iron (III) with the DFB occurred.

4.3.12. Iron (III) Uptake of Co-SiO₂-FB

Table 4.20 shows the iron (III) measured in FeCl₃ before and after it was stirred with the Co-SiO₂-FB for an hour. It also shows the amount of iron (III) measured in each of the oxalate washes performed on this sample before and after adding FeCl₃.

Table 4.20. Amount of Iron (III) in FeCl₃ Solution Before and After Stirring with Co-SiO₂-FB, in Oxalate Washes

Sample	Volume of Sample (mL)	Amount of Fe ⁺³ (μmol) in Sample
Oxalate Wash #1 (before adding FeCl ₃)	5	0.033 ± 0.002
Oxalate Wash #2 (before adding FeCl ₃)	5	0 ± 0.002
FeCl ₃ Solution (18.6 μM)	20	0.447 ± 0.004
FeCl ₃ Supernatant	20	0.218 ± 0.005
Oxalate Wash #1 (after adding FeCl ₃)	5	0.093 ± 0.002
Oxalate Wash #2 (after adding FeCl ₃)	5	0 ± 0.002

Before adding iron (III), the Co-SiO₂-FB particles were washed with oxalate to remove any iron (III) which may be present on the surface. In this case, only 0.033 μmol iron (III) was removed. This is less than the amount of iron (III) which adsorbed from the FeCl₃ solution when it was added – 0.229 μmol. This may indicate that some DFB not bound to iron (III) reacted with the surface. However, as pointed out in the previous section, TurboBeads Silica™ adsorb iron (III). Thus, there is no evidence to support specific binding of DFB on the surface with iron (III).

When washing the particles with oxalate after adding iron (III), only 0.093 μmol were recovered. This is 41% of the total amount of iron (III) which had adsorbed onto the particles. This is the same recovery rate from the particles with oxalate as seen with the Co-SiO₂-DFB.

4.4. Conclusions

First, an attempt was made to coat the Co-C nanoparticles in silica. This was followed by treatment with an anhydride silane. The anhydride functional groups were converted to carboxylic acid, which was then reacted with DFB. The IR evidence suggested that the silica coating successfully formed, and was successfully derivatized with carboxylic acid. It also suggests that an amide linkage was formed between the DFB and carboxylic acid. Thus, unlike the attempts to derivatize Co-C with DFB made in Chapter 2, this attempt was successful. However, the particles did not adsorb iron (III) and it was determined that the silica coating was coming off of the particles due to the hydrophobic nature of the carbon coating.

An alternative substrate was sought. Magnetic nickel nanoparticles were chosen because they lacked a hydrophobic coating, meaning that the silica coating process may work better. (This is discussed further in Section 4.3.2.) TurboBeads Silica™, Co-C particles with a silica coating, were discovered as well. Both were studied as candidates for derivatization with DFB.

DRIFT spectroscopy showed the presence of silica on both the TurboBeads Silica™ and silica-treated nickel nanoparticles. However, it was difficult to identify the C=O stretching peak due to the carboxylic acid, normally appearing at 1720 cm^{-1} , because each sample had a large peak in the same region even before derivatization. Therefore, after derivatizing TurboBeads Silica™ and Ni-SiO₂ with DFB, they were characterized with XPS.

Before derivatizing with DFB or DFB-Fe, the Ni-SiO₂ particles showed no XPS peak due to nitrogen, whereas afterward, they did show such a peak. DFB contains nitrogen, whereas no other component in the experiment did, indicating that DFB was successfully added to the surface. However, the XPS showed that the TurboBeads Silica™, even underivatized, do contain nitrogen, and so XPS characterization could not determine whether DFB was or was not successfully added to the surface in that case.

The iron (III) uptake of the Co-SiO₂-DFB, Co-SiO₂-FB, Ni-SiO₂-DFB, and Ni-SiO₂-FB particles was tested. The Ni-SiO₂-DFB particles did not take up iron (III) at all, whereas the Ni-SiO₂-FB did. However, two problems were encountered when removing iron (III) from the surface of Ni-SiO₂-FB with oxalate. First, the oxalate did not remove 100% of the iron (III) which adsorbed to the particles when it was added. Second, a peak which overlapped with the DFB-Fe peak appeared in the UV-Vis spectra of oxalate, which was exposed to Ni-SiO₂-FB particles. This peak appeared at 380 nm, which interfered with the accurate measurement of the absorbance of the DFB-Fe peak.

It was determined that the peak at 380 nm was due to a reaction between oxalic acid and the nickel, bringing nickel (II) ions into solution. Therefore, unless the nickel nanoparticles can be coated in such a way as to protect the nickel from pH 1.5 oxalate, these particles cannot be used to extract, concentrate or measure iron (III) from the ocean.

TurboBeads Silica™ was capable of removing iron (III) from a solution both before and after treatment with DFB or DFB-Fe. Therefore, iron (III) adsorbed by the

DFB-treated particles cannot necessarily be attributed to specific adsorption by capture with the DFB. After exposing the Co-SiO₂-DFB and Co-SiO₂-FB nanoparticle samples to iron (III), only 41% of the iron (III) adsorbed by the particles from solution could be removed from the surface with oxalate. Still, unlike with the Ni-SiO₂-FB particles, there did not appear to be any additional peaks in the UV-Vis spectra of oxalate solutions to interfere with the DFB-Fe peak.

To successfully concentrate and measure iron (III) from a sample with the magnetic particles, the oxalate must be able to remove all the iron (III) from the particles. Otherwise, an accurate measurement cannot be obtained. There are two possible ways in which iron (III) could have been lost – or more accurately, become unavailable to DFB, preventing it from being measured.

As discussed in Section 3.4, when the iron (III) on the particles is exposed to air (i.e. when changing the solution which the particles are immersed in) it may react to form iron oxyhydroxides. Although the oxalate may be able to remove these oxyhydroxides from the surface⁵, the iron (III) still may not be accessible to DFB. Measuring iron (III) in oxalate involves adding DFB to chelate the iron (III), then measuring the 430 nm peak produced by the DFB-Fe complex. The portion of iron (III) in the oxyhydroxides cannot be measured in this way, because the DFB will not chelate it. Still, the formation of iron oxyhydroxides on the surface may not occur if the iron (III) is bound to oxalate, so this explanation only applies to any non-specifically-bound iron (III).

Another explanation can be found in the fact that oxalate can promote the photocatalytic degradation of DFB-Fe to form iron (II). Kunkely and Vogler found that irradiating a mixture of DFB-Fe and oxalate with white light caused the absorbance of the DFB-Fe peak to decrease by about 50% over the course of an hour.⁶ During this project, to measure iron (III) in oxalate, DFB was added and the pH was raised. The solution was exposed to ambient light in the laboratory while the pH adjustment was performed, which generally took at least 5 minutes. It is possible that prior to measurement of this solution with UV-Vis spectroscopy, some of the iron (III) could have been reduced to iron (II), reducing the DFB-Fe signal which would have appeared. This would make it appear as though not all of the iron (III) was recovered in the oxalate. This explains how some iron (III) could have appeared to be lost even if it had not reacted on the surface to become oxyhydroxides.

4.5. References

1. Roy, E. G.; Jiang, C. H.; Wells, M. L.; Tripp, C., Determining Subnanomolar Iron Concentrations in Oceanic Seawater Using a Siderophore-Modified Film Analyzed by Infrared Spectroscopy. *Analytical Chemistry* **2008**, *80* (12), 4689-4695.
2. Chi, Y.; Yuan, Q.; Li, Y. J.; Zhao, L.; Li, N.; Li, X. T.; Yan, W. F., Magnetically Separable Fe₃O₄@SiO₂@TiO₂-Ag Microspheres with Well-Designed Nanostructure and Enhanced Photocatalytic Activity. *Journal of Hazardous Materials* **2013**, *262*, 404-411.

3. D'Antonio, M. C.; Wladimirsky, A.; Palacios, D.; Coggiola, L.; Gonzalez-Baro, A. C.; Baran, E. J.; Mercader, R. C., Spectroscopic Investigations of Iron(II) and Iron(III) Oxalates. *Journal of the Brazilian Chemical Society* **2009**, *20* (3), 445-450.
4. Grass, R. N.; Athanassiou, E. K.; Stark, W. J., Covalently Functionalized Cobalt Nanoparticles as a Platform for Magnetic Separations in Organic Synthesis. *Angewandte Chemie-International Edition* **2007**, *46* (26), 4909-4912.
5. Lee, S. O.; Tran, T.; Jung, B. H.; Kim, S. J.; Kim, M. J., Dissolution of Iron Oxide Using Oxalic Acid. *Hydrometallurgy* **2007**, *87* (3-4), 91-99.
6. Kunkely, H.; Vogler, A., Photoreduction of Aqueous Ferrioxamine B by Oxalate Induced by Outer-Sphere Charge Transfer Excitation. *Inorganic Chemistry Communications* **2001**, *4* (4), 215-217.

CHAPTER 5: FUTURE WORK

The work presented in this thesis was done toward the goal of capturing and concentrating iron (III) from a solution to improve measurement ability. It was found that bare Co-C, Ni-SiO₂-FB, Co-SiO₂-DFB, and Co-SiO₂-FB particles were all capable of removing iron (III) from a solution. The next step was to remove iron (III) from the particles using a solution of 0.1 M oxalate at a pH of 1.5 (or, in the case of the bare Co-C particles, 8 mM DFB), then measure the iron (III) in this solution. However, the maximum amount of iron (III) which could be recovered by the oxalate was 70% for the Ni-SiO₂-FB particles and 41% for the Co-SiO₂-DFB and Co-SiO₂-FB particles. For the bare Co-C particles, 100% recovery was obtained once, but this was not reproducible.

It was determined that the incomplete recovery could be due to the formation of iron hydroxides on the surface of the particles when exposed to air if any non-specific binding of iron (III) occurred. When changing supernatants (e.g. removing the iron (III) solution and adding oxalate), the particles were briefly exposed to the air, which would allow the iron (III) on the surface to react with atmospheric oxygen. Ultimately, any iron oxyhydroxides which formed as a result could not be captured by the DFB and therefore the iron (III) could not be measured. Therefore, in any further work done to capture and concentrate iron (III) from the particles must be done in such a way as to prevent exposure to air.

One way to avoid exposure to air would be to work under nitrogen. Another way would be to ensure that the particles never leave solution, as illustrated in Figure 5.1.

Simply put, to change a solution, the old solution would have to be drained out as new solution was added in. Either way, if more work was to be performed on this project, exposure of the particles to air would have to be avoided.

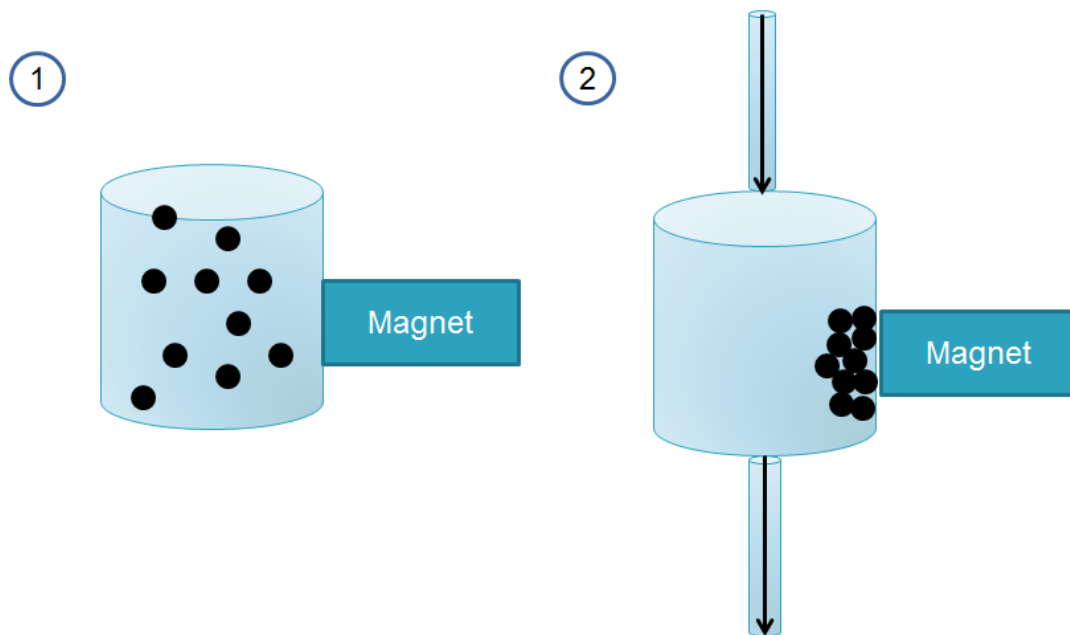


Figure 5.1. Scheme to prevent magnetic nanoparticles' exposure to air when changing solutions. 1) Draw particles to the side of the container with a magnet. 2) Allow old solution to drain while pumping new solution in.

Even if iron (III) was bound to DFB on the surface, preventing the formation of oxyhydroxides, loss could have occurred due to the reduction of DFB-Fe to iron (II) in the presence of oxalate caused by exposure to light (see Section 4.4). Therefore, when measuring iron (III) in solutions of oxalate, the oxalate solutions will have to be isolated from sources of light to prevent photodegradation prior to the measurement.

If any further work is performed on this project, the changes suggested above will have to be implemented.

BIBLIOGRAPHY

- Barrero, J. M.; Camara, C.; Perezconde, M. C.; Sanjose, C.; Fernandez, L., Pyoverdin-Doped Sol-Gel Glass for the Spectrofluorometric Determination of Iron(III). *Analyst* **1995**, *120* (2), 431-435.
- Byron, M. L.; Variano, E. A., Refractive-Index-Matched Hydrogel Materials for Measuring Flow-Structure Interactions. *Experiments in Fluids* **2013**, *54* (2), 6.
- Chapin, T. P.; Jannasch, H. W.; Johnson, K. S., In Situ Osmotic Analyzer for the Year-Long Continuous Determination Of Fe in Hydrothermal Systems. *Analytica Chimica Acta* **2002**, *463* (2), 265-274.
- Chi, Y.; Yuan, Q.; Li, Y. J.; Zhao, L.; Li, N.; Li, X. T.; Yan, W. F., Magnetically Separable Fe₃O₄@SiO₂@TiO₂-Ag Microspheres with Well-Designed Nanostructure and Enhanced Photocatalytic Activity. *Journal of Hazardous Materials* **2013**, *262*, 404-411.
- D'Antonio, M. C.; Wladimirsky, A.; Palacios, D.; Coggiola, L.; Gonzalez-Baro, A. C.; Baran, E. J.; Mercader, R. C., Spectroscopic Investigations of Iron(II) and Iron(III) Oxalates. *Journal of the Brazilian Chemical Society* **2009**, *20* (3), 445-450.
- Gamma, M. A UV-Vis. Spectroscopic Based Method for Iron Detection in Aqueous Solutions by Using DFB Tethered to Membranes. University of Maine, 2014, Ph.D Thesis.
- Garcia-Gonzalez, C. A.; Fraile, J.; Lopez-Periago, A.; Domingo, C., Preparation of Silane-Coated TiO₂ Nanoparticles in Supercritical CO₂. *Journal of Colloid and Interface Science* **2009**, *338* (2), 491-499.
- Grass, R. N.; Athanassiou, E. K.; Stark, W. J., Covalently Functionalized Cobalt Nanoparticles as a Platform for Magnetic Separations in Organic Synthesis. *Angewandte Chemie-International Edition* **2007**, *46* (26), 4909-4912.
- Gupta, R.; Bastani, B.; Goddard, N. J.; Grieve, B., Absorption Spectroscopy in Microfluidic Flow Cells Using a Metal Clad Leaky Waveguide Device With a Porous Gel Waveguide Layer. *Analyst* **2013**, *138* (1), 307-314.
- Hansen, K. Detection of Iron (III) Using Agarose Beads Derivatized with Desferrioxamine B. University of Maine, 2014, B.S. Thesis.

- He, H. Y.; Klinowski, J.; Forster, M.; Lerf, A., A New Structural Model for Graphite Oxide. *Chemical Physics Letters* **1998**, *287* (1-2), 53-56.
- Helm, Z. Determining Oceanic Iron Concentrations Using a Siderophore Based Sensor. University of Maine, 2013, M.S. Thesis.
- Hernlem, B. J.; Vane, L. M.; Sayles, G. D., Stability Constants for Complexes of the Siderophore Desferrioxamine B with Selected Heavy Metal Cations. *Inorganica Chimica Acta* **1996**, *244* (2), 179-184.
- Kanan, S. A.; Tze, W. T. Y.; Tripp, C. P., Method to Double the Surface Concentration and Control the Orientation of Adsorbed (3-aminopropyl)dimethylethoxysilane on Silica Powders and Glass Slides. *Langmuir* **2002**, *18* (17), 6623-6627.
- Keberle, H., The Biochemistry of Desferrioxamine and its Relation to Iron Metabolism. *Annals of the New York Academy of Sciences* **1964**, *119*, 758 - 768.
- King, D. W.; Lounsbury, H. A.; Millero, F. J., Rates and Mechanism of Fe(II) Oxidation at Nanomolar Total Iron Concentrations. *Environmental Science & Technology* **1995**, *29* (3), 818-824.
- Kunkely, H.; Vogler, A., Photoreduction of Aqueous Ferrioxamine B by Oxalate Induced by Outer-Sphere Charge Transfer Excitation. *Inorganic Chemistry Communications* **2001**, *4* (4), 215-217.
- Laes, A.; Vuillemin, R.; Leilde, B.; Sarthou, G.; Bournot-Marec, C.; Blain, S., Impact of Environmental Factors on In Situ Determination of Iron in Seawater by Flow Injection Analysis. *Marine Chemistry* **2005**, *97* (3-4), 347-356.
- Lam, C.; Jickells, T. D.; Richardson, D. J.; Russell, D. A., Fluorescence-Based Siderophore Biosensor for the Determination of Bioavailable Iron in Oceanic Waters. *Analytical Chemistry* **2006**, *78* (14), 5040-5045.
- Lebovka, N. I., Aggregation of Charged Colloidal Particles. In *Polyelectrolyte Complexes in the Dispersed and Solid State I: Principles and Theory*, Muller, M., Ed. Springer-Verlag Berlin: Berlin, 2014; Vol. 255, pp 57-96.
- Lee, S. O.; Tran, T.; Jung, B. H.; Kim, S. J.; Kim, M. J., Dissolution of Iron Oxide Using Oxalic Acid. *Hydrometallurgy* **2007**, *87* (3-4), 91-99.
- Lei, Q. P.; Lamb, D. H.; Heller, R. K.; Shannon, A. G.; Ryall, R.; Cash, P., Kinetic Studies on the Rate of Hydrolysis of N-Ethyl-N'-(Dimethylaminopropyl)carbodiimide in

Aqueous Solutions Using Mass Spectrometry and Capillary Electrophoresis. *Analytical Biochemistry* **2002**, *310* (1), 122-124.

Lohan, M. C.; Aguilar-Islas, A. M.; Bruland, K. W., Direct Determination of Iron in Acidified (pH 1.7) Seawater Samples by Flow Injection Analysis with Catalytic Spectrophotometric Detection: Application and Intercomparison. *Limnology and Oceanography-Methods* **2006**, *4*, 164-171.

Martel, A. E.; Smith, R. M., *Critical Stability Constants*. Plenum Press: New York 1982.

Martin, J. H.; Coale, K. H.; Johnson, K. S.; Fitzwater, S. E.; Gordon, R. M.; Tanner, S. J.; Hunter, C. N.; Elrod, V. A.; Nowicki, J. L.; Coley, T. L.; Barber, R. T.; Lindley, S.; Watson, A. J.; Vanscoy, K.; Law, C. S.; Liddicoat, M. I.; Ling, R.; Stanton, T.; Stockel, J.; Collins, C.; Anderson, A.; Bidigare, R.; Ondrusek, M.; Latasa, M.; Millero, F. J.; Lee, K.; Yao, W.; Zhang, J. Z.; Friederich, G.; Sakamoto, C.; Chavez, F.; Buck, K.; Kolber, Z.; Greene, R.; Falkowski, P.; Chisholm, S. W.; Hoge, F.; Swift, R.; Yungel, J.; Turner, S.; Nightingale, P.; Hatton, A.; Liss, P.; Tindale, N. W., Testing the Iron Hypothesis in Ecosystems of the Equatorial Pacific-Ocean. *Nature* **1994**, *371* (6493), 123-129.

Martin, J. H.; Fitzwater, S. E., Iron-Deficiency Limits Phytoplankton Growth in the Northeast Pacific Subarctic. *Nature* **1988**, *331* (6154), 341-343.

Nakajima, N.; Ikada, Y., Mechanism of Amide Formation by Carbodiimide for Bioconjugation in Aqueous-Media. *Bioconjugate Chemistry* **1995**, *6* (1), 123-130.

Owusu-Nkwantabisah, S. Polymer Adsorption on Solid Surfaces: Layer-by-Layer Studies and Development of an Iron (III) Sensor. University of Maine, 2014, Ph.D Thesis.

Quinten, M., The Color of Finely Dispersed Nanoparticles. *Applied Physics B-Lasers and Optics* **2001**, *73* (4), 317-326.

Roy, E. G.; Jiang, C. H.; Wells, M. L.; Tripp, C., Determining Subnanomolar Iron Concentrations in Oceanic Seawater Using a Siderophore-Modified Film Analyzed by Infrared Spectroscopy. *Analytical Chemistry* **2008**, *80* (12), 4689-4695.

Tripp, C. P.; Hair, M. L., Kinetics of the Adsorption of a Polystyrene-Poly(Ethylene Oxide) Block Copolymer on Silica: A Study of the Time Dependence in Surface/Segment Interactions. *Langmuir* **1996**, *12* (16), 3952-3956.

Witter, A. E.; Hutchins, D. A.; Butler, A.; Luther, G. W., Determination of Conditional Stability Constants and Kinetic Constants for Strong Model Fe-Binding Ligands in Seawater. *Marine Chemistry* **2000**, *69* (1-2), 1-17.

Witucki, G. L., A Silane Primer - Chemistry and Applications of Alkoxy Silanes. *Journal of Coatings Technology* **1993**, *65* (822), 57-60.

BIOGRAPHY OF THE AUTHOR

Kaiya Hansen was born in Whitefish, Montana but has lived in South Portland, Maine for most of her life. She graduated from South Portland High School in 2010. Then in May 2014, she graduated from the University of Maine with a B.S. in Chemistry and a minor in Mathematics. During most of her time at the University of Maine, she has been a member of the American Chemical Society. After graduating from the University of Maine for a second time, she plans to seek employment. She is a candidate for the Master of Science degree in Chemistry from the University of Maine in August 2015.